Nanomaterials with high solar reflectance as an emerging path towards energy-efficient envelope systems: a review

Rita Carvalho Veloso[1,2*], Andrea Souza[2], Joana Maia[2], Nuno Manuel Monteiro Ramos[2], João Ventura[1].

[1]IFIMUP, Departamento de Física e Astronomia, Faculdade de Ciências, Universidade do Porto, Rua do Campo Alegre s/n, 4169–007 Porto, Portugal

[2]CONSTRUCT-LFC, Departamento de Engenharia Civil, Faculdade de Engenharia, Universidade do Porto, Rua Dr. Roberto Frias, 4200-465 Porto, Portugal

* = corresponding author details, up201001431@edu.fe.up.pt

Abstract

The application of nanomaterials in the construction field is allowing the development of smart, green, durable and more efficient buildings. Among the most widely researched nanomaterials are nano-sized cool pigments, which are being enforced to achieve thermal and energy efficient façades, with the development of high reflectance and retro-reflectance coatings. Their peculiar optical and catalytic activity turns nanomaterials into suitable candidates to be use as dark coloured high solar reflectance without affecting aesthetic characteristics, thus improving the durability of coatings. The objective of this paper is to review the state-of-the-art on the benefits of using high reflectance nano pigments as coatings in building façades and their production and synthesis processes. It is thus divided into three main topics: (i) the benefits of using nanopigments on façades, (ii) the most important nanomaterials used as cool pigments and (iii) the main methods of synthesising nanopigments. One expects that the study of near-infrared nanopigmentation synthesis processes will be able to promote and disseminate the use of nanotechnology in construction, assessing the production problems and limitation and thus helping to disseminate new products by reducing production costs and increase availability.

Keywords: Nanomaterials; Buildings Envelope Systems; Near-Infrared Reflectance; Cool Pigments; Energy Efficiency

Introduction

Nanomaterials are gaining widespread importance due to their key characteristics and applications in diverse fields such as agriculture [1, 2, 3], energy [4, 5], electronics [6, 7], catalysis [8, 9], pharmaceuticals [10, 11], engineering [12, 13], technology [14, 15] or the food industry [16, 17]. The reduced size of nanomaterials affects their fundamental characteristics, altering the corresponding physical, chemical and biological behaviours. Research on nanomaterials then focuses on understanding and improving these properties, aiming novel effects and functional devices [18]. Among the many favourable characteristics often exhibited by nanomaterials, one just mentions their increased reactivity related with the enhanced surface area-to-volume-ratio, their high degree of crystallinity, chemical stability, high adsorption capacity or the possibility to tune their morphology [19, 20].

Among these unique characteristics, the optical and electronic properties of nanomaterials standout. In particular, optical properties such as emission and adsorption (related with electronic transitions between energy levels) are critically affected by dimensionality. Thus, as particle size decreases and the density of states becomes more quantized, the absorption spectra vary [21, 18]. Indeed, the mid-gap energy levels distribution leads to a wide range of absorption in nanoparticles, the crucial factor for their large optical and catalytic activity [22]. This opens the prospect of using nanoengineered materials to fine tune emission and adsorption for specific applications.

Nanotechnology is already starting to play an essential part in the development of new and improved construction materials [23]. As one moves towards nearly zero-energy buildings [24], there is the mandatory necessity to reduce the thermal gains in the urban environment. Around 40% of energy consumption and greenhouse gas emissions of European countries are attributed to buildings [25, 26, 27, 28]. The assessment and enhancement of the sustainability of buildings is thus becoming a major necessity for the consolidated development of the construction sector worldwide, ultimately aiming to design new buildings with minimal energy requirements, reduced energy use and CO_2 emissions [29].

To achieve this goal, it is important to reduce the amount of solar radiation absorbed by buildings [30]. In fact, part of the sunlight that hits a surface is absorbed as heat [29] and the resulting temperature rise in buildings can lead to large refrigeration necessities to maintain the comfort of residents. The use of reflective coatings that reflect a large portion of solar radiation (the so-called cool pigments) is thus a decisive factor for the reduction of the thermal gains and overheating in buildings [31]. Even though sunlight intensity is larger in the visible region, invisible NIR radiation accounts for around half of all solar energy reaching us [32]. Thus, research in cool pigments focuses on NIR-reflecting materials that can be an economical, ecologically and passive method to help increase energy savings in buildings decreasing the energy required for cooling loads and enhancing indoor thermal comfort by reducing the surface and ambient temperatures [33]. Figure 1 shows the main thermal properties of cool materials.

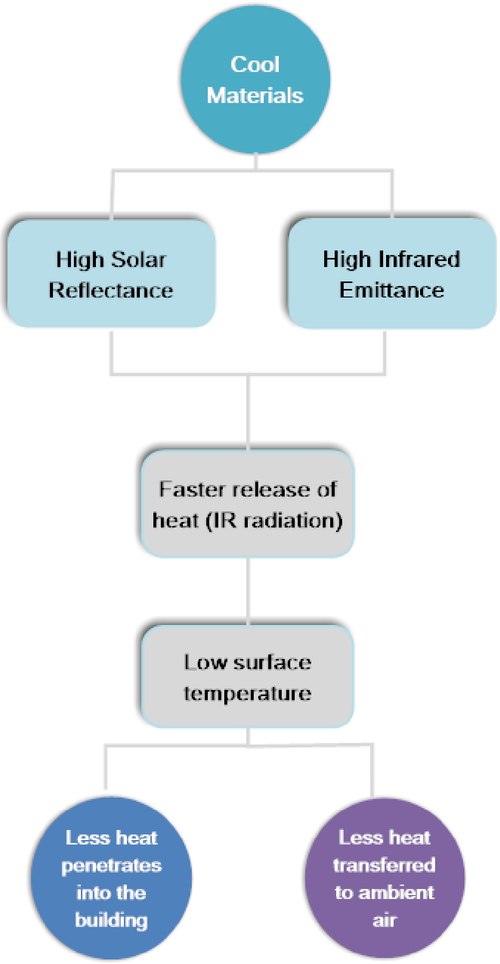

Figure 1: Cool material properties. Reproduced with permission from ref. **[33]**, Copyright 2011, Elsevier.

This is where nanomaterials with tuned optical properties have a significant opportunity in the construction sector, as reviews in this manuscript. Several authors have already presented the progress and performance of reflective materials, as well as their implementation in buildings (roofs, pavements, …) for a high cooling potential [34, 35, 36, 37, 38, 39, 40, 41]. As Santamouris et al. [34] stated, recent research focus on the improvement of already available materials or the development of new cool materials.

Rawat et al. [36], for instance, highlighted the energy-saving advantages using reflective materials in roofs structures, in different climatic zones. However, there is a limited number of literature reviews that focus on the actual reflective materials and their physical properties. Here, we will comprehensively assess the state-of-art of near-infrared (NIR) reflecting nanomaterials, emphasising NIR reflective inorganic pigments and nanopigments applicable as cool materials in buildings, grouping them by crystalline class and physical properties. The inclusion and exclusion criteria for analysing the articles in this review were the synthesis process, crystalline class, spectral and solar reflectance studies, colour and the applicability in buildings surfaces, such as roofs and façades. For that, the manuscript is divided into three main sections. Section 2 will give an introduction to nanomaterials in the construction sector motivated by thermal comfort problems in buildings. Section 3 will detail the most important materials currently being researched for cool pigments, starting with near-infrared (NIR) reflecting inorganic nanopigments (including the most important metal oxide nanoparticles TiO_2, ZnO, Cr_2O_3 and ZrO_2), complex inorganic coloured pigments (particularly spinel-type oxides), perovskites-based, rare-earth-based pigments and core-shell structures. Section 4 will briefly present how nanoscience can provide new routes for the development of advanced adaptive structures in civil engineering and architectural design as smart building skins. Section 5 will summarize the main routes to obtain nanopigments, including solid-state, sol-gel, hydrothermal, molten salt and sonochemical synthesis and examples of relevant materials synthesized by each route. The final section will give a prospect for the future of cool nanopigments in construction.

Nanomaterials in building envelopes

Nanotechnology can offer improved materials and applications for the construction sector. The main goal of the incorporation of novel construction technologies is to move towards green, smart and efficient buildings. As we have seen, the unique optical properties of nanomaterials offer the possibility to develop reflective nanopigments [42] for increasing thermal comfort and energy saving. Furthermore, besides their use as reflecting cool pigments, nanomaterials can bring additional value to construction materials. They can improve cementitious materials properties, increase composites durability, reduce weight, reduce heat transfer, promote energy efficiency and selfcleaning features [43, 44] or improved mechanical properties (including hardness, strain-to-failure or scratch resistance) in coatings [45, 46]. Novel construction materials play a crucial part in making buildings more sustainable by enabling the development of energy-efficient façades [47]. In this respect, enhancing the thermal performance of the envelope system is a critical way to decrease building energy consumption [48]. This may even involve cool coloured materials with high reflectivity in the NIR when the aesthetic of darker colours is favoured [49]. One of the most exciting technological applications is precisely to replace usual dark pigments that absorb NIR radiation, by cool materials with similar colours but with enhanced solar reflectance [50, 51]. Typically, cool materials have high solar reflectance and infrared emittance [52, 53]. By employing materials with tuned absorption and reflection of specific spectral wavelengths, the total energy absorbed by the surface where the cool pigment is applied is reduced [54, 55, 56]. According to Gobakis et al. [57], the definition of cool roofing materials depends on the specific Certification Program, but usually is required a minimum of 0.65 for solar reflectance and 0.85 for thermal emittance.

Angular dependence of the Solar reflectance

The solar reflectance of surfaces varies according to the angular distribution of the incident solar radiation, from a minimum value analogous to the normal incidence of a light beam to a maximum value corresponding to an incidence angle of 90^o, depending on the surface roughness [58]. According to Fresnel equations, reflections in smooth surfaces are strictly dependent on the angle of incidence and have high angular reflectance values, while reflections from rough surfaces are less affected by incident angle variations [59].

This issue is particularly pertinent in cool materials, since they can undergo treatments to become smoother and increase the solar reflectance. For instance, coatings for roof application usually present smooth surfaces. Thus, it is important to understand how the incident angle affects the solar reflectance in order to estimate the solar gains of building components [58]. Such estimation of solar gains of buildings should also include diffuse and specular reflections of the incident irradiation. Usually, solar gains can be determined using [58]:

$$Q_{SG} = I_b.(1-\rho) + I_d.(1-\rho) = (I_b + I_d).(1-\rho) = I_g.(1-\rho), \qquad (1)$$

where Q_{SG} is the solar gain heat power [W/m^2], I_b the beam irradiance [W/m^2], I_d the diffuse irradiance [W/m^2], I_g the global irradiance [W/m^2] and ρ the solar reflectance [-].

Building materials are commonly considered Lambertian due to their ability to reflect diffuse incident radiation on their surface. Such statement cannot be strictly valid since the reflectance of a material surface is the result of the combination of the incident (diffuse, hemispherical also called specular beam) and reflected (diffuse or specular) radiation geometries, associated with the contribution of the proper spectrum wavelength [Infrared (IR), visible, ultraviolet (UV)], as well as the incidence angle (Figure 2). While the reflectance of a surface under specular reflectance (such as in glass and metal coatings) depends on the incident angle, that of diffuse irradiation (as in most of the paint and cementitious coatings) is constant regardless of the incidence angle, as mentioned before [59].

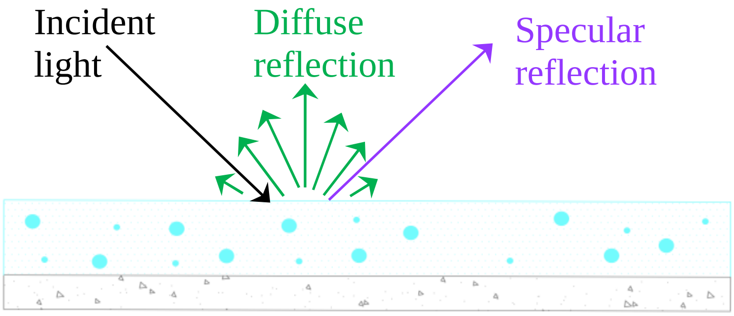

Figure 2: Reflection properties of the incident light on an opaque façade.

The main difference between conventional and cool coloured material products is that the latter can include paints, pigments, coatings and membranes to smooth the surface. This promotes a partly specular surface and reduces the absorption due to surface roughness. On the contrary, traditional materials can comprise rough finishing and diffuse performance. However, many opaque construction materials frequently present a mixed behaviour, which includes specular and diffuse performances (Figure 3).

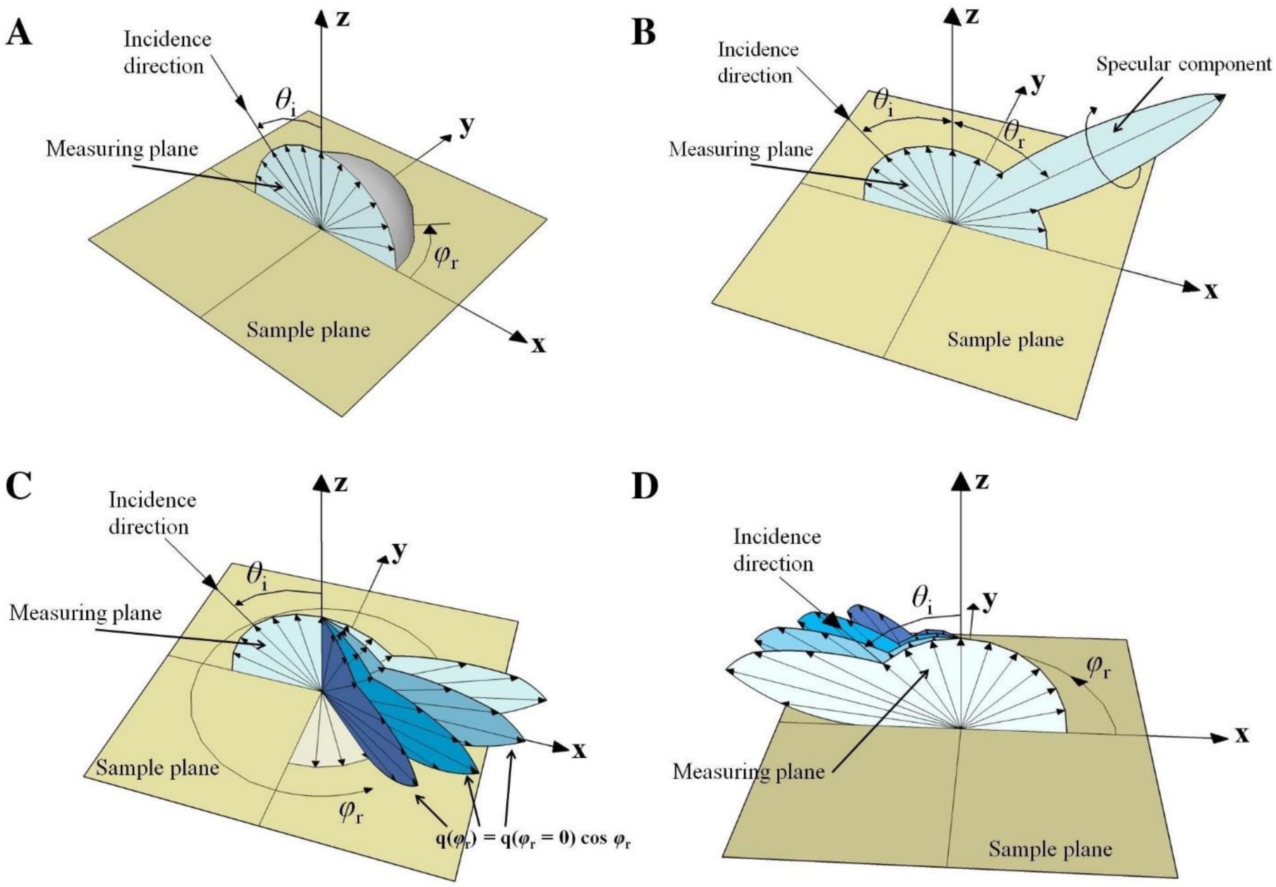

Figure 3: 3D images of calculations of the directional-hemispherical reflectance of materials: (a) mainly Lambertian; (b) mainly specular; (c) mixed behavior; (d) backscattering mixed. Reproduced with permission from Ref. **[59]**, Copyright 2015, Elsevier.

As such, Carnielo et al. [58] considered two different reflectance components. The first is an angular component (ρ_θ) related with the variation of the solar beam irradiance with the incidence angle (θ) that can be calculated from the interpolation of experimental values obtained at various θ-values. The second component is a constant reflectance (ρ_d) related with the diffuse solar irradiance that uniformly hits a surface:

$$\rho_d = \int_0^{\pi/2} \rho(\theta) \, . \, d_\theta . \qquad (2)$$

The authors then proposed a method to calculate the dependence of solar gains on the incident angle using:

$$Q_{SG}(\theta) = I_b . (1 - \rho_\theta) + I_d . (1 - \rho_d) . \qquad (3)$$

Regarding the building envelope system, in Figure 4, Takebayashi [60] identified that the reflection of solar radiation on diffuse conventional façades (e.g. concrete, paints or wood) results in 12.5% being reflected to the sky, 12.5% to the ground and 75% being absorbed by the building façade. However, the use of high reflectance cool coatings can reduce the thermal load to approximately 25%. If the façade has a high reflectance specular property, the reflection can even reach 75%. However, in this case, despite reducing the thermal absorption of the wall, the beam could cause pedestrian glare.

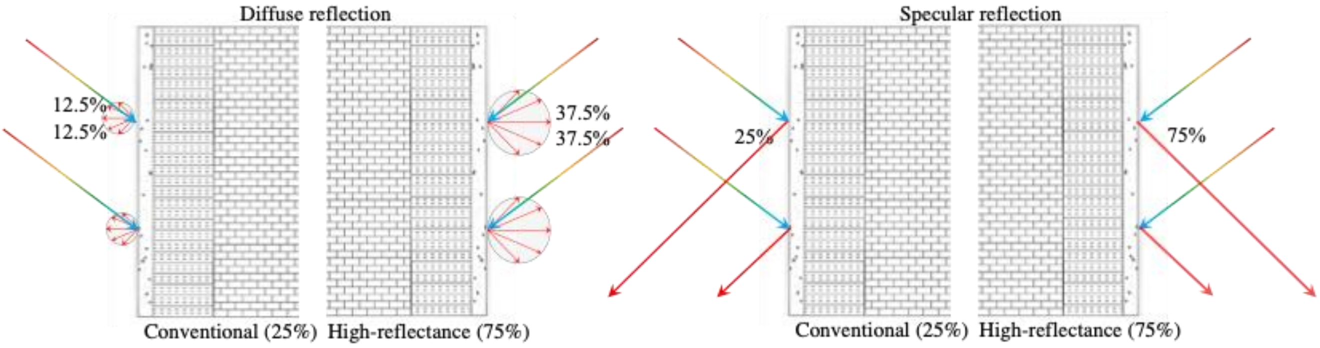

Figure 4: Example of diffuse and specular reflections on the façades of a building. Reproduced with permission from ref. **[60]**, Copyright 2016, Elsevier.

Although the application of materials with high solar reflectance seems relatively easy with plenty space to implement this strategy in hot climates, there are still urgent difficulties that must be taken into account. For example, surfaces with high reflectance can cause glare problems leading to hazards and discomfort [61]. Another potential problem is the limited range of colours/hues to be applied to buildings. However, these problems can be avoided by providing materials with a broad range of colour palette (for aesthetic reasons) but controlled near-infrared reflectance to achieve the desired effects [62].

Near-infrared reflecting inorganic pigments and nanopigment

Typically, cool pigments are chosen from materials displaying the highest reflectances, with complex metal oxides being the main source of NIR reflective inorganic pigments, selectively reflecting radiation in the visible and infrared regions. In particular, white materials, such as titanium dioxide, present the best heat reflection performance with a solar reflectance of around 87% [63] and are thus the most used cool materials. Such high reflectance leads to a lower sunlight absorption from exterior surfaces, such as roofs, decreasing the cooling necessities of the building. Low light absorbance and high dispersion of radiation in the visible regions are other relevant properties of white pigments (400-800 nm). Nevertheless, conventional dark tones (such as black pigments; highly absorbing and reflecting only ≈5% of the total solar irradiation) are still abundantly used on exteriors, either because of aesthetic reasons or to conceal soiling.

The reflectivity and absorptivity of a pigment are independent, opening the possibility to design coloured NIR reflective coatings [64], with the corresponding heat reflection being strongly related with the pigment colour. Furthermore, reflective nanopigments can be designed in order to selectively reflect visible and infrared radiation (Figure 5). To design a NIR- reflecting pigment it is required to maximise the total reflectance and emissivity and, withal, minimise the possible contamination by infrared absorbing materials white pigments [65]. Another key parameter to design a cool pigment is the used particle size, which allows engineering the scattering power [66].

The optical properties of a coating depend on (i) the refractive indices of the pigment and binder; (ii) the thickness of the film; and (iii) the size, shape and concentration of the pigment particles [67, 68]. Painted coatings are considered thin films, so that their optical properties can be classified in three broad cases: (a) transparent films that allow most light to pass but can absorb some of it; (b) translucent films in which light is scattered in both directions; and (c) opaque films where the concentration of colorant or pigment particles is high and a portion of light is absorbed and the other is scattered back to the top [69].

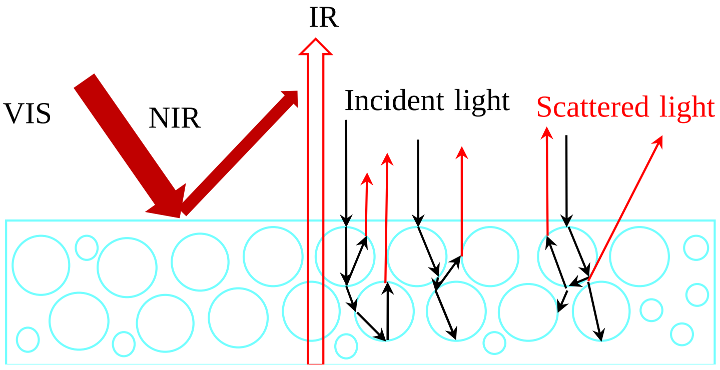

Figure 5: Schematic of reflective nanopigment coating. Reproduced with permission from ref. **[70]**, Copyright 2014, Elsevier.

Light scattering by particles can be modelled by Maxwell's equations but exact solutions can only be found for specific particle geometries (e.g. spherical). Concerning the influence of the size of a scattering particle, one can define a size parameter ($\mathcal{X}$) given by (in which r is the particle radius r and λ the wavelength of the incident radiation):

$$\varkappa = \frac{2\pi r}{\lambda}. \qquad (4)$$

Two cases then follow: if the size parameter is small ($\varkappa \leq 0.3$) the particles are classified as small and light scattering is defined by Rayleigh theory; on the other hand, if the size parameter is between $0.3 \leq \varkappa \leq 0.5$, the particles are considered large and scattering is treated by Mie theory [71], which is a complete analytical solution of Maxwell's equations used to characterize the scattering from any spherical particle with an arbitrary size.

The multiple-scattering phenomena that arises in the scattering of light from surfaces is fundamental in nature and several models are described in the literature [72, 73]. The simplest model to predict and explain the optical properties of colorant layers is the Kubelka- Munk (KM) theory [74, 75]. This two-flux model is widely applied in the pigment industry and translucent/opaque films [68]. For the latter, the effective scattering coefficient S is particularly high because of the high concentration of the pigment and light is completely scattered [69], giving origin to the Kubelka-Munk equation:

$$\frac{K}{S} = \frac{(1-R_\infty)^2}{2R_\infty}, \qquad (5)$$

where K is the absorption coefficient and R_∞ is the reflectance at an infinite thickness.

However, the use of the KM model is limiting since it assumes that the light passes through the film only in a diffuse mode and refractive index changes are not considered. On the other hand, the Sauderson correction [76] adjusts the coating's reflectance by considering the refractive index gap that can possible exist between the layer coating and air. In real films, there is a scattering effect, with the light propagating in any direction. The KM model contemplates two fluxes with diffused light in both directions (upwards and downwards). Applying the Sauderson correction on the classical KM theory actually estimates the difference of the refractive indexes and gives a better approach on the reflectance values.

Metal oxides nanoparticles

Inorganic pigments are commonly used in different applications, including paints and coatings [77]**.** Table 1 shows the most common metal oxide compounds used as cool pigments. As readily seen, the largest solar radiation reflections are obtained using white coatings, from which the most typical is titanium dioxide (TiO_2). Nevertheless, other oxides or their synthetic analogues can be used as pigments after suitable modifications.

Table 1: Common pigments used as cool material and their relevant properties.

Compound	Crystal Structure	Colour	Particle Size	Form	% NIR reflectance	Reference
TiO_2	Tetragonal, Rutile	White	Micrometres	powder	~ 87%	[63]
ZnO	Hexagonal, Wurtzite	White	Nanometres	powder	~ 85%	[78, 79]
ZrO_2	Monoclinic, baddeleyite	White	Micrometres	NA	NA	[80]
Cr_2O_3	Sesquioxide	Green	Nanometres	powder	50-57%	[81, 82]

TiO_2 is the most used pigment in coatings formulation, improving the quality and coverage power, durability and brightness of the coating [83, 84]. Besides that, there are other metal oxides nanomaterials such as ZrO_2, ZnO or Cr_2O_3, that have been used as key-enabling technologies for the production of control functional coatings to minimise energy usage in buildings [85]. However, the use of heavy metals is beginning to be worrying and alarming [86, 81] and an ideal approach is the use of naturally occurring oxides or the production of their analogues with appropriate modifications that make then suitable to be used as pigments.

Titanium Dioxide (TiO_2)

Titanium Dioxide (TiO_2) is a white colour pigment widely used for eco-friendly applications, including in construction materials (tiles, concrete, coatings or glasses), because of its unique properties (low cost, non-toxicity, optical transparency, large refractive index, chemical stability or good thermal performance) [87, 88]. In these applications, the behaviour of TiO_2 nanomaterials is largely influenced by their electronic and optical properties, particle size, morphology and crystalline structure [89]. Anatase (tetragonal), brookite (orthorhombic) and rutile (tetragonal) are the three main crystalline phases of TiO_2 [90]. The most stable modification is the rutile phase, while anatase irreversibly transforms into rutile during heating at a transformation temperature that depends on the synthesis process, annealing atmosphere, crystallinity degree and impurity content [91, 92].

Relevant Properties

From the TiO_2 phases, rutile {crystal system: tetragonal (4/mmm), space group: P42/mnm–D_{14}^{4h}}, anatase {tetragonal (4/mmm), I41/amd–D_{19}^{4h}} and brookite {orthorhombic (mmm), Pbca–D_{15}^{2h}}, only the first two have an important role in industrial applications. Brookite has a much smaller significance due to the drawback in fabricate pure-phase crystal, when compared to rutile and anatase TiO_2 (Figure 6) [93, 90].

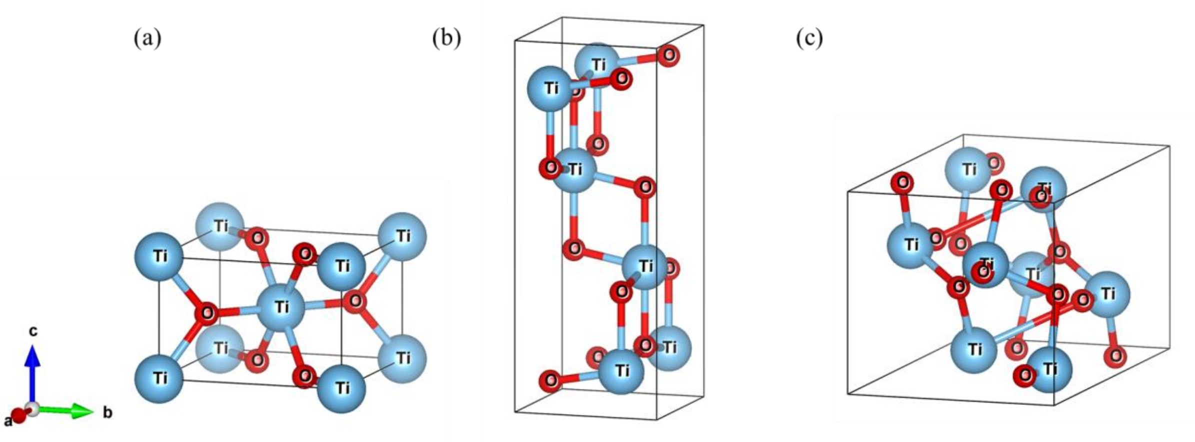

Figure 6: Planar building-block representation of TiO_2 in the (a) rutile (b) anatase and (c) brookite phases.

Being a large bandgap (>3 eV) n-type semiconductor, most of the practical applications of TiO_2 use its light adsorption capacity, particularly photocatalysis and photovoltaics. However, its large band gap and the fast recombination of photo-excited carries limit its light adsorption properties to UV light that constitutes only ≈5% of the total solar radiation [94, 95]. Table 2 summarizes the main properties of the anatase and rutile phases of TiO_2.

Table 2: Structural and physical characteristics of TiO_2 (anatase and rutile). Adapted from ref. **[95, 96]**.

Property	Anatase	Rutile
Molecular Weight (g/mol)	79.88	79.88
Melting Point (°C)	1825	1825
Boiling Point (°C)	2500-3000	2500-3000
Light Absorption (nm)	<390	<415
Mohr’s Hardness	5.5	6.5-7.0
Refractive Index	2.55	2.75
Dielectric Constant	31	114

Crystal Structure	Tetragonal	Tetragonal
Lattice Constant (Å)	a=3.7842 b=3.7842 c=9.5146	a=4.5937 b=4.5937 c=2.9581
Density (g/cm^3)	3.79	4.13
Ti-O Bond Length (Å)	1.94 (4) 1.97 (2)	1.95 (4) 1.98 (2)
Bandgap Energy (eV)	3.20	3.0

Applications in the coating industry

TiO_2 has been extensively used in building materials and in the coating industry due to a diversified set of properties. Compared with other metal oxide materials, it provides high photocatalytic activity and is highly effective under weak solar irradiation. Furthermore, TiO_2 can be incorporated in traditional construction materials without degrading the original performance [97].

With the development of the coating industry, several studies have been directed to take advantage of the characteristics and properties of TiO_2. It has already been reported that TiO_2 is the most effective UV protector [98] and improves the solar reflectance of coatings. For instance, Godnjavec et al. [99] modified the surface characteristics of TiO_2 nanomaterials to be used as additives in clear acrylic coatings. Looking at the results, it appears that TiO_2 improved the dispersion in the acrylic coating, as well as UV protection. In general, particle size influences a large variety of properties of materials [100]. Consequently, it will determine the appearance (colour and brightness), as well as the reflectance of coatings. In the coatings industry, commercial rutile TiO_2 generally has a particle size in the order of nanometres (200-300 nm) and efficiently reflects radiation with a wavelength between 400 and 1700 nm. However, larger sized titanium dioxide particles (≈10 µm) reflect better radiation in the 800 and 2300 nm range, but is less effective in the 400-800 nm range. Song et al. [101] studied how the particle size distributions of commercial TiO_2 pigments [TiO_2 Pure (280 nm), Altiris 550 (360 nm) and Altiris 800 (410 nm)] influences the corresponding optical properties. They showed that the sunlight reflectance decreases with increasing pigment particle size (Figure 7).

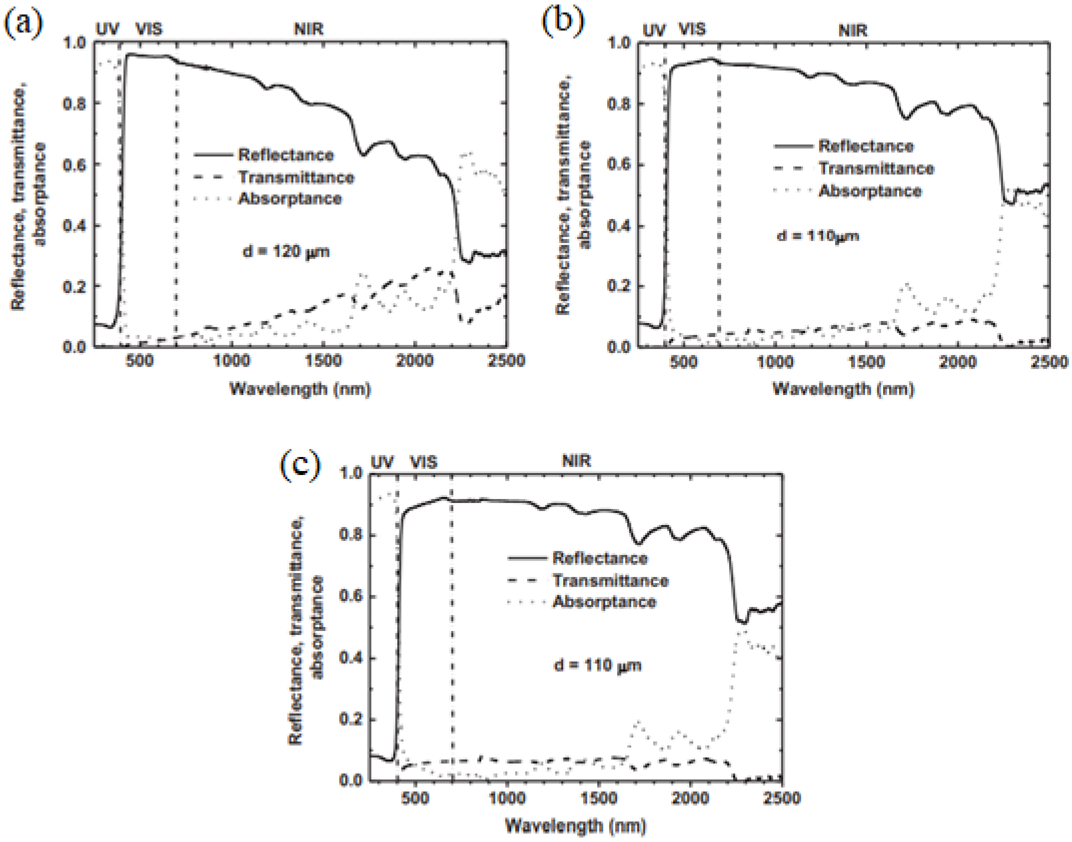

Figure 7: Optical properties of paint coatings with (a) rutile TiO_2 (280 nm), (b) Altiris 550 (360 nm) and (c) Altiris 800 (410 nm) pigments (28 wt%). Reproduced with permission from ref. **[101]**, Copyright 2014, Elsevier.

Another study, conducted by Piri et al. [102], aimed to characterise the reflectance, transmittance and absorption of different surfaces coated with TiO_2 particles of different size (35, 120 and 250 nm) and concentration (0.1, 0.5, 1.0, 5.0, 10% wt) (Figure 8). This study confirmed that the optical properties of the coatings are strongly dependent on particle size and corresponding concentration. It was shown that the TiO_2 nanoparticles strongly absorb light in the UV region, but reflect most of VIS and NIR radiation.

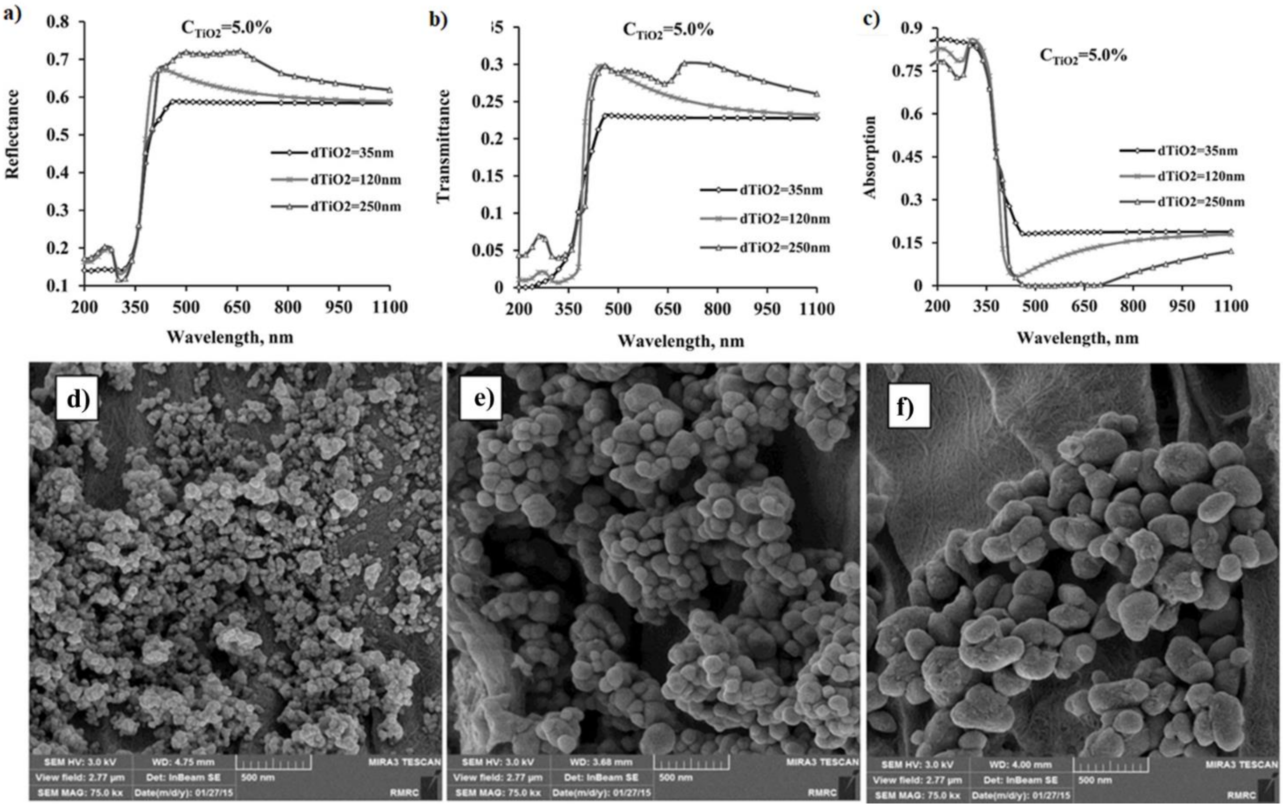

Figure 8: Effect of the diameter of TiO_2 nanopigments on the corresponding reflectance, transmittance and absorption (a, b and c); SEM (Scanning Electron Microscopy) images of TiO_2 with diameters of 35 nm (d), 120 nm (e) and 250 nm (f). Reproduced with permission from ref. **[102]**, Copyright 2017, Elsevier.

Shen et al. **[88]** studied how the concentration and particle size of TiO_2 nanoparticles affect the thermal and mechanical properties of coatings applied in thermal insulation. The solar reflectance with different gradations was also tested, with the results indicating an improvement of the solar reflectance and thermal insulation of the coating with increasing nanosized particles content.

Modifications on TiO_2

The higher cost of nanosized TiO_2 when compared with regular TiO_2 will necessarily result in the increase of a production costs. Moreover, two other major characteristics limit the use of nanosized TiO_2. First, the small particle size and enhanced surface area of nano TiO_2 typically lead to an incompatibility with the polymeric matrix and thus to agglomeration and to a decrease of the overall UV protection efficiency which is determined by the dispersion of the TiO_2 nanoparticles. Second, it is necessary to avert the formation of free radicals, which can occur due to the photochemical reactivity of TiO_2 [99, 103]. To overcome these challenges, several physical and chemical routes are used to modify the TiO_2 structure. One of the solutions is the modification of the surface of the nanoparticles with inorganic oxides that can further decrease the difference in the refractive index of the coating.

Narrowing the bandgap in order to improve TiO_2 photostability and reactivity under solar radiation is one of the motives to research modifications in TiO_2. The mains goal in doping TiO_2 is to cause interstitial or substitutional defects or create vacancies in order to change colour, magnetic and optical properties, reactivity or conductivity of the original oxides used [96]. Much effort has been made to enhance the optical properties of TiO_2 by bandgap engineering including metal, non-metal and self-doping.

A very efficient methodology for narrow the bandgap of semiconductors is, for example, the incorporation of non-metallic compounds. In order to achieve photoactivity in visible light, dopants such as nitrogen, carbon, fluorine, boron or phosphorous are added to the structures of titanium dioxide [104]. Likewise, metallic elements such as, lithium (Li), aluminium (Al) and potassium (K) are also used to improve the reflectance of the particles of TiO_2. Usually, commercial TiO_2 Rutile is doped with Al_2O_3 to improve its photochemical stability. Kumar et al. [105] applied Al-doped TiO_2 nanoparticles on plastic substrate coatings to develop light reflectors. These reflectors showed a diffuse reflectance of over 98% for a coating thickness of 0.25 mm (Figure 9) due to defects in the rutile lattice created by the Al doping, acting as traps for the photogenerated charges [64, 106].

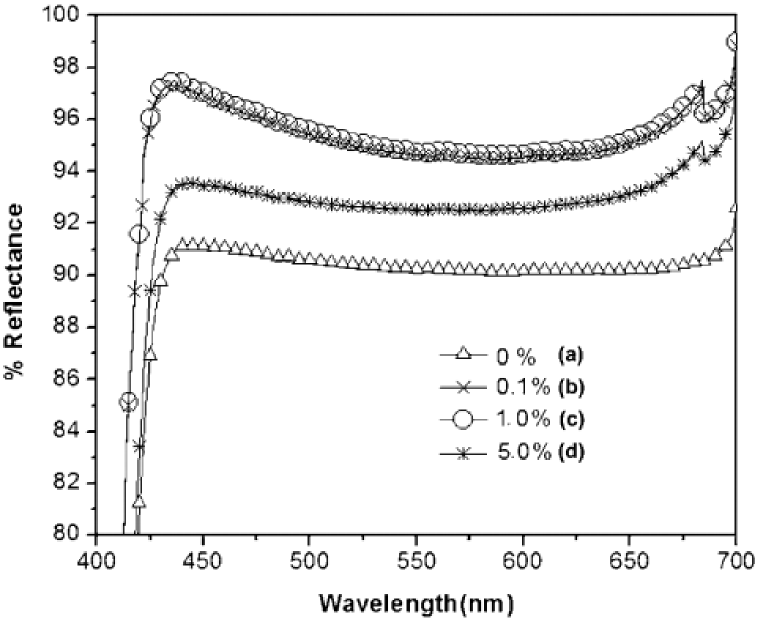

Figure 9: Diffuse reflectance of Al-doped TiO_2 nanoparticles exposed to light radiation with 0% (a), 0.1% (b), 1.0% (c), and 5.0% (d). Reproduced with permission from ref. **[105]**, Copyright 2013, Cambridge University Press.

Such procedures give rise to impurity states in the TiO_2 bandgap that improve visible-light harvesting. Nevertheless, doping leaching, thermal instability, or less efficient recombination of charges induced by additions and/or traps, still presents some limitations, raising environmental issues [107, 108]. The largest problem with doped TiO_2 at present may be the loss of photoactivity during recycling and long-term storage [108]. Therefore, major areas of future research should include the development of new nanodopants, a new method of nanodopant incorporation into the TiO_2 structure as well as new applications for coating technologies.

Zinc Oxide (ZnO)

In the last few years, one of the most promising metal oxides is zinc oxide due to its wide range of radiation absorption, high chemical and mechanical stability, good catalytic activity, electrochemical coupling coefficient and low toxicity [109]. Zinc oxide can be applied in the most diverse areas such as cosmetics, pharmacy, paints and coatings, floor coverings, plastics and rubber products, storage batteries, detergents or soaps, textiles and also electrical equipment [79].

Relevant properties

Due to its stability in harsh processing conditions, it is considered an excellent antibacterial agent, as well as its use is considered safe for animals and humans [110]. It belongs to the group II-IV of the semiconductors with a wide range of direct bandgap at room temperature of 3.37 eV [111], belonging to the hexagonal crystalline system (Figure 10) a much simpler crystal growth technology that turns manufacturing costs ZnO-based pigments potentially lower. Such structure develops a crystal lattice of a Wurtzite type since the Zn-O tetrahedra join at a common zinc atom forming a nucleus for additional tetrahedra [112].

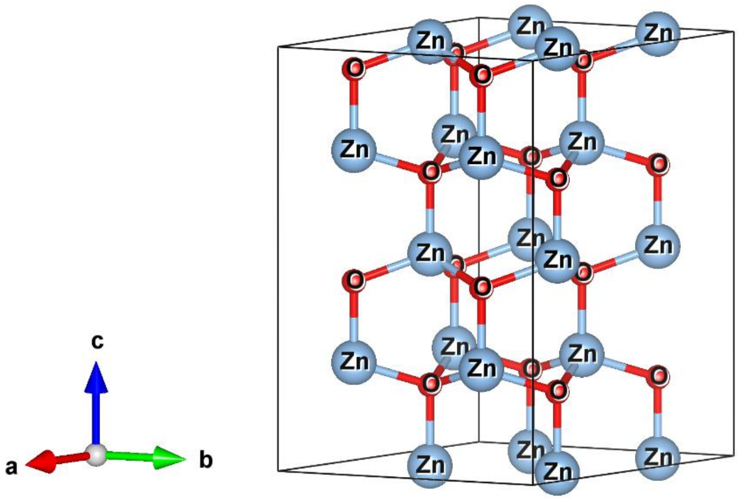

Figure 10: Crystalline structure of polyhedral zinc oxide (wurtzite).

Applications in the coating industry

Together with titanium dioxide, ZnO is a widely used white pigment, found both in decorative and artistic paints, even though it cannot compete with the hiding power (a particle's ability to scatter light) of TiO_2 rutile (n=2.75), due to its low refractive index, n = 2.02 [64, 113]. Mixtures of ZnO with barium sulphate, lead white or titanium dioxide are often found in oil paints to enhance the hiding power [114]. It is expected that pigments optimized in size and morphology will achieve optimum diffuse solar reflectance for smaller film thicknesses, which contributes to improving the durability of the system as the volume of pigment required is reduced. Kiomarsipour et al. [79] developed a novel ZnO pigment morphology to increase its scattering ability. They synthesised five different morphologies of ZnO pigments (nanoparticle-decorated, nanorods, microrods, submicrorods and scale-like) by a simple hydrothermal procedure and studied the effects of the ZnO morphology on the spectral reflectance (Figure 11). As shown in Figure 11 for TiO_2, the decorated surface with ZnO nanoparticles showed increased light scattering.

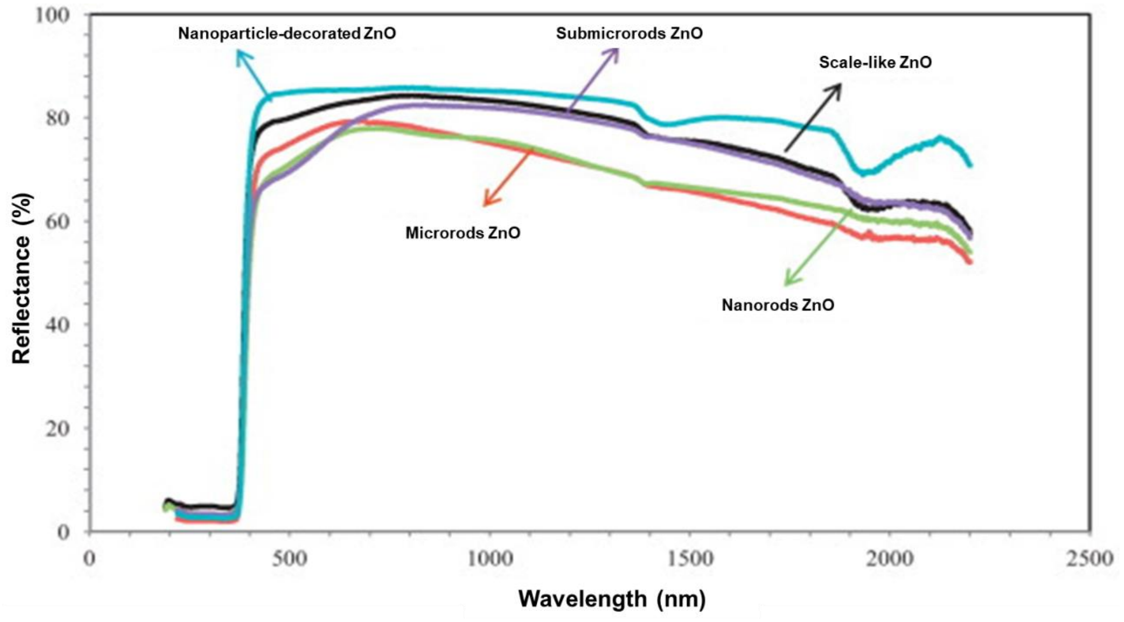

Figure 11: UV/VIS/NIR spectral reflectance of different morphology ZnO pigments. Reproduced with permission from ref. **[79]**, Copyright 2013, Elsevier.

Nevertheless, ZnO is no longer used as a principal pigment, but instead as an additive in exterior paint for wood preservation. It improves the durability and resistance of coatings from mildew and can absorb UV radiation [115]. However, ZnO pigments (as TiO_2; see Table 1) are also active photocatalysts so that the absorption of UV light can result in the degradation of the organic binders and thus in coatings with decreased lifetime [116].

To improve their properties, it is possible to engineering the bandgap of ZnO. This technology allows the fabrication of energy-saving windows by alloying, for example, with MgO, which increases the bandgap, or with CdO, which decreases the bandgap. Doping with compounds such as Aluminium (Al) or gallium (Ga) turns ZnO into a modest electrical conductor with the ability to reflect NIR light. As such, it was proposed as a piece of a multi-layered coating system for windows with the capability of energy-saving or heat-rejecting. In this realization, the coating is transparent to visible light, while reflecting infrared radiation into the outside (rejecting radiant heat in hot weather) or back into the room (lowering heating necessities in cold weather). [66].

Zirconium Dioxide (ZrO_2)

Zirconium dioxide (zirconia) occurs naturally as the mineral baddeleyite and is fabricated by calcining other zirconium compounds. Bulk ZrO_2 is a wide bandgap (~5 eV) insulting material. ZrO_2 has three stable phases at normal conditions: cubic above 2370°C, tetragonal between 1170 and 2370 °C and monoclinic bellow 1170°C [117] (Figure 12). Contrarily to TiO_2, in which all phases have six-coordinate Ti, monoclinic zirconia presents seven-coordinate Zr centres due to the larger size of the Zr atom. [118].

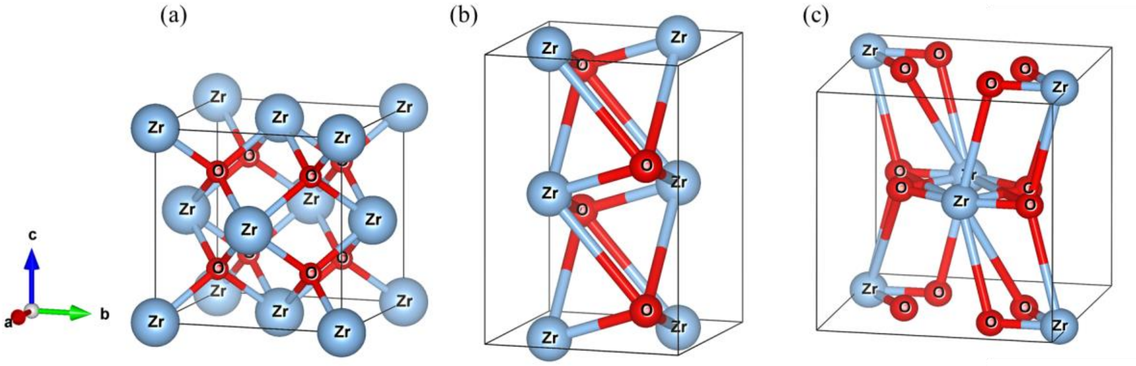

Figure 12: Crystal structures of ZrO_2: cubic (a), tetragonal (b), and monoclinic (c).

Zirconia is particularly interesting for coatings in the near-UV to IR ranges due to its good refractive index and low absorption properties. It can be used in exterior service paint as a coating for the surface of titanium oxide pigment particles. Such coating reduces UV excitation of titanium dioxide, minimizing the interaction with organic paint binder and extend the service life. Zirconia has also been used in white camouflage paints for use in snow environments as a substitute of TiO_2 pigments since it more closely simulates snow in microwave and infrared spectra. [80]. Besides, aqueous solution zirconium compounds can have the ability to crosslink carboxylates resins, which can be used in both water-based inks and paints to improve both heat and scrub resistances [119].

Chromium Oxide (Cr_2O_3)

In spite of their excellent performance as reflective materials, white pigments present several disadvantages such as light pollution, poor stain resistance or monochrome. Thus, with the increasing necessity for additional functions and attractiveness, cool pigments are still unsatisfactory for society [81]. There is a large necessity to substitute conventional coloured pigments with reflective pigments which, although absorbing smaller amounts of NIR radiation, offer coatings with analogous coloration to conventional buildings materials but with enhanced solar reflectance. [120].

Cr_2O_3 is the only solid chromium oxide phase stable above 773 K. Below this temperature, different oxygen-rich phases can occur in the Cr_2O_3-CrO_3 composition range [121]. Chromium (III) oxide is a highly stable sesquioxide (Figure 13) and is isomorphous with corundum [122], α-$A1_2O_3$, in which oxygen is positioned in an approximate hexagonal close packing lattice, with Cr^{3+} occupying 2/3 of the octahedral interstices. Like corundum, Cr_2O_3 is a hard, brittle and antiferromagnetic material [123].

Cr_2O_3 has a high melting temperature of approximately 2435 K, which makes chromium sesquioxide an important refractory compound. For this reason, it is a proper material for coatings due to their wear resistance and thermal protection. By employing nanosized chromium (III) oxide, it is possible to obtain newer or enhanced applications in surface coatings [124].

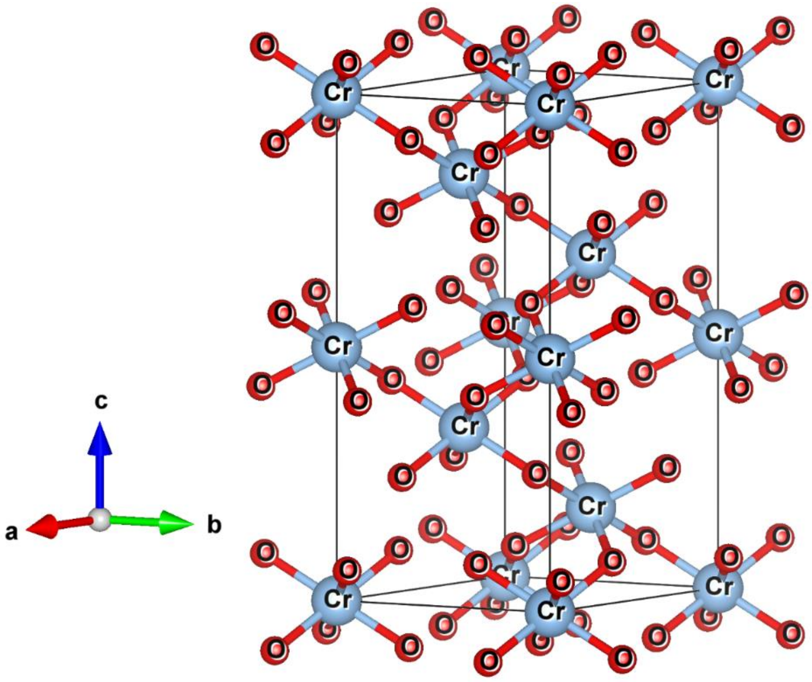

Figure 13: Unit Cell of Chromium (III) sesquioxide.

In the past, chromium oxide has already been used by military in camouflage coatings to avoid objects detection. Green pigments, such as Cr_2O_3, have medium-high NIR solar reflectance, between 50 and 57% [81], being used as roofing material that efficiently reduce their surface temperature and simultaneously improves the appearance of the roof [82, 125].

Due to the dark green tone, different efforts are being performed to obtain a brighter green. For example, Liang et al. [82] prepared pure Cr_2O_3 from the thermal decomposition of CrOOH, obtaining both high NIR reflectance and good colour performance (Figure 14).

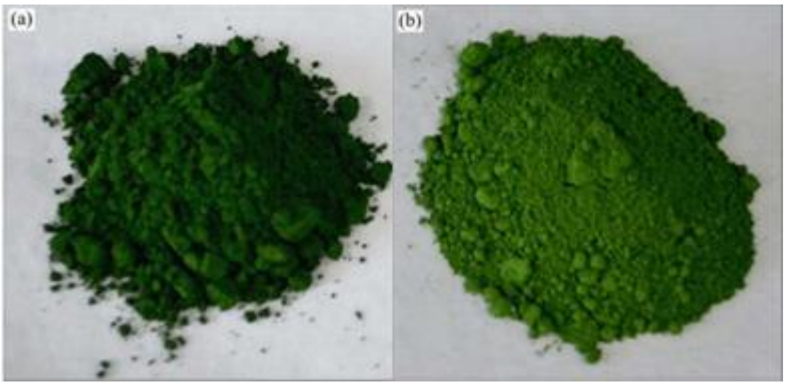

Figure 14: Photographs of (a) regular dark green Cr_2O_3 pigments and (b) yellowish-green Cr_2O_3 prepared by calcination. Reproduced with permission from ref. **[82]**, Copyright 2015, Elsevier.

Based on the Cr_2O_3 composition, a large variety of colour pigment systems have been developed with enhanced NIR reflectance [126, 127]. In order to obtain high NIR reflectance (70%−82%), small amounts of metal ions such as aluminium, [128, 129], titanium (Figure 15) [82], vanadium, cobalt or bismuth, are normally introduced into Cr_2O_3. Other reports have shown that doping with rare-earth elements (La, Pr) can lead to the production of environmental benign, high reflective (>85%) nano-pigments based on Cr_2O_3 [130].

Nonetheless, the chromatic properties of the final products are still undesirable, acquiring a dark green hue. Besides, rarely is reported the phenomenon or principle why doping with such elements changes the NIR reflectance of Cr_2O_3 host. [82].

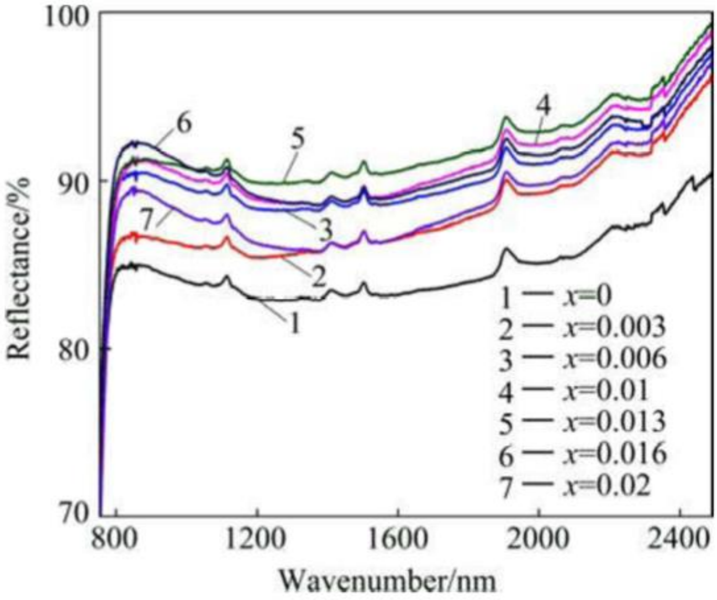

Figure 15: The reflectance spectra of $Cr_{2-x}Ti_xO_{3+\delta}$ pigments in the near infrared region. Reproduced with permission from ref. **[82]**, Copyright 2015, Elsevier.

However, usual Cr_2O_3 fabrication processes cause several problems, including the high cost of production and environmental pollution from dust containing hexavalent chromium (Cr-VI) which is highly toxic and a human carcinogenic. Recently, several procedures have been developed to prepare high quality green chromic oxide nanoparticles taking into account health safety and environmental protection [131]. Thus, there is an assertive motivation to develop coloured cool pigments through green processes and materials that are less harmful to the environment

Mixed metal oxides or complex inorganic coloured pigments

Mixed metal oxides or complex inorganic coloured pigments (CICPs) are the primary variety of inorganic NIR reflective pigments [42, 130], with a large number of patents being reported on these pigments. This shows their broad and significant interest, which comprises two main areas: (i) reduce heat build-up and (ii) visual camouflage. In particular, nano mixed metal oxides are attracting large interest for their potential as pigments, further offering exceptional resistance to acid, bases and organic solvents [132]. Nanocrystalline metal oxides possess some significant optical applications, which include anti-reflective properties in optical coatings, better photonic bandgap materials, and improved optical limiting materials for eye protection [42]. Examples of such compounds are listed in Table 3.

Among these systems, spinel-type oxides (Figure 16) with the general formula AB_2O_4 or, depending on the cations distribution on the crystalline structure, the inverse formula $B(AB)O_4$, are attracting large attention due to their thermal and chemical stability [45, 133, 134, 135].

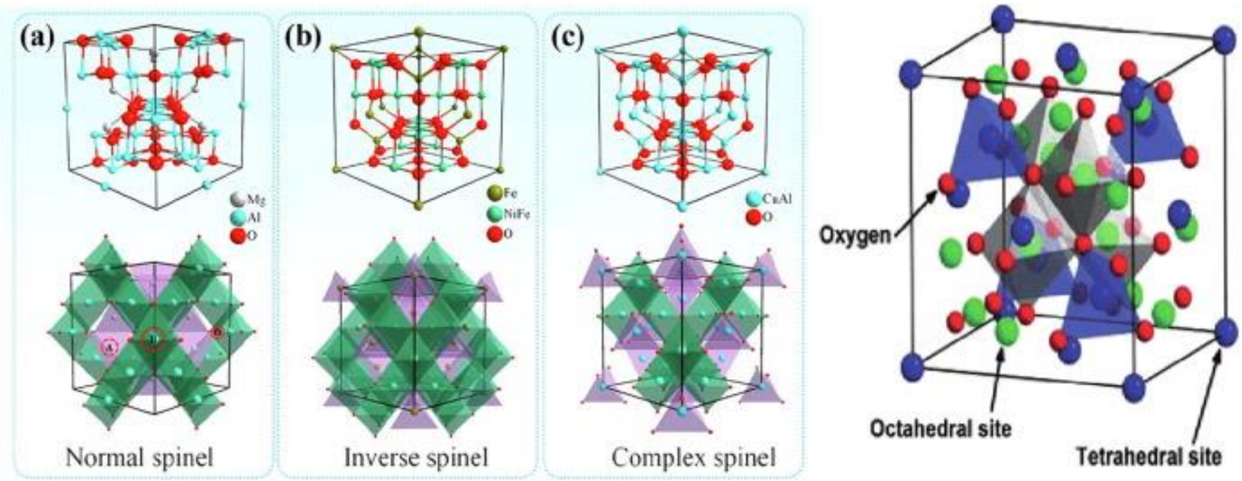

Figure 16: Examples of typical spinel structures. Reproduced with permission from ref. **[134]**, Copyright 2017, Elsevier.

Table 3: Examples of mixed metal oxides used as NIR reflecting pigments.

Compound	Crystal Structure	Colour	Particle Size	% NIR reflectance	Reference
$CoAl_2O_4$	Spinel	Intense Blue	Nanometres	51%-79%	[136, 137]
$ZnAl_2O_4$	Spinel	White	Nanometres	85%	[138]
$CoCr_2O_4$	Spinel	Blue Greenish	Nanometres	43%	[139]
$ZnCr_2O_4$	Spinel	Grey	Nanometres	~ 60%	[139]
$NiAl_2O_4$	Spinel	Blue Greenish	Nanometres	24%-53%	[140]
$NaZnPO_4$- based	Monoclinic	Intense Blue	Micrometres	32%-52%	[141]
$BiVO_4$	Monoclinic	Bright Yellow	Nanometres	~50%	[142]
$BiPO_4$	Monoclinic	White	Micrometres	80%	[143]
Ta^{5+} doped $BiVO_4$	Monoclinic	Bright Yellow	Nanometres	~85%	[144]
P^{5+} doped $BiVO_4$	Monoclinic	Bright Yellow	Nanometres	~90%	[144]
V^{5+} doped $BiPO_4$	Monoclinic	Bright Yellow	Micrometres	~90%	[143]
Mn and Mn/N doped- $ZnAl_2O_4$	Spinel-type	White to Brown	Nanometres	15%-50%	[138]
$Zn_{0.9}Co_{0.1}Al_2O_4$	Spinel-type	Intense Blue	Nanometres	63%	[145]
$Co_{0.25}Zn0_{.75}Cr_2O_4$	Spinel-type	Light Blue	Nanometres	52%	[139]
$Co_{0.5}Mg_{0.5}Al_2O_4$	Spinel-type	Blue	Nanometres	54,2%	[146]
$Co_{0.5}Mg_{0.5}Al_{2-x}Fe_xO_4$	Spinel-type	Dark Blue to Black	Nanometres	45.7%-54.2%	[146]
$CoCr_{0.5}Al_{1.5}O_4$	Spinel-type	Blue	Nanometres	43%	[139]

Ce and Fe doped $ZnAl_2O_4$	Spinel-type	Reddish yellow	Nanometres	65-86%	[147]

Cobalt aluminate ($CoAl_2O_4$) an important intense blue pigment, is an example of a compound with a normal spinel structure (Figure 17 (a)) [137] and is extensively used as a colouring agent in several applications due to its inherent properties (colour performance, chemical and thermal stability, high refractive index) [148] (Figure 17 (b)). Ali et al. [136] prepared, via a combustion method, nanopigment $CoAl_2O_4$ exhibiting a blue colour (in the visible region) and a high solar reflectance (~51.8%).

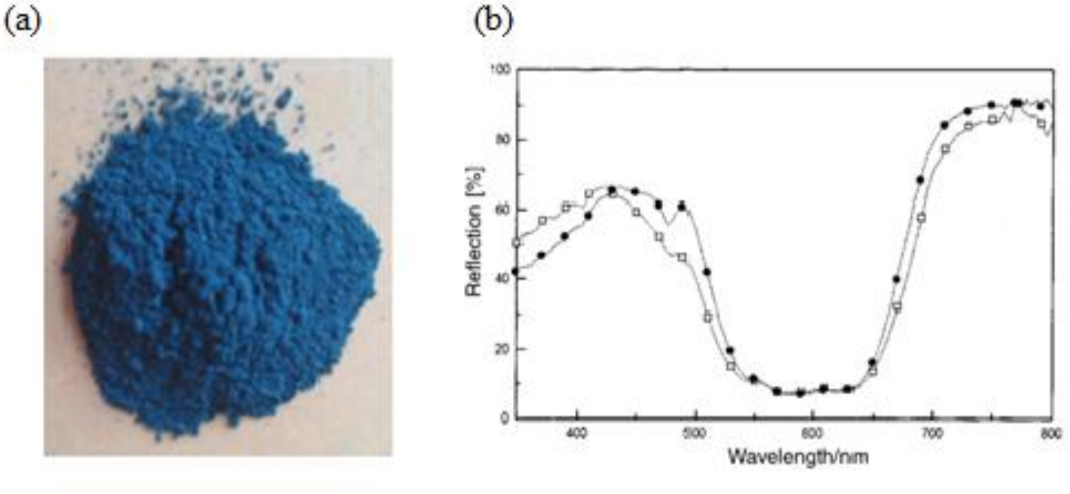

Figure 17: (a) Photograph of $CoAl_2O_4$ nanopigment obtained via self-propagation combustion method. Reproduced with permission from ref. **[137]**, Copyright 2017, Hindawi; (b) Diffuse reflectance of $CoAl_2O_4$ after 15 min at 600ºC (squares) and standard $CoAl_2O_4$ pigment (circles). Reproduced with permission from ref. **[148]**, Copyright 2000, Royal Society of Chemistry.

However, the manufacturing cost for cobalt-based product is high, since cobalt is scarce. Therefore, Bao et al. [146] modified $CoAl_2O_4$ with Mg^{2+} for Co^{2+} ions by a sol-gel route. On the other hand, due to the capability of spinel-type materials to accommodate different cations, the authors also doped with Fe^{3+} for Al^{3+} in $Co_{0.5}Mg_{0.5}Al_2O_4$ to obtain various colours and tonalities with a particle size in the 40-100 nm range (Figure 18 (a)). Through this study, it was possible to achieve a vast range of colours by incorporating in the $Co_{0.5}Mg_{0.5}Al_{2-x}Fe_xO_4$ matrix appropriated Fe^{3+} ions through bandgap engineering. Most prominently, these engineered pigments exhibited various colour tonalities in the visible range and high NIR solar reflectance (>43%) (Figure 18 (b) and (c)).

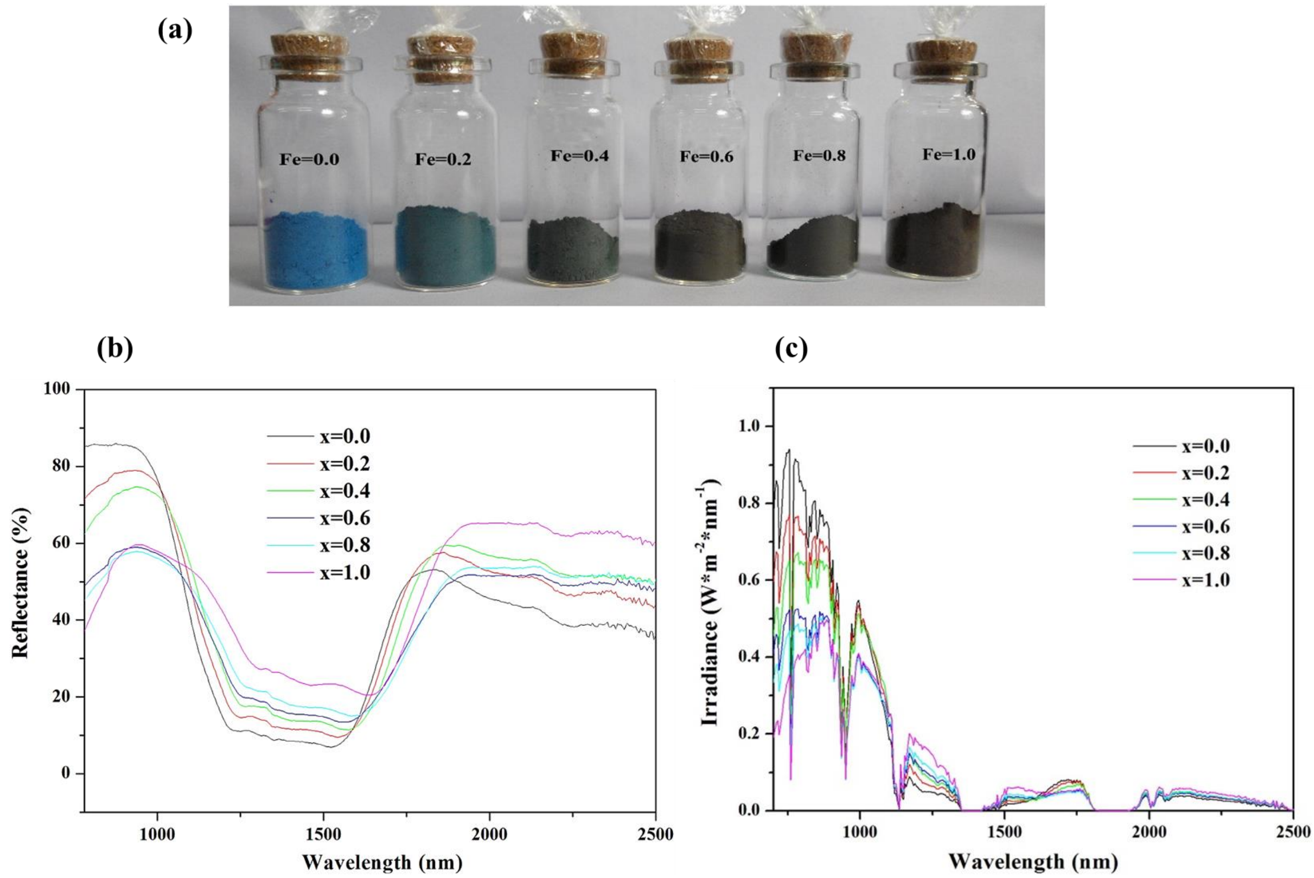

Figure 18: (a) Photographs of Co$_{0.5}$Mg$_{0.5}$Al$_{2-x}$Fe$_x$O$_4$ (x=0, 0.2, 0.4, 0.6, 0.8, and 1.0) powdered pigments; (b) NIR reflectance and (c) NIR irradiance of Co$_{0.5}$Mg$_{0.5}$Al$_{2-x}$Fe$_x$O$_4$ powdered samples. Reproduced with permission from ref **[146]**, Copyright 2016, Elsevier.

Another notable spinel-type pigment is Zinc Aluminate ($ZnAl_2O_4$). Such compound possesses a wide bandgap and appears as a white pigment in the visible region, which has potential on optical coating applications. $ZnAl_2O_4$ and $ZnAl_2O_4$-based pigments synthesised by different techniques are being widely reported because of the simple fabrication process and low cost. Yang et al. [138] fabricated, by a sol-gel synthesis, a variety of coloured pigments of Mn-doped $ZnAl_2O_4$ and Mn/N co-doped $ZnAl_2O_4$ (Figure 19 (a)). The particle range of such materials was around 27-31 nm with results of NIR solar reflectance (Figure 19 (b) and (c)) in the 85% (x=0.0) to 50% (x=0.5) range, indicating that co-doped samples are suitable candidates for cool materials.

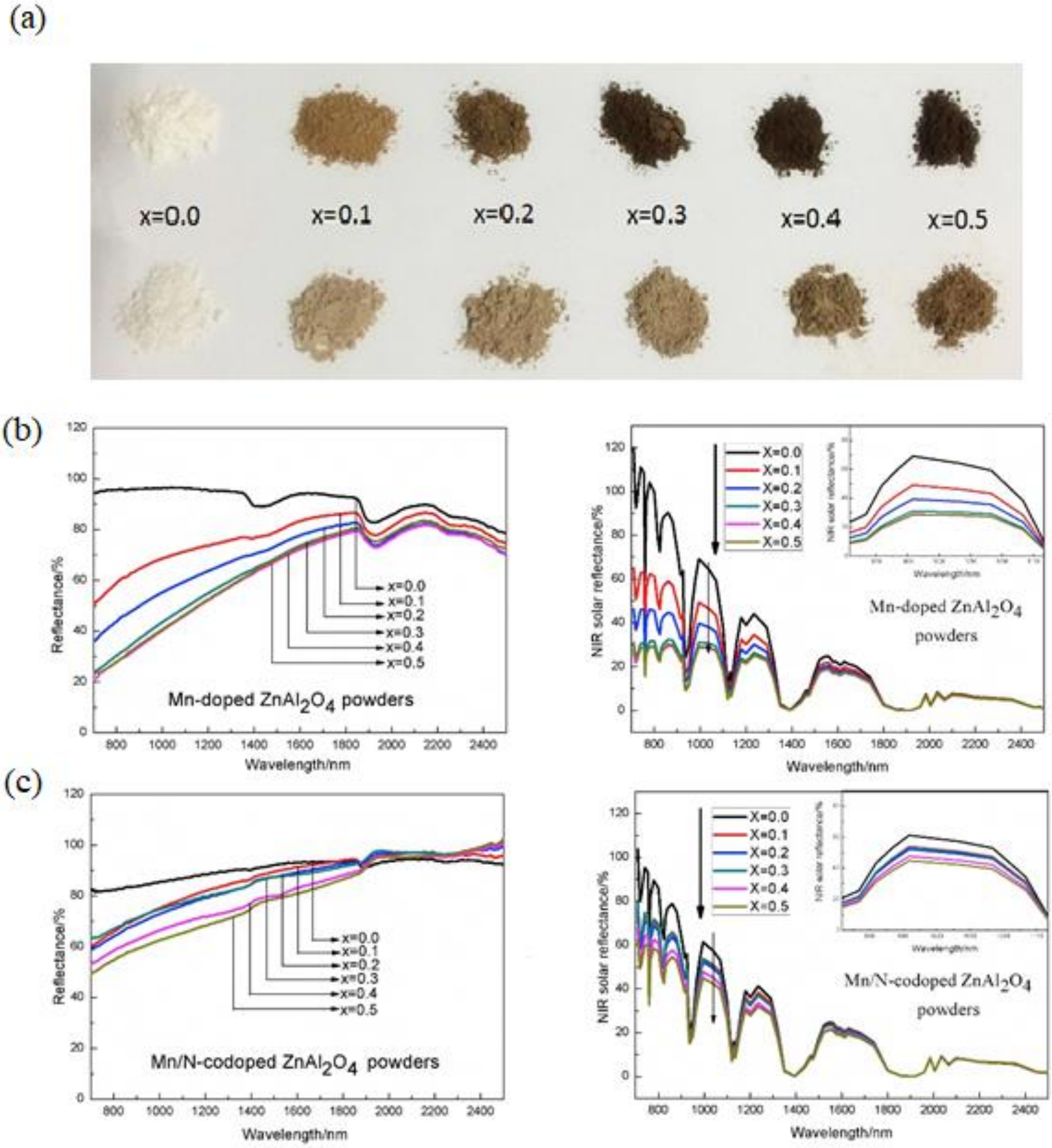

Figure 19: (a) Photographs of Mn-doped $ZnAl_2O_4$ and Mn/N co-doped $ZnAl_2O_4$ compounds (x = 0.0, 0.1, 0.2, 0.3, 0.4, and 0.5); NIR reflectance and NIR solar reflectance of (b) Mn-doped $ZnAl_2O_4$ powders and (c) Mn/N co-doped $ZnAl_2O_4$ powders. Reproduced with permission from ref. **[138]**, Copyright 2017, Elsevier.

An important commercially CICPs widely used as a pigment is cobalt chromite ($CoCr_2O_4$), which acts as an intense bluish-green hue [149]. Since chromium and cobalt are harmful and rare, it is mandatory to incorporate low cost and less toxic elements to $CoCr_2O_4$ thus, reducing environmental damages and fabrication costs. However, the optical properties of such pigment has not been often reported. Hedayati el al. [139] modified $CoCr_2O_4$ with Al^{3+} and Zn^{2+}, via a sol-gel route obtaining particles with sizes between 100 and 250 nm. Their results showed that the NIR solar reflectance was enhanced by increasing the Zn^{2+} and A^{l3+} concentrations (Figure 20), demonstrating their potential use as cool pigments.

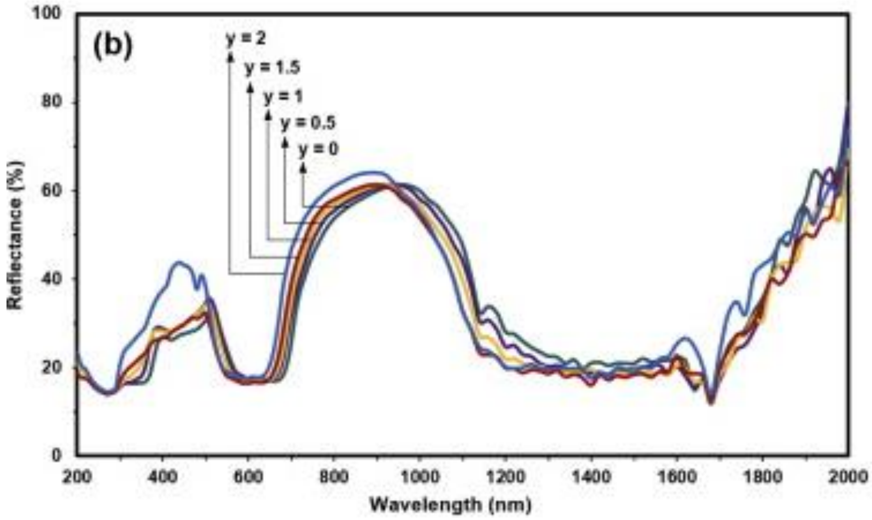

Figure 20: Diffuse reflectance spectra of $CoCr_{2-y}Al_yO_4$ (y = 0, 0.5, 1, 1.5 and 2) pigments. Reproduced with permission from ref. **[139]**, Copyright 2015, Elsevier.

ABO_3 type perovskites-based pigments

ABO_3 type oxides are extremely interesting, particularly due to their optoelectronic properties. Generally, these compounds can exhibit diverse crystal structures, such as perovskite and ilmenite [150], but the majority of ABO_3-type oxides crystallise in the simple mineral perovskite ($CaTiO_3$) structure or similar. These oxides exist in varied range of A and B cations [151, 152, 153] (with A larger than B). In ideal perovskite structures, A occupies the eight corner positions, while B (which can be 3d, 4d or 5d transition metal ions) occupies the body centre position. The O ions are located at the centres of the six faces (Figure 21) [154].

Several ABO_3 type complex or doped oxides can be used as near-infrared pigments (Table 4). For example, Meenakshi el al. [155] synthesised pale-yellow perovskite-like bismuth titanate ($Bi_4Ti_3O_{12}$) using a simple hydrothermal method. Their results (Figure 22) showed that such nanopigment (around 250-500 nm) acts as a better near-infrared reflective pigment and has superior cooling property than the TiO_2 conventional white pigment.

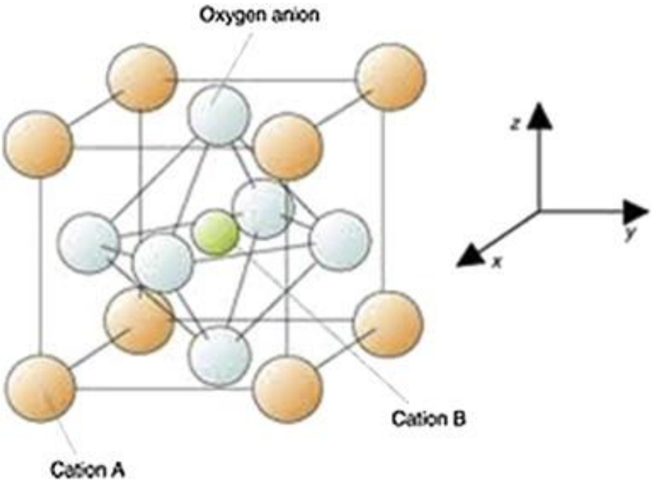

Figure 21: An example of a typical ABO_3 perovskite-type unit-cell structure. Reproduced with permission from ref. **[154]**, Copyright 2014, Elsevier.

Table 4: Examples of ABO_3 type based oxides used as NIR reflecting pigments.

Compound	Crystal Structure	Colour	Particle Size	% NIR reflectance	Reference
$MgTiO_3$	Ilmenite	White	Nanometres	60%-75%	[156, 157]
$NiTiO_3$	Ilmenite	Yellow	Nanometres	60%-80%	[158, 159]
$CoTiO_3$	Ilmenite	Green	Nanometres	~ 50%	[160]
$ZnTiO_3$	Perovskite	White	Nanometres	95%	[116]
$SrTiO_3$	Perovskite	White to Grey	Nanometres	85%	[161, 162]
$CaTiO_3$	Perovskite	Yellow	Micrometres	90%	[163]
$YMnO_3$	Perovskite	Blue-Greenish	Nanometres	53.4%	[164, 165]
$BiFeO_3$	Perovskite	Dark Brown	Nanometres	53%	[63]
$Bi_4Ti_3O_{12}$	Perovskite	Pale-yellow	Nanometres	95%	[155]
$CaCu_3Ti_4O_{12}$	Perovskite	Pale-Brown	Nanometres	57%	[166]
$Ca_2Mn_{0.85}Ti_{0.15}O_4$	Perovskite-like	Black	Micrometres	66.2%	[167]
$SrSn_{0.075}Cr_{0.025}O_{3-\delta}$	Perovskite-like	Pink	Nanometres	~ 60%	[168]
$Bi_{0.6}La_{0.4}O3$	Perovskite-like	Reddish-Brown	Nanometres	72%	[63]
Cr^{3+} doped $CaTiO_3$	Perovskite-like	Dark Brown	Nanometres	~ 80%	[163]
Cr^{3+} doped $BaTiO_3$	Perovskite-like	Yellow greenish	Nanometres	68%-79%	[169]
Y (In,Mn) O_3- based	Perovskite-like	Ochre to deep blue	Nanometres	63%-90%	[170, 171, 172]
Fe^{3+} doped $YMnO_3$	Perovskite-like	Nearly black	Micrometres	~80%	[173]
Mg^{2+} doped $CaCu_3Ti_4O_{12}$	Perovskite-like	Light Brown	Nanometres	~62%	[166]

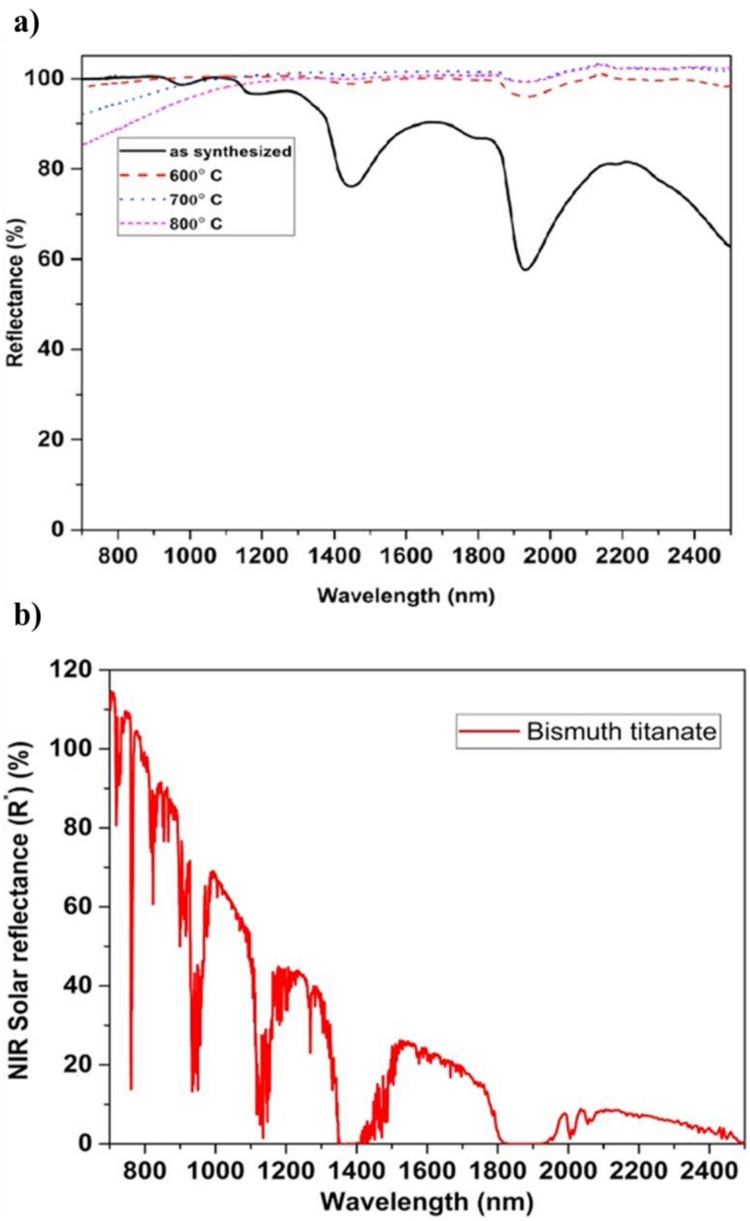

Figure 22: (a) Reflectance spectra of $Bi_4Ti_3O_{12}$ (BTO) for different calcination temperatures. (b) BTO NIR solar reflectance. Reproduced with permission from ref. **[155]**, Copyright 2018, Elsevier.

Another promising candidate to be used as a cool pigment is zinc titanate. Since there is restricted literature about the cooling effects of $ZnTiO_3$, Lv et al. [116] studied the possibility to synthesise, by a simple solid-state technique, such pigment, which turns out to be a challenge due to the delicate phase equilibria of the ZnO–TiO_2 system. They successfully produced hexagonal $ZnTiO_3$, with a distribution range between 100 nm and 1 µm, which has an optical bandgap as high as 3.75eV and has superior near-infrared reflectance (about 95%) and cooling properties when compared to conventional white pigments (Figure 23). In the interest of avoiding degradation of organic binders of paint by high-energy UV light, there is a blue shift of the absorption edge from 380 (ZnO) to 320 nm, overcoming the challenge of using white pigment such as TiO2 and ZnO.

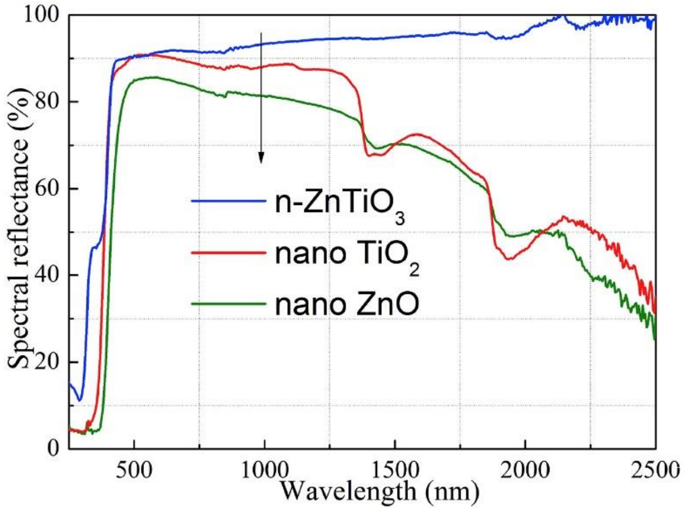

Figure 23: Diffuse reflectance spectra of nanosized ZnO, nanosized TiO_2 and nanosized $ZnTiO_3$ samples. Reproduced with permission from ref. **[116]**, Copyright 2019, Elsevier.

Although light colours are important in the pigments industry, there is a necessity to expand the range of colours to darker ones. As we have seen, the interest is to introduce pigments that possess colour due to visible light absorption while at the same time providing a cooling effect by reflecting NIR. To increase the colour range, Yuan et al. [63] doped perovskite $BiFeO_3$ with rare-earth elements (La^{3+}) to adjust the colour performance by controlling energy gaps and displacement phenomenon in the valence and conduction bands. Interestingly, although the $BiFeO_3$ NIR reflectance can be enhanced to around 72% by doping with La^{3+}, the visible colour becomes lighter (Figure 24).

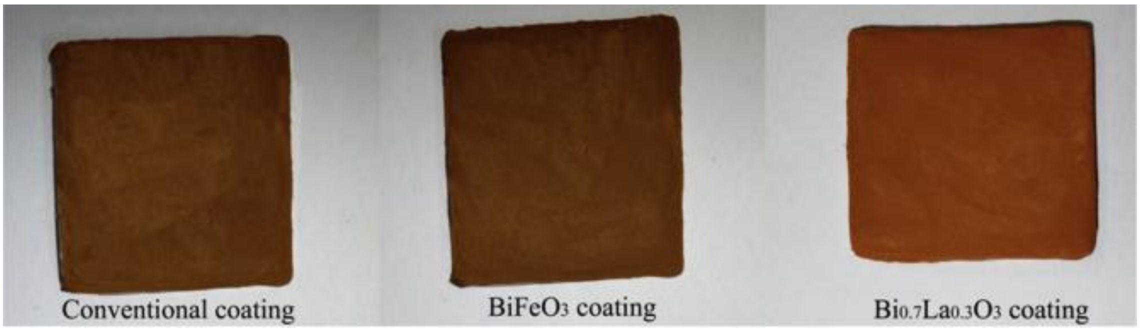

Figure 24: Concrete cement substrates coated with different pigments. Reproduced with permission from ref. **[63]**, Copyright 2018, Elsevier.

Former reports on Cr-doped perovskites showed that these pigments have darker tones and a high absorption in the visible region. As no NIR reflectance results had been presented, Zou et al. [163] synthesised such pigments by the calcination of $CaCO_3$ and the Cr-dopant at the surface of TiO_2 particles and achieved dark colours with only 1% Cr doped $CaTiO_3$ having a size distribution between 0.5 to 2µm, with around 80% near-infrared reflectance (Figure 25).

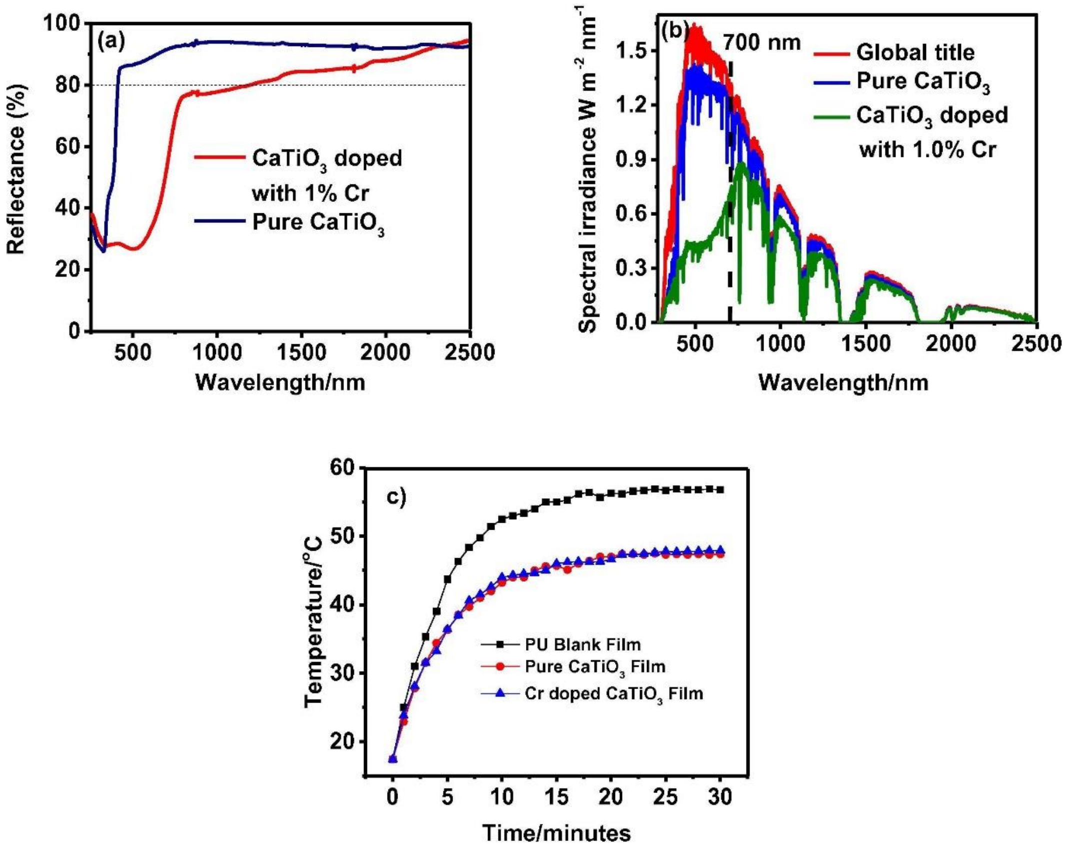

Figure 25: (a) Graphs of the UV–VIS-NIR diffuse and (b) solar irradiance reflection curves. (c) Variation of the surface temperatures of ceramic tiles of undoped and 1% Cr doped $CaTiO_3$ pigments. Reproduced with permission from ref. **[163]**, Copyright 2019, Elsevier.

Other attracting pigments are doped compounds [($In_{2x-1}Cu_xTi_x$), ($In_{1-x}Fe_x$), ($In_{1-x}Mn_x$) and ($In_{1-x-2y}Mn_xTi_yZn_y$)] based on $YInO_3$ structure with intense bright colours. They have higher stability, improved NIR reflectance and they are environmentally friendly. Li et al. [170] were able to build a multi-coloured pattern through rational design by a simple solid-state method based on the $YInO_3$ perovskite structure (Figure 26 (a)). In addition to their bright colour, these pigments were able to reflect NIR. For instance, the purple samples reflect around 90% of NIR radiation (Figure 26 (b)) [170], this led to the development of low-cost, eco-friendly and extremely stable inorganic ABO_3 type oxide near-infrared reflecting pigments.

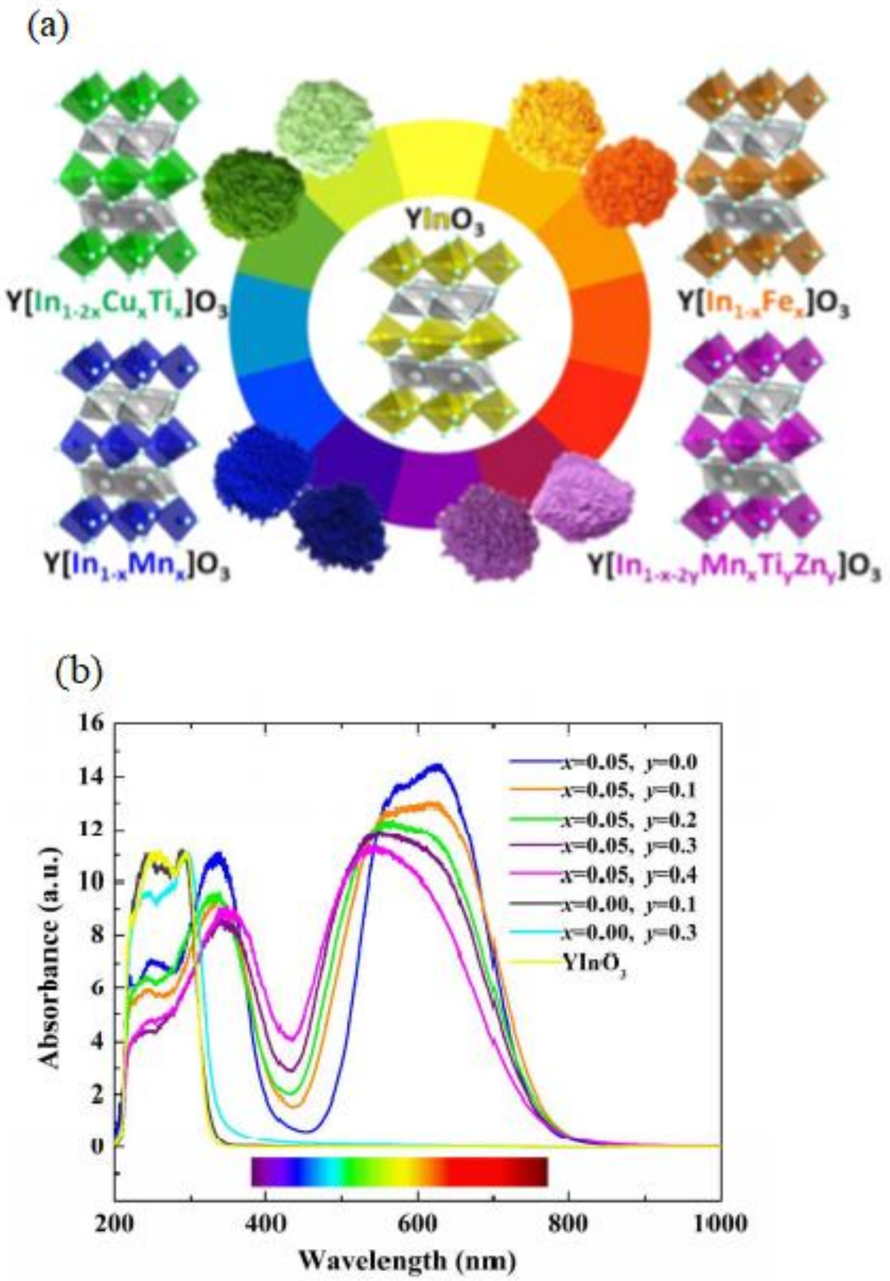

Figure 26: (a) Range of colours created by doping YInO$_3$;(b) diffuse reflectance curve of purple pigments Y[In$_{1-x-}$2yMn$_x$Ti$_y$Zn$_y$] O$_3$ (x = 0.05, y = 0.1~0.4). The blue YIn$_{0.95}$Mn$_{0.05}$O$_3$, YInO$_3$ and compositions without Mn chromophore (x = 0.00, y = 0.1 and 0.3) are also shown. Reproduced with permission from ref. **[170]**, Copyright 2016, American Chemical Society Publications.

Pigments based on rare-earth elements

Traditional inorganic pigments generally contain heavy metals, which cannot satisfy society needs for environmental protection and energy-saving. As a result, many researchers have employed rare earth metals to modify pigments to improve their NIR reflectivity and colour. The industrial utilisation of rare-earth elements has been increasing quickly because of their non-toxic nature, stability and intense shades.

Therefore, a huge variety of NIR-reflecting materials based on rare-earths are being studied as substitutes for conventional cool pigments, favouring the use of lanthanide oxides [174]. The most representative pigments based on rare-earth element are listed in Table 5.

Transition metal ions are typically integrated as chromophores into $A_2B_2O_7$ stoichiometry materials to obtain coloured materials [175]. Because of the toxicity of some of these ions (Cr, Ni, Co …), the use of different, harmless elements will be decisive in the future. With their ideal properties, lanthanides oxides are perfect candidates to substitute the harmful ions in the $A_2B_2O_7$ structure towards environmentally friendly materials [176, 177, 174].

Table 5: Pigments based on rare-earth elements used as NIR reflecting materials.

Compound	Crystal Structure	Colour	Particle Size	% NIR reflectance	Reference
CeO_2	Face-cantered cubic	Pale yellow white	Nanometres	~80%	[176, 178]
$Y_2Cu_2O_5$	Orthorhombic	Green Blue	Nanometres	~40%	[179]
Y_2BaCuO_5	Orthorhombic	Green	Nanometres	61%	[180]
$Bi_2Ce_2O_7$	Monoclinic	Yellow	Micrometres	~ 90%	[181]
$LaYO_3$	Fluorite-type	White	Nanometres	92%	[182]
$LaFeO_3$	Orthorhombic	Dark Orange	Nanometres	65.4%	[183]
$Y_2Ce_2O_7$	Cubic fluorite	Ivory White	Nanometres	~90%	[184, 185]
$La_2Ce_2O_7$	Fluorite-type	White	Nanometres	95.95%	[186]
$Sm_2Ce_2O_7$	Cubic fluorite	Yellow cream	Micrometres	~80%	[187]
$GdCeO_{3.5}$	Cubic fluorite	Yellow	Nanometres	91%	[188]
$Bi_{2-x}Y_xCe_2O_7$	Cubic fluorite	Yellow	Micrometres	93%	[176]
$Bi_2Ce_{2-x}Tb_xO_7$	Cubic fluorite	Red	Micrometres	88%	[176]
Fe^{3+} doped $Y_2Ce_2O_7$	Cubic fluorite	Light Yellow	Nanometres	~80%	[184]
Mo^{6+} doped $Y_2Ce_2O_7$	Cubic fluorite	Yellow	Micrometres	80.5%	[185]
Pr^{4+} doped $Y_2Ce_2O_7$	Cubic fluorite	Red	Micrometres	57.5%	[185]
Tb^{4+} doped $Y_2Ce_2O_7$	Cubic C-type	Red	Micrometres	55.1%-86.9%	[189]
W^{6+}/Fe^{3+} doped $La_2Ce_2O_7$	Fluorite-type	Yellow to Orange	Nanometres	83.27%-89.55%	[190]
Tb^{4+}/ Pr4+ doped $La_2Ce_2O_7$	Fluorite-type	Soft Orange to Dark Orange	Nanometres	~90%	[186]
Bi^{3+} doped $LaYO_3$	Cubic bixbyite type	Light Yellow to Bright Yellow	Nanometres	~91%	[182]
Bi^{3+}/Tb^{4+} co-doped $LaYO_3$	Cubic bixbyite type	Soft Orange to Dark Orange	Nanometres	84.13%-92.41%	[182]
Al^{3+} doped $LaFeO_3$	Orthorhombic	Orange to Yellow	Nanometres	53.7%-56.7%	[183]
Bi_3YO_6 doped with Fe_2O_3	Fluorite-type	Bright yellow to ochre red	Nanometres	88.64-99.58%	[191]

V doped $LaPO_4$	Monoclinic	White to greyish yellow	Nanometres	62.14-87.86%	[192]
Fe doped $Pr_2Zr_2O_7$	Fluorite-type with pyrochlore	Reddish orange	Micrometres	~70%	[193]

Amongst the lanthanide oxides, materials based on Cerium oxide (CeO_2) are being studied for cool pigment applications due to their opacity and low toxicity [194]. $Bi_2Ce_2O_7$ has a low bandgap of 2.3 eV that allows its easy fine-tuning to produce various colours [181]. To analyse the effect of substitutions on the structure and colour characteristics of $Bi_2Ce_2O_7$, Raj et al. [176] synthesized a cerium oxide-based material with Bi^{3+} being substituted by yttrium and Ce^{4+} substituted for terbium, by a solid-state path to produce $Bi_{2-x}Y_xCe_2O_7$ and $Bi_2Ce_{2-x}Tb_xO_7$ ($x = 0.25, 0.50, 0, 75, 1.0, 1.25$ and 1.50) materials. With such substitution, it was possible to achieve novel series of red and yellow, low toxicity cool pigments with high NIR reflectance at a particle size of 1-3 µm (Figure 27 (a)). As shown in Figure 27 (b), the $Bi_{2-x}Y_xCe_2O_7$ and $Bi_2Ce_{2-x}Tb_xO_7$ spectra display an extraordinary reflectance in the range of 70–88% and 90–94%for the red and yellow pigments making them suitable to be used as NIR reflecting coatings [176].

Due to the excellent chemical and thermal stabilities of the rare-earth oxides, a lanthanum and cerium mixed oxide ($La_2Ce_2O_7$), with low thermal conductivity has been used as a turbine blade coating [186]. Huang et al. [186] then focused their study on exploring the influence of doping $La_2Ce_2O_7$ with Pr^{4+} and Tb^{4+} on the colour shade and NIR reflectance. A series of new pigments with the formula $La_2Ce_{2-x}M_xO_7$ (M= Pr, Tb) were fabricated via a sol-gel route with a particle size around 500 nm. Doping Tb^{4+} for Ce^{4+} in $La_2Ce_2O_7$ caused a decrease of the bandgap from 3.34 to 2.24 eV with increasing dopant (up to 0.5%). Hence, the colours of the fabricated pigments were varied from yellow to dark orange, an evolution analogous to that of Pr-doped pigments (Figure 28 (a)). To study the thermal properties of the synthesised pigments, $La_2Ce_{2-x}Pr_xO_7$ and $La_2Ce_{2-x}Tb_xO_7$ pigments were chosen as coating of a metal sheet of roof surface. The results showed that these coatings significantly improve the NIR and solar reflectances, confirming that the synthesised materials possess potential as new cool pigments (Figure 28 (b)) [186].

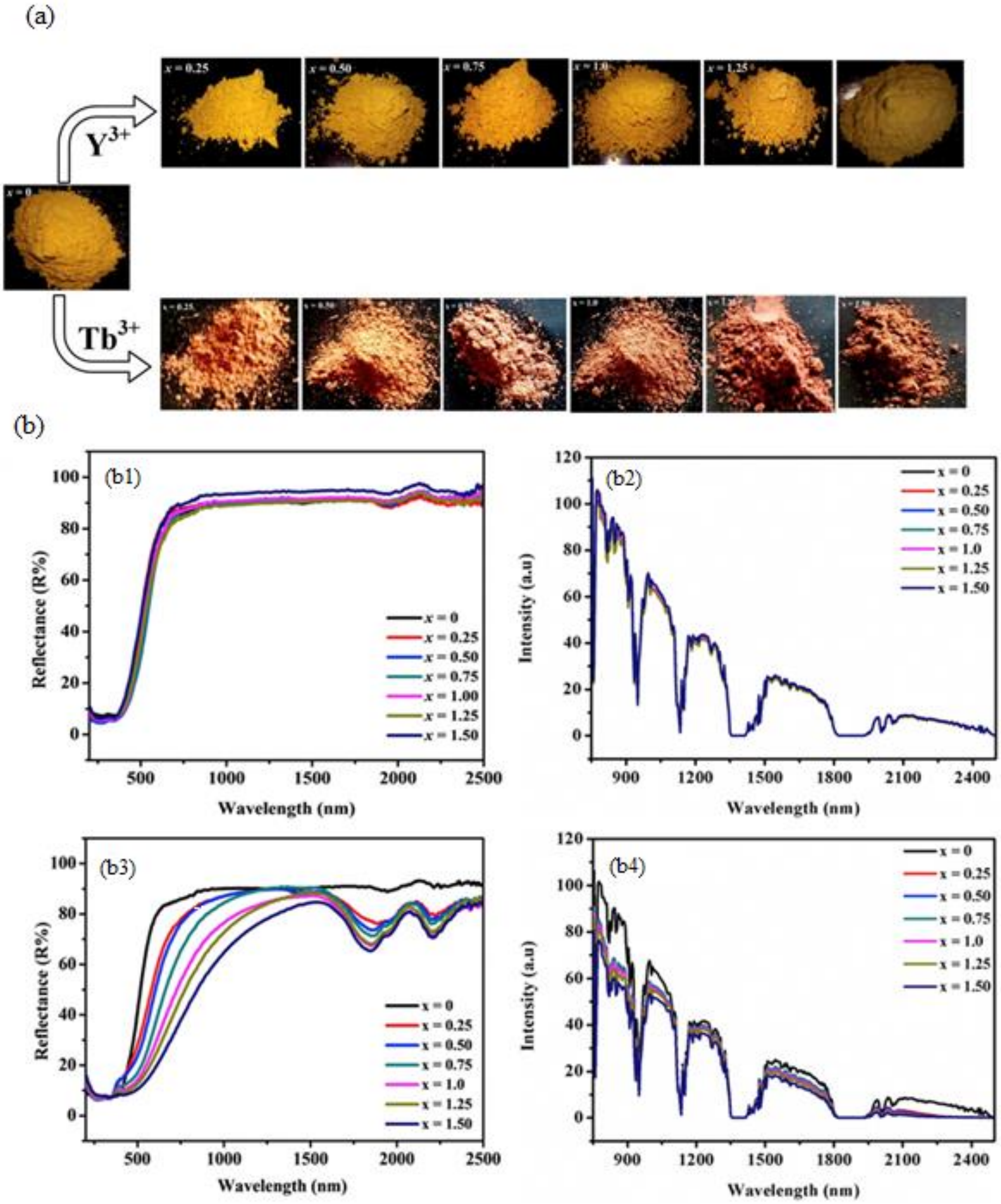

Figure 27: (a) Photographs of $Bi_{2-x}Y_xCe_2O_7$ and $Bi_2Ce_{2-x}Tb_xO_7$ (x = 0, 0.25, 0.5, 0.75, 1.0, 1.25 and 1.50) pigments. (b) NIR reflectance spectra of (b1) $Bi_{2-x}Y_xCe_2O_7$ and (b2) $Bi_2Ce_{2-x}Tb_xO_7$ (x = 0, 0.25, 0.50, 0.75, 1.0, 1.25 and 1.50) pigments and solar NIR reflectance spectra of (b3) $Bi_{2-x}Y_xCe_2O_7$ and (b4) $Bi_2Ce_{2-x}Tb_xO_7$ (x = 0, 0.25, 0.50, 0.75, 1.0, 1.25 and 1.50) pigments. Reproduced with permission from ref. **[176]**, Copyright 2019, Elsevier.

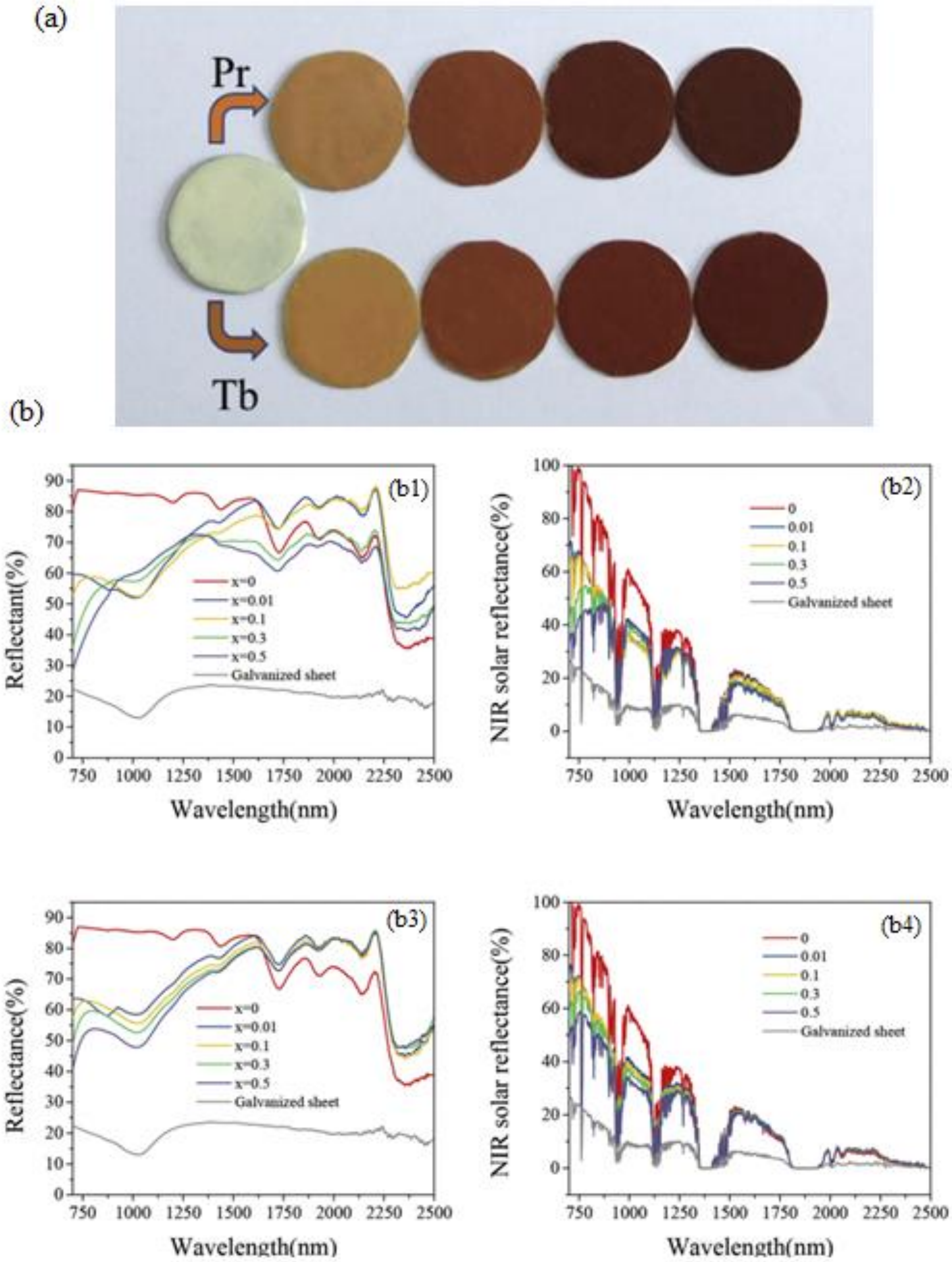

Figure 28: (a) Photograph of the coatings coloured with $La_2Ce_{2-x}Pr_xO_7$ and $La_2Ce_{2-x}Tb_xO_7$ (x= 0, 0.01, 0.1, 0.3, 0.5) pigments. (b) NIR reflectance and solar reflectance curves of the coloured coatings with (b1, b2) $La_2Ce_{2-x}Pr_xO_7$ and (b3, b4) $La_2Ce_{2-x}Tb_xO_7$ (x=0, 0.01, 0.1, 0.3, 0.5). Reproduced with permission from ref. **[186]**, Copyright 2017, Elsevier.

Cheng et al. [190] developed, also using a sol-gel route, a series of non-toxic yellow-orange NIR reflecting pigments based on $La_2Ce_2O_7$. The W^{6+} and Fe^{3+} co-doping contributed to enhancing the solar reflectance since the samples possessed high NIR reflectance (Figure 29 (a)) to test the suitability of the $La_2Ce_{1.7}W_{0.15}Fe_{0.15}O_{7+\delta}$ pigment, a galvanised sheet was used, demonstrating an increase of the NIR solar reflectance from 19% to 71% with the application of the coating (Figure 29 (b)). Thus, the synthesised pigments can be considered potential candidates for energy-saving coatings in building façades to reduce the interior temperature [190].

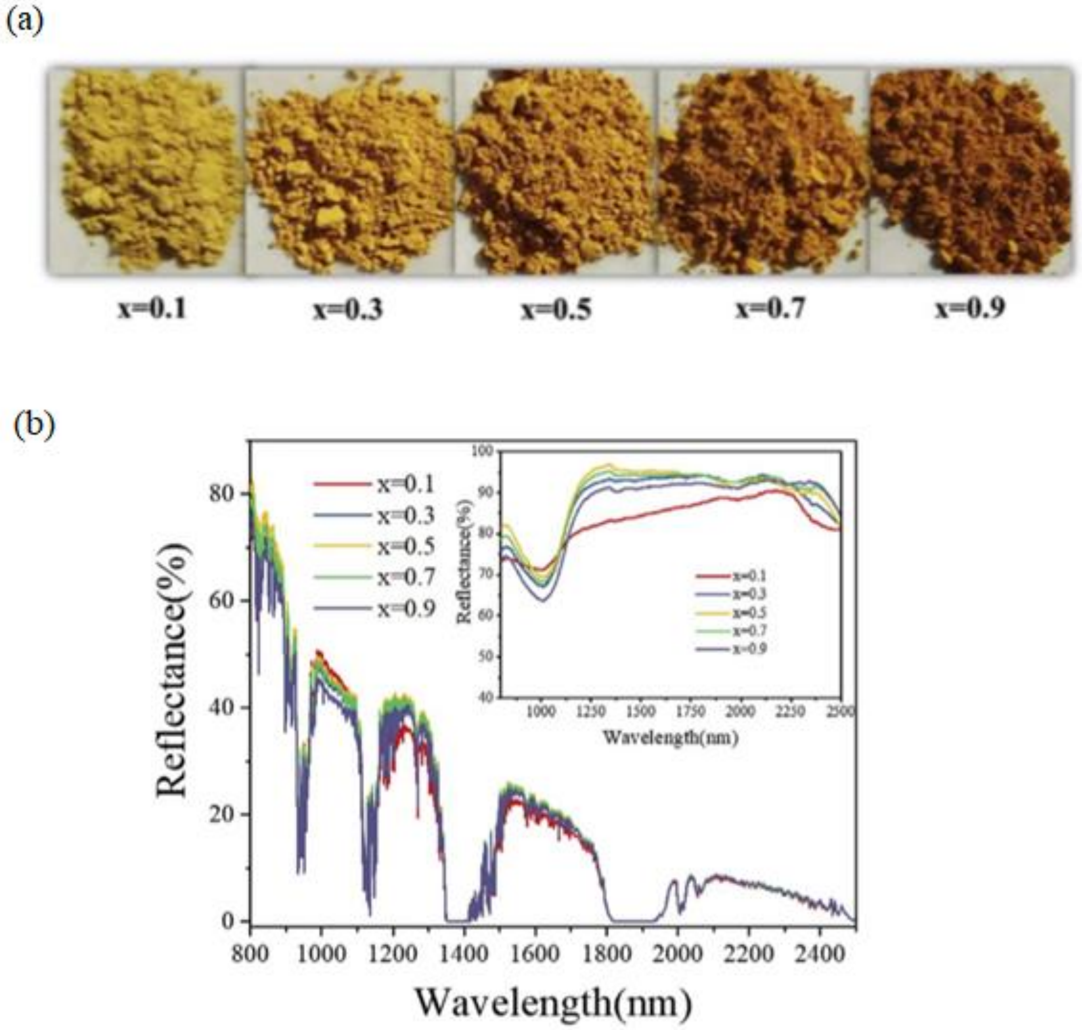

Figure 29: (a) Photographs and (b) NIR solar reflectance spectra of $La_2Ce_{2-x}W_{0.5x}Fe_{0.5x}O_{7+\delta}$ (x=0.1, 0.3, 0.5, 0.7, 0.9) pigments. Reproduced with permission from ref. **[190]**, Copyright 2018, Elsevier.

$Y_2Ce_2O_7$, with a bandgap of 3.11 eV, was recently synthesised from a CeO_2 based host lattice with substituted terbium for Ce^{4+}. Raj et al. [189] successfully prepared, by a typical solid-state approach, a novel series of red pigments based on $Y_2Ce_{2-x}Tb_xO_7$. These powder samples with a size of approximately 100 nm demonstrated a very high solar reflectance after tested onto various building substrates (Figure 30).

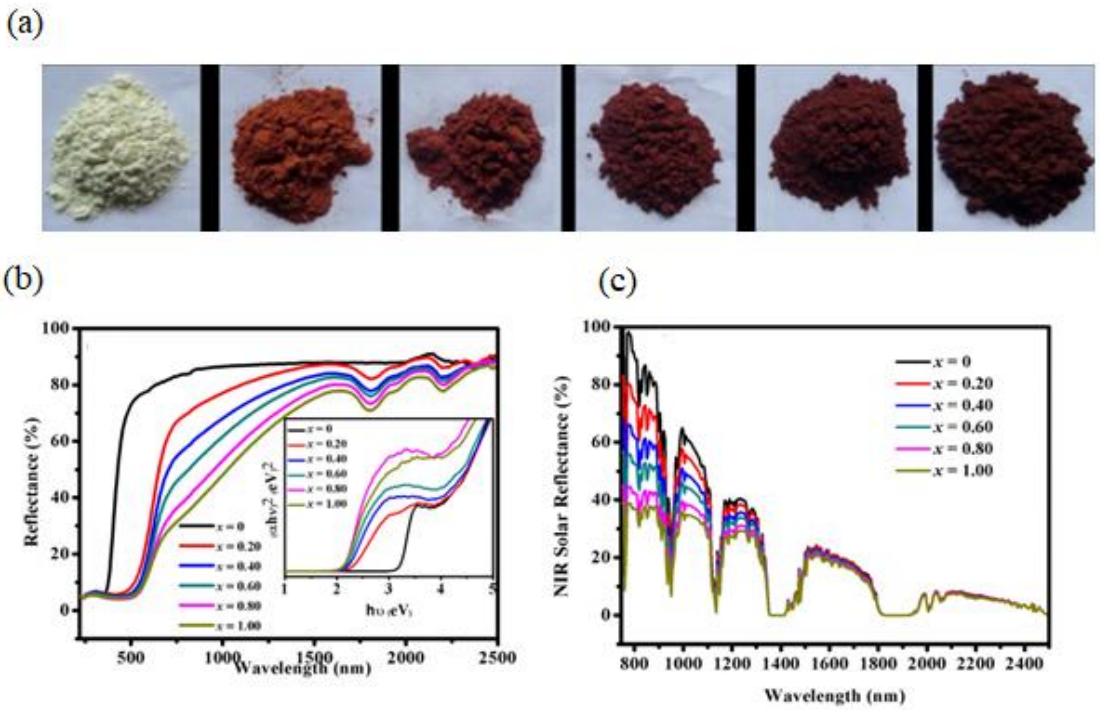

Figure 30: (a) Photographs of $Y_2Ce_{2-x}Tb_xO_7$ (x=0, 0.2, 0.4, 0.6, 0.8, and 1.0) red pigments. (b) Reflectance spectra and (c) solar reflectance of $Y_2Ce_{2-x}Tb_xO_7$ (x=0, 0.2, 0.4, 0.6, 0.8, and 1.0) red pigments (Tauc plots in the inset). Reproduced with permission from ref. **[189]**, Copyright 2015, Elsevier.

A similar research was conducted by Vishnu et al. [185] that developed a new range of environmentally friendly NIR reflecting inorganic pigments (with a particle size of around 10 µm) based on yttrium cerate doped with Mo^{6+} and Pr^{4+} metal ions using a solid-state reaction. The Mo^{6+}-doped pigments denoted an intense yellow tone with a high NIR solar reflectance in the 700-2500 nm range. On the other hand, the praseodymium doped pigments exhibited a variety of colours, from red to dark brown. These results confirm that, by bandgap engineering, it is possible to achieve various colour shades in the visible region while simultaneously achieving high NIR solar reflectance (80.5% for yellow and 57.5% for reddish-brown).

Although rare-metal-based pigments are being studied to potentially replace traditional pigments because of their low toxicity and high reflectivity, the higher cost of some rare-earth metals is a key liming factor still preventing their widespread use as pigments [195].

Core-Shell Structures

A good approach for producing high-performance multifunctional materials is the core-shell structures, with an outer shell encapsulating the inner core. Such structures not only enhance the physical-chemical properties of pigments, but also successfully prevent the inner core from interacting with the environment [196]. Compared with pigments mixtures, core-shell structures can enhance the darkness of colours and the solar reflectivity [195].

The materials morphology and structure are crucial factors for the application of core-shell particles (Table 6). As noticed before, the morphology and particle size affect the optical properties of cool pigments [197]. When mixed with TiO_2 pigments that have higher NIR reflectance, the NIR reflectance of colour materials is also improved. Nevertheless, the colour intensity is also reduced. This clearly shows that there is still the need to enhance the NIR reflectance of colour pigments while at the same time improving their colour intensity [196, 197].

Table 6: Examples of core-shell structures used as NIR reflecting pigments. (HGM: Hollow Glass Microspheres).

Compound	Colour	Particle Size	% NIR reflectance	Reference
TiO_2@CuO	Grey to Dark Grey	Nanometres	61-96.1%	[195]
$NiTiO_3$@TiO_2	Bright Yellow	Nanometres	~70%	[196]
TiO_2@$CoTiO_3$	Green	Nanometres	~60%	[160]
TiO_2@$NiTiO_3$	Yellow	Nanometres	~70%	[198]
$(Fe, Cr)_2O_3$@TiO_2	Brown	Nanometres	57.8%	[199]
Fe_2O_3@SiO_2@TiO_2	Reddish Brown	Nanometres	~ 68%	[200]
Fe_2O_3@SiO_2	Brown	Nanometres	~ 45%	[201]
(HGMs)@ZnS_xSe_{1-x}	Light Yellow	Micrometres	~85%	[202]
(HGMs)@ZnS_xSe_{1-x}: Cu/In	Bright Red	Micrometres	~75%	[202]
(HGMs)@ZnO	White	Nanometres	~95.7%.	[203]
(HGM)@$BiOCl_{1-x}I_x$	Yellow to Light Orange	Micrometres	92.6-94.7%	[204]
Mica-titania	White	Nanometres	~97.4%	[205]
$BiFe_{1-x}Al_xO_3$@mica-titania	Brown to Orange	Nanometres	63.5-73.6%	[206]

Yao et al. [195] prepared composite inorganic pigments with TiO_2@CuO core-shell structure (Figure 31 (a)) by a co-precipitation method, which had a dark colour and high NIR reflectivity. Copper oxide is a common black metal oxide used in the industry and can exhibit NIR reflectance with dark colours in a certain composition range (Figure 31 (b) to (f)). When used as a blending pigment, rutile TiO_2 further enhances the NIR reflectivity (from around 61% to 96%) (Figure 31 (g) e (h)). Therefore, this blended pigment might be a promising candidate for inexpensive, environmentally friendly cool pigments [195].

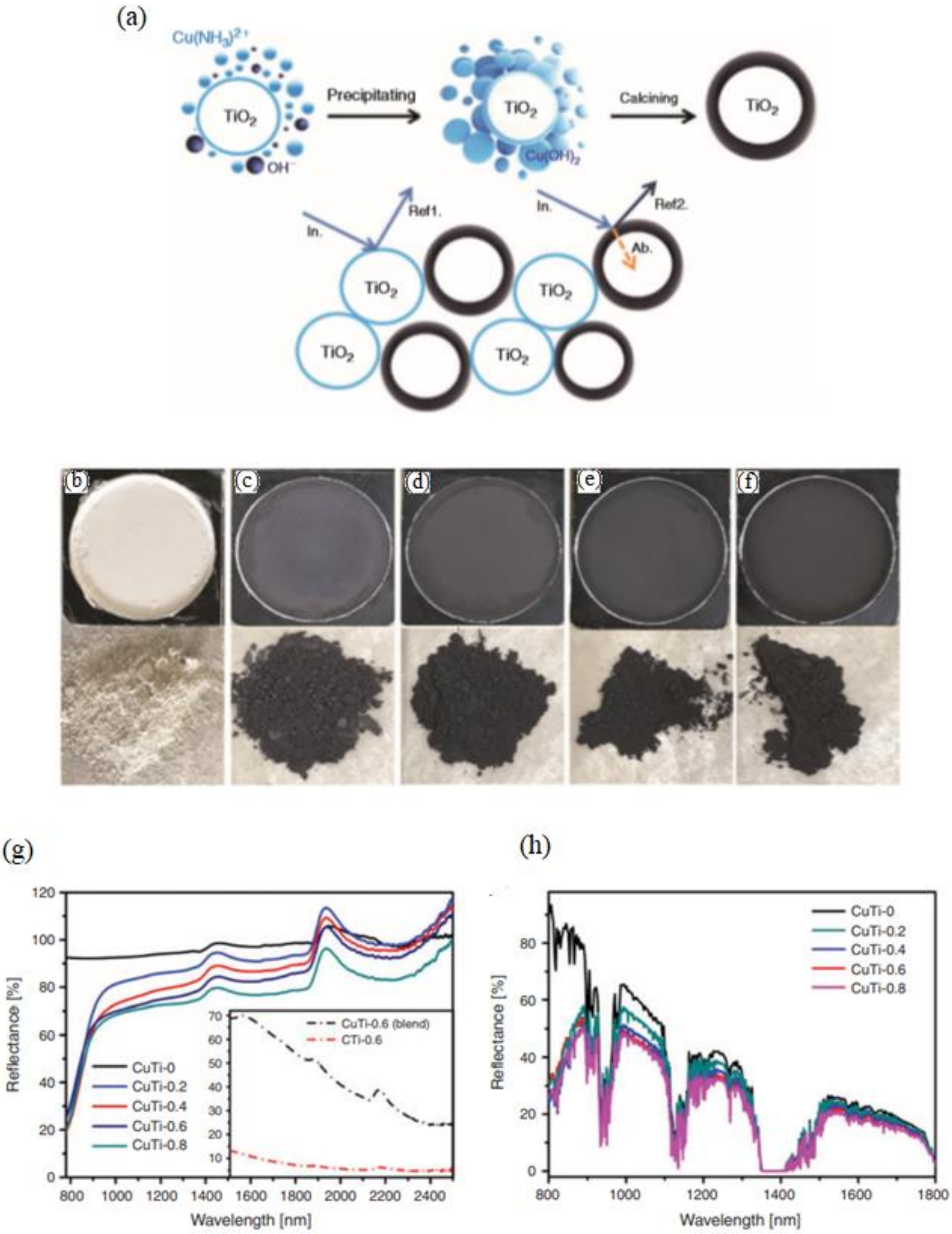

Figure 31: (a) Scheme of the formation of CuO@TiO$_2$ particles and corresponding light/pigment interaction. Photographs of composite pigments: (b) Cu@Ti 0%, (c) Cu@Ti 0.2%, (d) Cu@Ti 0.4%, (e) Cu@Ti 0.6% (f) and Cu@Ti 0.8%; (g) NIR reflectance and (h) NIR solar reflectance curves of Cu@Ti composite pigments. Reproduced with permission from ref. **[195]**, Copyright 2018, CSIRO Publishing.

Nickel titanate (NiTiO$_3$), a standard yellow pigment, also displays enhanced solar reflectance [158, 159]. Incorporating NiTiO$_3$ in TiO$_2$ structure can help to further improve their NIR reflectance. He et al. [196] produced by a sol-gel route core-shell NiTiO$_3$@TiO$_2$ yellow particles, with around 850 nm diameters.

Furthermore, a reduced amount of $NiTiO_3$ particles would result in the decrease of the NIR absorption, while the incorporation of rutile TiO_2 (with a superior NIR reflectance) stimulates the NIR reflection of the core-shell structure. Nevertheless, the $NiTiO_3$ and TiO_2 mixture was able to reflect light and prevent the $NiTiO_3$ from absorbing part of the visible light [196]. Consequently, the mixed pigment exhibits a faded hue. Thus, the unique core-shell structure of the $NiTiO_3$@TiO_2 pigment showed improved NIR reflectance and bright yellow colours.

Niaraki et al. [199] prepared two different NIR reflecting nanocomposites based on Fe, Cr and Ti oxides. The first consisted on $(Fe,Cr)_2O_3$@TiO_2 core-shell particles, using mixing and co-precipitation methods; the second was a physical mixture of Fe-Cr-Ti oxides materials. The effects of the thermal treatment (500 °C and 1000 °C) and of the preparation method were investigated. In both cases, it was noticed that the average particle sizes were ≈30 nm, and that, by increasing the treatment temperature to 1000ºC, the NIR reflectance increased for both cases (core-shell and mixture) (Figure 32 (a) and (b)). However, the core-shell structure reveals much higher NIR reflectance (57.8%) than that of the mixture composed by the mixed oxides (47.8%). The enhanced rate of the NIR reflectance of the $(Fe,Cr)_2O_3$@TiO_2 calcinated at 1000 ºC was attributed to the improved refractive index of the core-shell structure. A simple schematic of the reflectance mechanism of the two pigments is shown in Figure 32(e) [199].

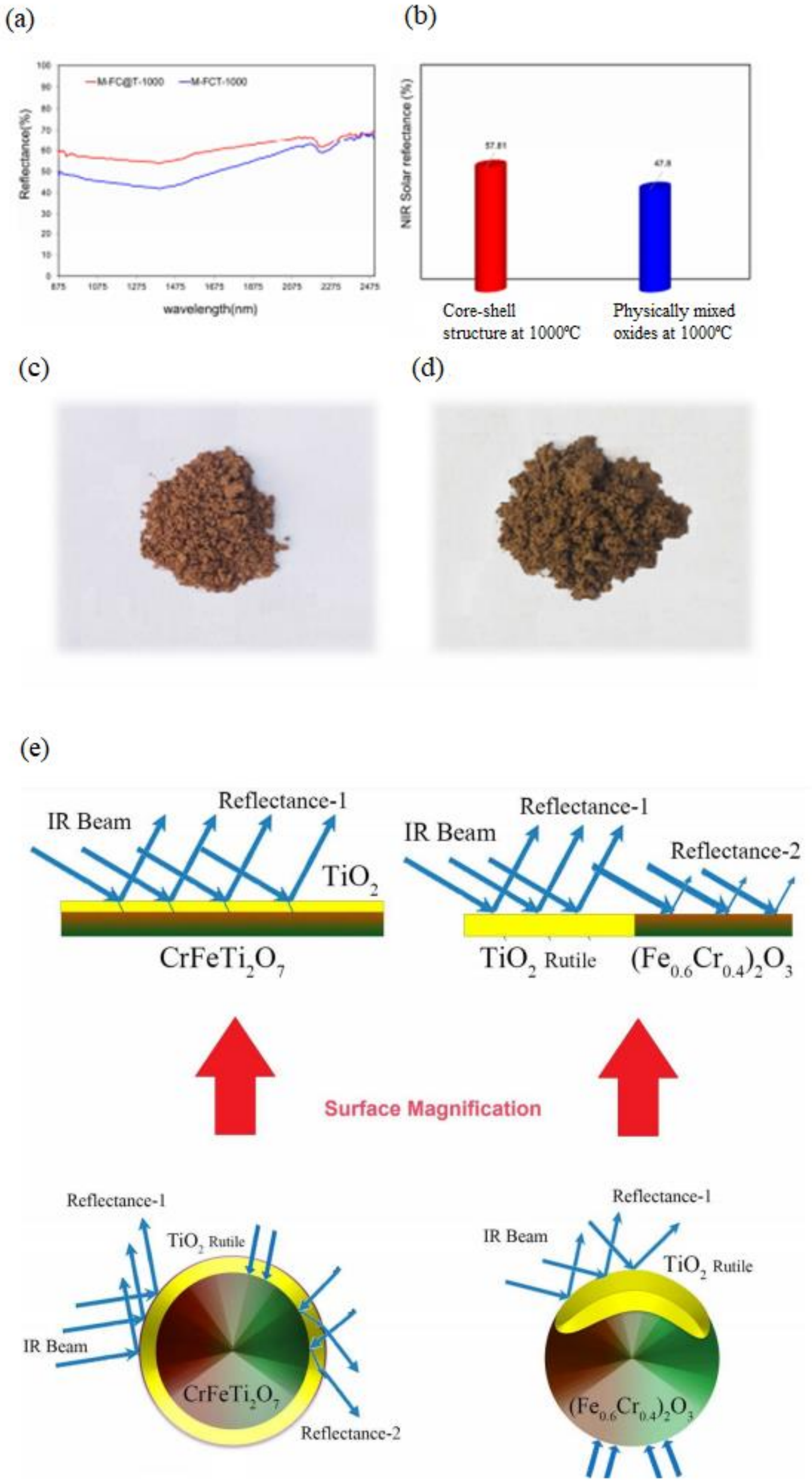

Figure 32: (a) NIR reflectance spectrum and (b) solar NIR reflectance value; photographs of: (c) core-shell structure ($(Fe,Cr)_2O_3@TiO_2$) and (d) physically mixed Fe-Cr-Ti oxides (at 1000 ºC); (e) reflectance

mechanism in core-shell structure and physically mixed samples. Reproduced with permission from ref. **[199]**, Copyright 2019, Elsevier.

Building façade's smart and adaptive nanomaterials

Smart and adaptive façades are gaining more interest besides just the use of cool pigments due to their ability to interact with and adjust to the environment, adapting their behaviour and functionality (Figure 33) [207]. Such envelope systems are capable to modify their properties and regulate the indoor characteristics and heat transfer in response to load variations or to changes in indoor or outdoor parameters, to improve comfort [208].

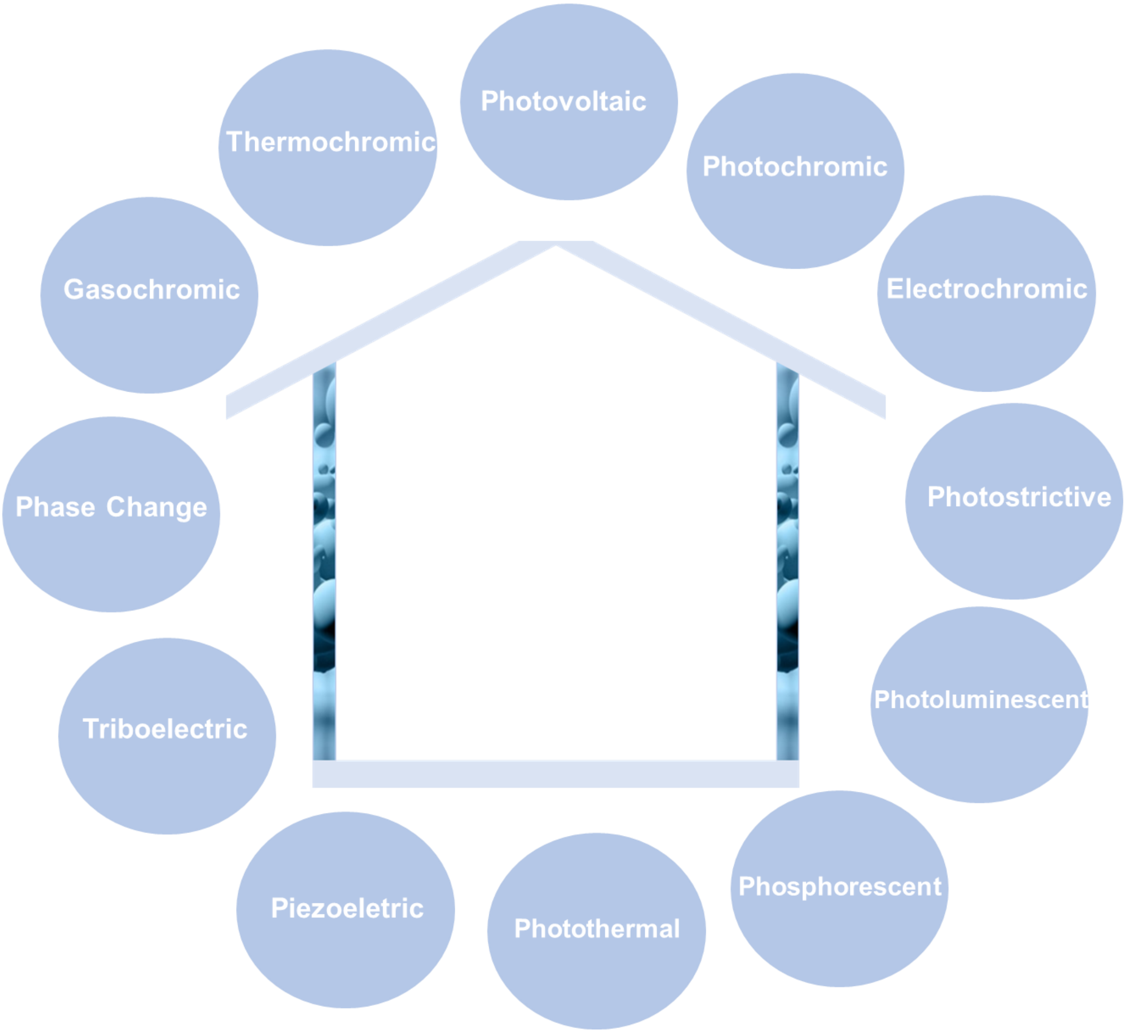

Figure 33: Selection of building façade's smart and adaptive materials.

One of the most critical issues is to select the best material to incorporate in the building's façade since different properties, such as durability, insulation, quality, cost, aesthetics and strength, must be considered [209]. Table 7 shows the typical and function of several smart and adaptive materials used in building façades, from which we highlight a few in the following.

Table 7: Identification of building façade´s smart and adaptive materials. Adapted from ref. **[209]**.

Materials	Function	Typical material	Reference
Thermochromic	Reversibly change of colour (related with a change in the crystalline phase and structure) due to a temperature variation	In_2O_3, VO_2	[210] [211] [212] [213]
Photovoltaic	Convert solar radiation into electrical energy	TiO_2, ZnO, SnO_2, Nb_2O_5, SiO_2, CNT's	[214]
Photochromic	Exhibit changes in the optical properties in reaction to light	TiO_2 quantum dots, NiO/Ni_2O_3, MoO_3, azobenzenes	[215] [216] [217]
Phosphorescent	Convert ultraviolet into white light	$SrAl_2O_4$: $Eu^{2+,}$ Dy^{3+}; $Sr4Al_14O_25$:Eu^{2+},Dy^{3+},$B+^{3+}$;	[218]
Photostrictive	Exhibit changes in shape in reaction to light	Liquid crystalline polymer	[219]
Photoluminescent	When excited by light, the transition from the excited state back into the ground state is accompanied by delayed or simultaneous light emission according to the material's nature	$CaAl_2O_4$: Eu^{+2}, Nd^{+3}, La^{+3}; $Sr_2MgSi_2O_7$: Eu, Dy	[220] [221]
Photothermal	Generate thermal energy when photoexcited	Aluminum-doped zinc oxide (AZO), ZnO thin layers, TiO_2/Ag/TiO_2, fluorine-doped tin oxide (FTO)	[222] [223] [224]
Piezoelectric	Generate an electric potential in response to pressure	$Pb[Zr_xTi_{1-x}]O_3$; $NaNbO_3$	[225] [226] [227]
Triboelectric	Type of contact electrification in which certain materials become electrically charged after coming in contact with a different material	Liquid crystals, indium tin oxide (ITO)	[228] [229] [230]
Phase Change (PCM)	Release/absorb energy at the phase transition to provide useful heat/cooling	Paraffins, fatty acids, salt hydrates, metallic	[231] [232] [233] [234]
Electrochromic	Colour or opacity of a material changes when a voltage is applied	WO_3, IrO_2, MoO_3, In_2O_3:Sn,	[235] [236] [237]

Gasochromic	Reversibly switches its optical transmittance when exposed to diluted hydrogen and oxygen gases.	Pt-WO_3 thin film	[238]

The disadvantage of the intermittent nature of solar energy can be overcome through a transferal system between the energy supply and demand sectors based on Phase Change Materials technology (see e.g. [239]). Some studies have found that PCMs integrated into buildings can mitigate energy by 10% to 87% for cooling purposes. As a result, PCMs have been recognized as one of the most progressive materials to enhance energy efficiency and sustainability in buildings especially for heating and cooling [231]. However, the performance enhancement of buildings using PCMs is a complex research and optimized situation, as there are many variables and significant uncertainties involved in building physics. Chromogenic devices (e.g. gaso-, thermo-, electro- and photochromic) are also a technology used to vary the amount of solar energy through windows (or other substrates) in buildings. Such materials experience a change in their optical properties in the visible and/or infrared region, due to the application of a specific external stimulus [240]. As an example, Piccolo et al. showed that cooling energy saving can increase by 38% when using electrochromic coatings in glass when compared to a clear glass [241]. Therefore, combining NIR reflective nanopigments with other smart or adaptive materials could be a powerful tool in designing net zero energy buildings.

Methods to synthesize pigments/nanopigments

Different approaches can be used for the production of inorganic pigments, including solid-state method [35, 242], sol-gel [243, 244, 245], hydrothermal processes [246, 247], molten salts routes [248, 249] or the sonochemical approach [250, 251, 252]. The properties of the synthesised products depend critically on the particle size and the method adopted to fabricate the pigments is crucial for the obtained optical properties [35].

Solid-State Route

In a typical solid-state reaction, nanoparticles preparation necessitates high-temperature treatments above 1000 °C for long periods until the disappearance of the intermediary phases (Figure 35). The precursor oxides are mixed in a stoichiometric ratio and homogenised by wet milling in an agate mortar, using solvents such as ethanol, water or acetone. The residual solvent is, therefore, evaporated and the resultant powders calcinated in the furnace. However, problems have arisen with this method, such as poor sintering behaviour, heterogeneous and imprecise control of stoichiometry. This process can also lead to bulky, robust powder agglomerates, unwanted phases, irregular grain growth and poor reproducibility [242].

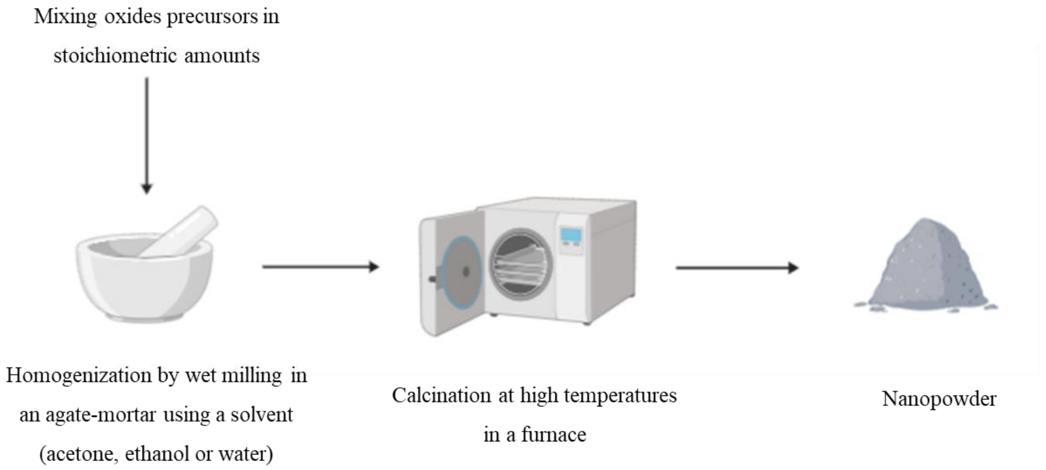

Figure 34: Schematic representation of a solid-state synthesis procedure.

As an example, Oka e Masui [167], synthesised $Ca_2Mn_{1-x}Ti_xO_4$ using the conventional solid-state procedure to identify whether such a compound could be the right candidate for a novel NIR reflective black pigment. A part of Mn^{4+} was substituted by Ti^{4+} to improve the reflectance of the pigment. Stoichiometric amounts of $CaCO_3$, MnO_2 and TiO_2 were mixed and the powder has heated in air at 1200 ºC for 6 h. The composition $Ca_2Mn_{0.85}Ti_{0.15}O_4$ was optimised to satisfy both enough blackness and high NIR reflectance compared to conventional black pigments (<50%) (Figure 35).

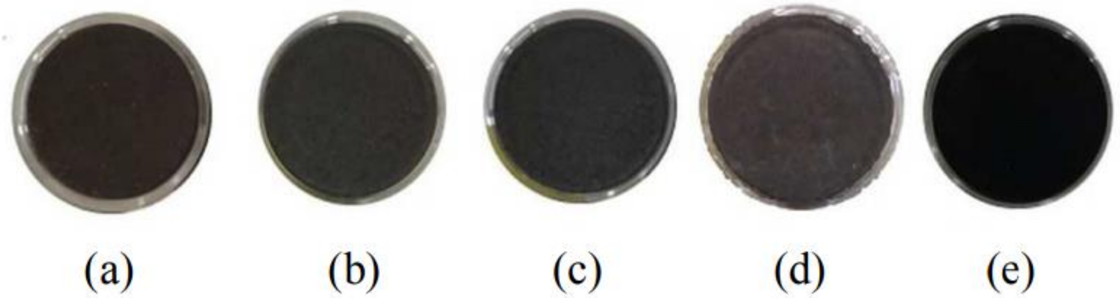

Figure 35: (a) Photographs of $Ca_2Mn_{0.85}Ti_{0.15}O_4$ synthesised by conventional solid-state route (a), (b) Black 6350 (iron and chromium oxide), (c) Black 6301 (manganese and bismuth oxide), (d) MPT-370 (calcium, manganese, and TiO_2) and (e) carbon black. Reproduced with permission from ref. **[167]**, Copyright 2016, Elsevier.

Sol-Gel

Sol-Gel is a wet chemical process that includes the development of an inorganic system by the formation of a colloidal suspension (sol) and the gelation of the sol forming a continuous liquid phase gel; (Figure 36). Compared with other conventional routes, sol-gel offers several advantages: low temperature, high purity control, controlled composition, microstructure and textural properties since there is an intimate mixing of the components, which ultimately ensures the homogeneity of the final product [243, 244, 245].

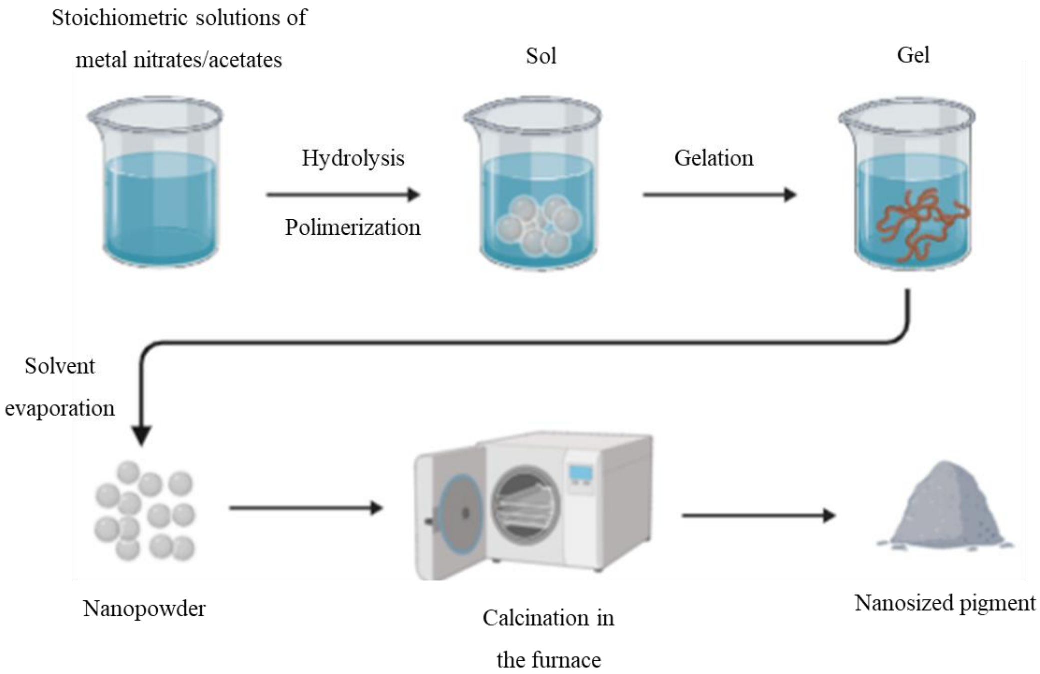

Figure 36: Representation scheme of a sol-gel route.

Radhika et al. [188] were able to control the morphology of gadolinium-doped cerium oxide powders using a facile synthesis process mixing traditional citrate gel and calcination methods, resulting in highly dispersed mixed oxides (Figure 37).

Figure 37: Photographs of Gd:Ce:Mo oxides prepared by a sol-gel method: (a) 1:1:0; (b) 1:0.95:0.05; (c) 1:0.9:0.1; (d) 1:0.85:0.15; (e) 1:0.8:0.20; (f) 1:0.75:0.25; (g) 1:0.65:0.35. Reproduced with permission from ref. **[188]**, Copyright 2014, American Chemical Society Publications.

Hydrothermal method

The hydrothermal procedure (Figure 38) has great prospect to produce materials that would normally be obtained by conventional high-temperature routes of solid-state chemistry. In hydrothermal methods, a solvent allows the quick mixture of many chemical compounds, leading to homogenous products, offering the possibility to control crystal growth and particle morphologies. This method represents a large opportunity to produce multivalued oxides with two or more metals, where the fast mixing of the constituent elements provides a large synthesis advantage [246]. Wet-chemical routes, like hydrothermal synthesis, offer the opportunity for synthesize high purity, highly crystallised, homogenous, ultrafine, well-dispersed nanopowders [247].

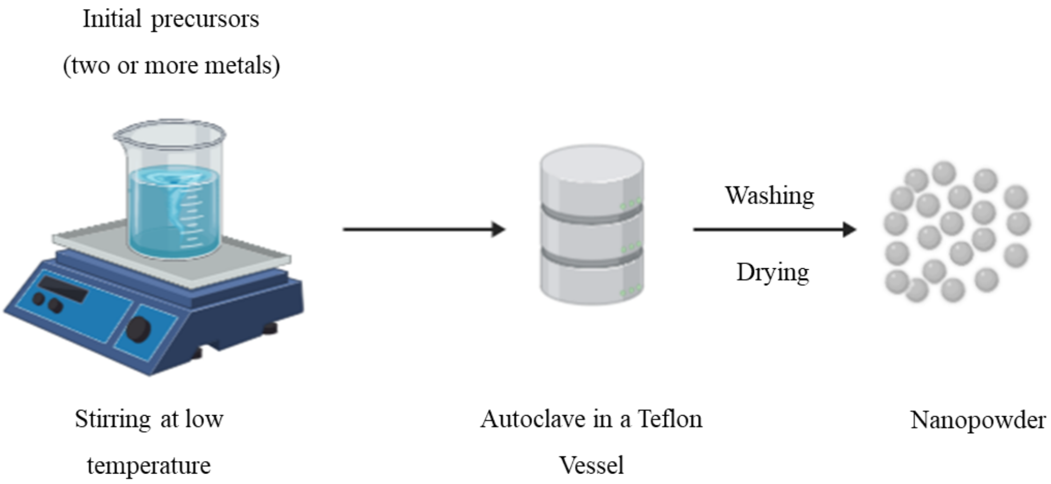

Figure 38: General representation of a hydrothermal synthesis method.

Ding et al. [143], prepared a series of V^{5+} doped $BiPO_4$ pigments (Figure 39) exhibiting high NIR reflectance using a simple hydrothermal method. Stoichiometric amounts of bulk materials were added to 80 mL of glycerol/distilled water solvent to obtain $BiP_{1-x}V_xO_4$ (x=0, 0.01, 0.05, 0.08, 0.10, 0.15). To dissolve the mixture fastly, the authors used an ultrasonic cleaner. Lastly, the mixture was transferred into an autoclave at 160 °C for 24 h.

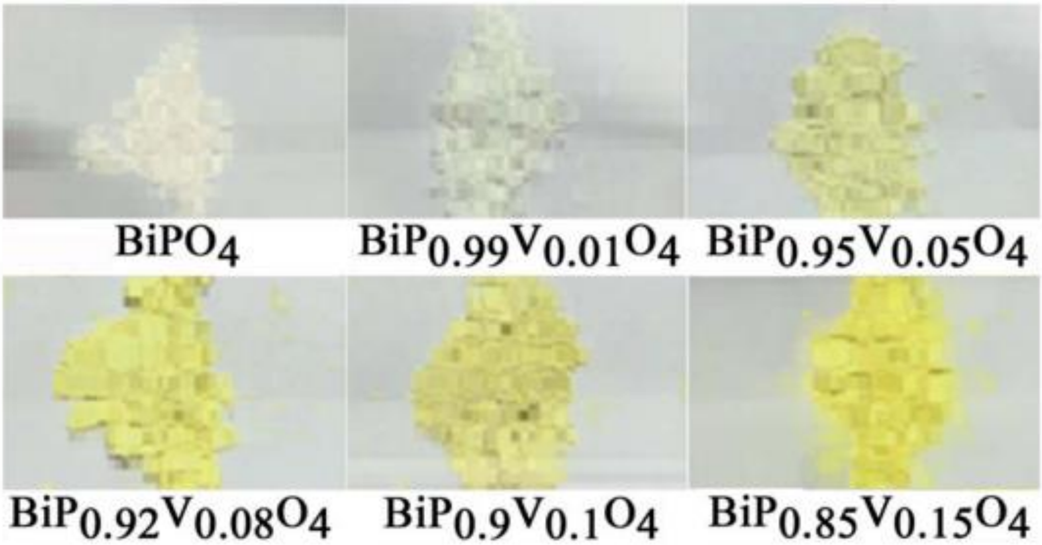

Figure 39: Photographs of $BiPO_4$-based pigments synthesised by a hydrothermal process. Reproduced with permission from ref. [143], Copyright 2018, Royal Society of Chemistry.

Molten Salt Synthesis

Sol-gel and hydrothermal processes are wet-chemical materials fabrication methods that still present several disadvantages, such as being difficult and expensive routes. Thus, one still needs alternative routes to synthesise nanopowders having precise diameters and morphology. Recently, a large range of oxide nanopowders was synthetized using molten-salt synthesis (MSS) (Figure 40) [249]. Molten salts can form a liquid above the melting point of the selected salts, acting as a solvent for reactant dissolution, diffusion and precipitation. This route permits the melt-solid to react much quicker due to the small diffusion distances and large mobility of the melted oxides, resulting in complete reactions in moderately short times. Compared to other synthetic methods, MSS offers a low processing temperature and control of the nanopowders morphology [248].

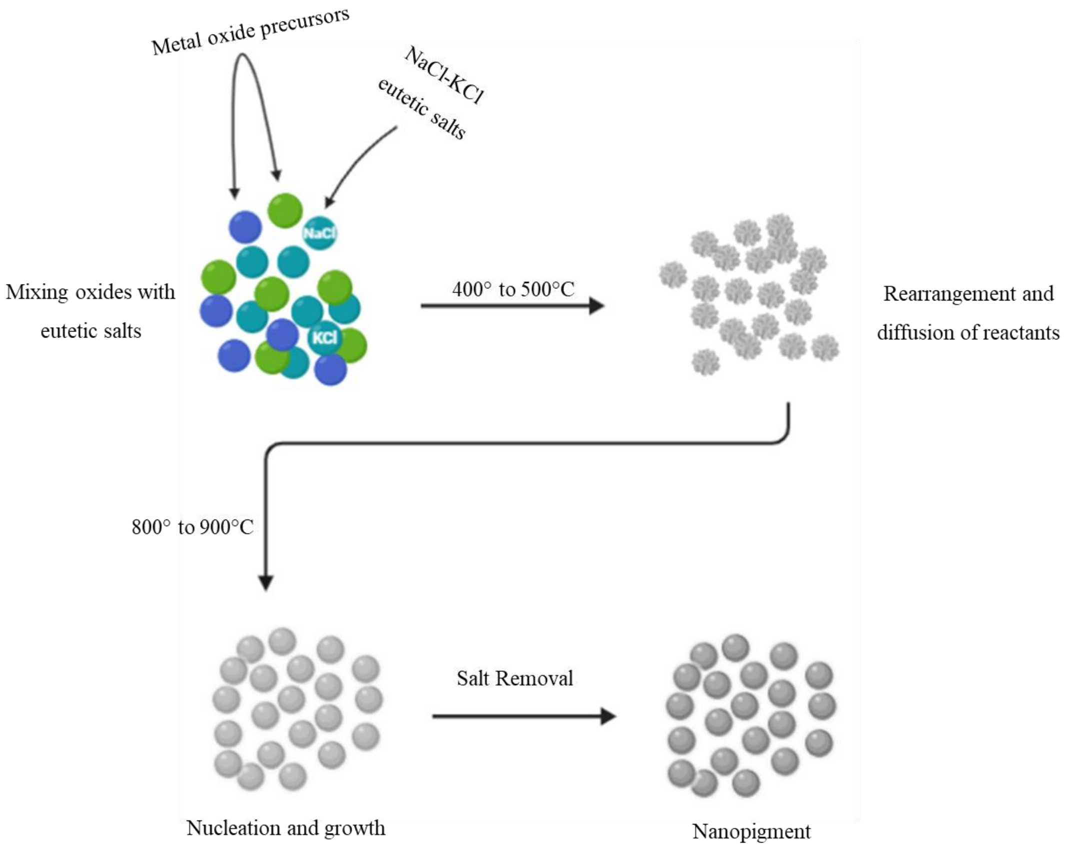

Figure 40: Schematic representation of a molten salt assisted synthesis reaction.

Xing et al. [249] used a molten salt assisted synthesis to prepare pure $ZnTiO_3$ powders from standard ZnO and TiO_2 oxides in sodium/potassium chlorides (the melting point of 670 °C at the eutectic composition).

Green synthesis: Sonochemical approach

Sonochemistry (Figure 41) has proven to be an important tool in the preparation of metal oxides. The interesting characteristic of power ultrasounds arises from the fact that it provides a form of energy for the modification of chemical reactivity. It is well known that ultrasonic irradiation promotes cavitation in an aqueous medium where the formation, growth, and collapse of microbubbles occurs. Cavitation can form at high temperatures and pressures (≈5000 ºC and above 1800 kPa), thus allowing the occurrence of uncommon chemical reactions. In many cases, thermally induced procedures offer crystalline nanoparticles [251].

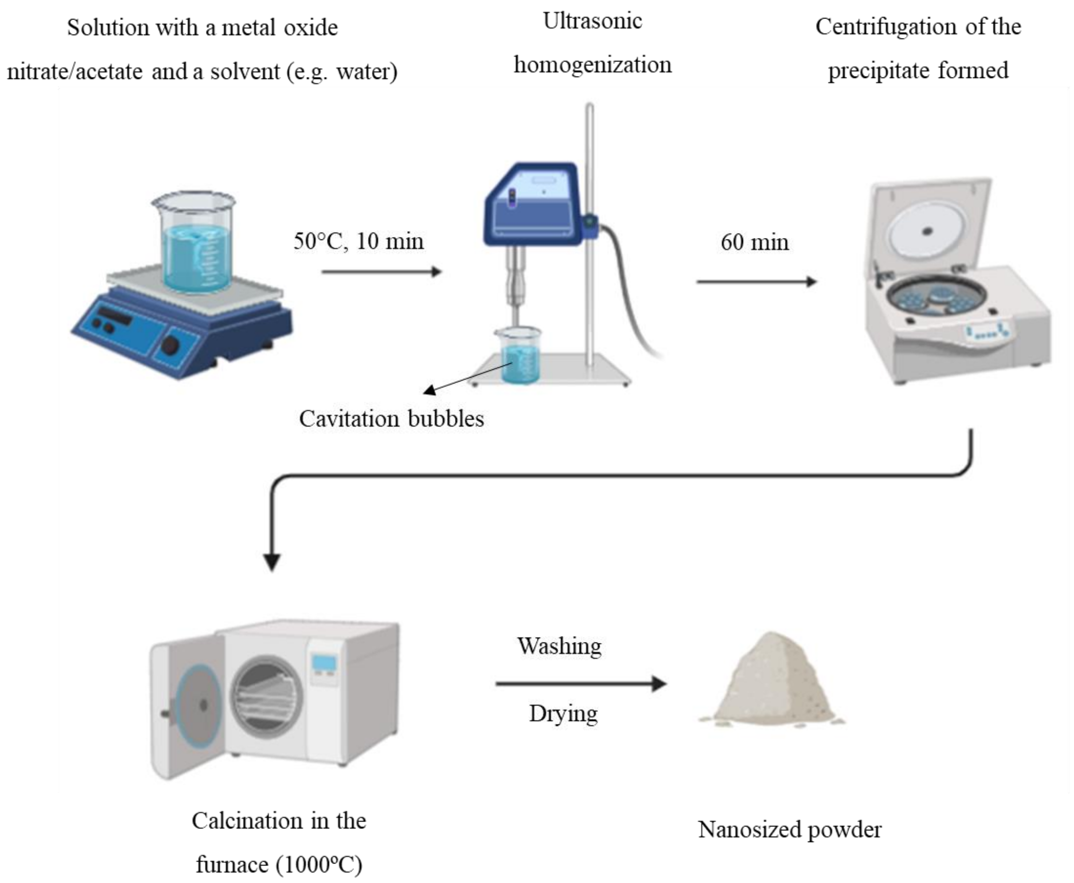

Figure 41: Schematic representation of green sonochemical synthesis.

For example, Pholnak et al. [250] successfully used a commercial ultrasonic homogeniser to obtain single-phase spheroidal ZnO nanomaterials using the sonochemical synthesis. Compared with conventional techniques, the synthesis that uses ultrasounds can often be initiated without the need for additives and sonochemistry, making use of cruder reagents. Thus, the reactions may be accelerated or performed under less forcing conditions when sonication is applied [252].

Summary and Outlook

In this review we presented the state-of-the-art of near-infrared reflective nanomaterials. This paper aimed to classify such nanomaterials according to their crystal structure, identifying the best routes to a successful production and to demonstrate their current importance. In the literature, there is a large number of reported reflective inorganic pigments, which reveals their great importance when applied in buildings. As seen, there is a large interest in obtaining novel NIR reflective nanomaterials that are more ecological and resilient, less dangerous and that can replace conventional toxic and heavy metal materials. The use of adaptive materials to reduce the quantity of absorbed solar energy in buildings can indeed be a promising solution to soften the urban heat island effect. By reduction the amount of absorbed radiation, the incorporation of near-infrared reflecting pigments in coatings can be a strategy to help decrease the cooling load demand. Its combination with other technologies will enable achieving improved energy performance in buildings. The current barriers for the implementation of such nanomaterials is the relatively high initial cost that could be solved by their widespread uptake in the building industry in the future.

Further research should also focus on the life cycle assessment of these new and functional reflective nanopigments to be applied on building envelope systems, since their low environmental impact are strictly related with their durability. Moreover, such studies should assess the long-term durability on coatings (using full-size prototypes), analyse the impact of surface reflectivity on the overall energy consumption and thermal comfort in both air-conditioned and non-air-conditioned buildings.

Conflict of interests

The authors declare no conflict of interests regarding the publication of this article.

References

1. Kumar S, Bhanjana G, Sharma A, et al (2017) Development of nanoformulation approaches for the control of weeds. Science of The Total Environment 586:1272–1278. https://doi.org/10.1016/j.scitotenv.2017.02.138

2. Begum P, Fugetsu B (2012) Phytotoxicity of multi-walled carbon nanotubes on red spinach (Amaranthus tricolor L) and the role of ascorbic acid as an antioxidant. Journal of Hazardous Materials 243:212–222. https://doi.org/10.1016/j.jhazmat.2012.10.025

3. Rico CM, Hong J, Morales MI, et al (2013) Effect of Cerium Oxide Nanoparticles on Rice: A Study Involving the Antioxidant Defense System and In Vivo Fluorescence Imaging. Environmental Science & Technology 47:5635–5642. https://doi.org/10.1021/es401032m

4. Li F, Jiang X, Zhao J, Zhang S (2015) Graphene oxide: A promising nanomaterial for energy and environmental applications. Nano Energy 16:488–515. https://doi.org/10.1016/j.nanoen.2015.07.014

5. Ma X, Luo W, Yan M, et al (2016) In situ characterization of electrochemical processes in one dimensional nanomaterials for energy storages devices. Nano Energy 24:165–188. https://doi.org/10.1016/j.nanoen.2016.03.023

6. Yu R, Lin Q, Leung S-F, Fan Z (2012) Nanomaterials and nanostructures for efficient light absorption and photovoltaics. Nano Energy 1:57–72. https://doi.org/10.1016/j.nanoen.2011.10.002

7. Mishra YK, Murugan NA, Kotakoski J, Adam J (2017) Progress in electronics and photonics with nanomaterials. Vacuum 146:304–307. https://doi.org/10.1016/j.vacuum.2017.09.035

8. Ede SR, Anantharaj S, Sakthikumar K, et al (2018) Investigation of various synthetic protocols for self-assembled nanomaterials and their role in catalysis: progress and perspectives. Materials Today Chemistry 10:31–78. https://doi.org/10.1016/j.mtchem.2018.07.003

9. Das SK, Bhunia MK, Bhaumik A (2010) Self-assembled TiO2 nanoparticles: mesoporosity, optical and catalytic properties. Dalton Transactions 39:4382.

https://doi.org/10.1039/c000317d

10. de Jong (2008) Drug delivery and nanoparticles: Applications and hazards. International Journal of Nanomedicine 3:133. https://doi.org/10.2147/ijn.s596

11. Jha AK, Prasad K (2019) Nanomaterials from biological and pharmaceutical wastes – a step towards environmental protection. Materials Today: Proceedings 18:1465–1471. https://doi.org/10.1016/j.matpr.2019.06.615

12. Juárez-Moreno K, Pestryakov A, Petranovskii V (2014) Engineering of Supported Nanomaterials. Procedia Chemistry 10:25–30. https://doi.org/10.1016/j.proche.2014.10.006

13. Tomar R, Abdala AA, Chaudhary RG, Singh NB (2020) Photocatalytic degradation of dyes by nanomaterials. Materials Today: Proceedings 29:967–973. https://doi.org/10.1016/j.matpr.2020.04.144

14. Lewis NS (2016) Developing a scalable artificial photosynthesis technology through nanomaterials by design. Nature Nanotechnology 11:1010–1019. https://doi.org/10.1038/nnano.2016.194

15. Wu S, Xu R, Lu M, et al (2015) Graphene-Containing Nanomaterials for Lithium-Ion Batteries. Advanced Energy Materials 5:1500400. https://doi.org/10.1002/aenm.201500400

16. Zeng Y, Zhu Z, Du D, Lin Y (2016) Nanomaterial-based electrochemical biosensors for food safety. Journal of Electroanalytical Chemistry 781:147–154. https://doi.org/10.1016/j.jelechem.2016.10.030

17. Lv M, Liu Y, Geng J, et al (2018) Engineering nanomaterials-based biosensors for food safety detection. Biosensors and Bioelectronics 106:122–128. https://doi.org/10.1016/j.bios.2018.01.049

18. Louise Liu J, Bashir S (2015) Advanced nanomaterials and their applications in renewable energy. Elsevier, Amsterdam

19. Sekoai PT, Ouma CNM, du Preez SP, et al (2019) Application of nanoparticles in biofuels: An overview. Fuel 237:380–397. https://doi.org/10.1016/j.fuel.2018.10.030

20. Khin MM, Nair AS, Babu VJ, et al (2012) A review on nanomaterials for environmental remediation. Energy & Environmental Science 5:8075. https://doi.org/10.1039/c2ee21818f

21. Wegner F (1981) Bounds on the density of states in disordered systems. Zeitschrift für Physik B Condensed Matter 44:9–15. https://doi.org/10.1007/bf01292646

22. Ullattil SG, Narendranath SB, Pillai SC, Periyat P (2018) Black TiO2 Nanomaterials: A Review of Recent Advances. Chemical Engineering Journal 343:708–736. https://doi.org/10.1016/j.cej.2018.01.069

23. Pacheco-Torgal F, Jalali S (2011) Nanotechnology: Advantages and drawbacks in the field of construction and building materials. Construction and Building Materials 25:582–590. https://doi.org/10.1016/j.conbuildmat.2010.07.009

24. Comission Communication from the Comission to the European the Council, European Economic and Social Commitee, Commitee of the Regions Energy (2011) Directive 2010/31/EC. European Comission

25. Lechtenböhmer S, Schüring A (2010) The potential for large-scale savings from insulating residential buildings in the EU. Energy Efficiency 4:257–270. https://doi.org/10.1007/s12053-010-9090-6

26. Santamouris M (2007) Heat Island Research in Europe: The State of the Art. Advances in Building Energy Research 1:123–150. https://doi.org/10.1080/17512549.2007.9687272

27. Hammad F, Abu-Hijleh B (2010) The energy savings potential of using dynamic external louvers in an office building. Energy and Buildings 42:1888–1895. https://doi.org/10.1016/j.enbuild.2010.05.024

28. Brambilla A, Salvalai G, Imperadori M, Sesana MM (2018) Nearly zero energy building renovation: From energy efficiency to environmental efficiency, a pilot case study. Energy and Buildings 166:271–283. https://doi.org/10.1016/j.enbuild.2018.02.002

29. Cozza ES, Alloisio M, Comite A, et al (2015) NIR-reflecting properties of new paints for energy-efficient buildings. Solar Energy 116:108–116.

https://doi.org/10.1016/j.solener.2015.04.004

30. Doulos L, Santamouris M, Livada I (2004) Passive cooling of outdoor urban spaces. The role of materials. Solar Energy 77:231–249. https://doi.org/10.1016/j.solener.2004.04.005

31. Song Z, Zhang W, Shi Y, et al (2013) Optical properties across the solar spectrum and indoor thermal performance of cool white coatings for building energy efficiency. Energy and Buildings 63:49–58. https://doi.org/10.1016/j.enbuild.2013.03.051

32. Wake L (1989) Principles and Formulations of solar reflecting and low IR emitting coatings for defense use. In: Defense Technical Information Center, Washington, DC, USA, AD-A218429

33. Santamouris M, Synnefa A, Karlessi T (2011) Using advanced cool materials in the urban built environment to mitigate heat islands and improve thermal comfort conditions. Solar Energy 85:3085–3102. https://doi.org/10.1016/j.solener.2010.12.023

34. Santamouris M, Yun GY (2020) Recent development and research priorities on cool and super cool materials to mitigate urban heat island. Renewable Energy 161:792–807. https://doi.org/10.1016/j.renene.2020.07.109

35. Jose S, Joshy D, Narendranath SB, Periyat P (2019) Recent advances in infrared reflective inorganic pigments. Solar Energy Materials and Solar Cells 194:7–27. https://doi.org/10.1016/j.solmat.2019.01.037

36. Rawat M, Singh R N. (2021) A study on the comparative review of cool roof thermal performance in various regions. Energy and Built Environment in press: https://doi.org/10.1016/j.enbenv.2021.03.001

37. Falasca S, Ciancio V, Salata F, et al (2019) High albedo materials to counteract heat waves in cities: An assessment of meteorology, buildings energy needs and pedestrian thermal comfort. Building and Environment 163:106242. https://doi.org/10.1016/j.buildenv.2019.106242

38. Cheela VRS, John M, Biswas W, Sarker P (2021) Combating Urban Heat Island Effect—A Review of Reflective Pavements and Tree Shading Strategies. Buildings

11:93. https://doi.org/10.3390/buildings11030093

39. Hernández-Pérez I, Álvarez G, Xamán J, et al (2014) Thermal performance of reflective materials applied to exterior building components—A review. Energy and Buildings 80:81–105. https://doi.org/10.1016/j.enbuild.2014.05.008

40. Wang C, Wang Z-H, Kaloush KE, Shacat J (2021) Cool pavements for urban heat island mitigation: A synthetic review. Renewable and Sustainable Energy Reviews 146:111171. https://doi.org/10.1016/j.rser.2021.111171

41. Yenneti K, Ding L, Prasad D, et al (2020) Urban Overheating and Cooling Potential in Australia: An Evidence-Based Review. Climate 8:126. https://doi.org/10.3390/cli8110126

42. Jeevanandam P, Mulukutla RS, Phillips M, et al (2007) Near Infrared Reflectance Properties of Metal Oxide Nanoparticles. The Journal of Physical Chemistry C 111:1912–1918. https://doi.org/10.1021/jp066363o

43. Papadaki D, Kiriakidis G, Tsoutsos T (2018) Applications of nanotechnology in construction industry. In: Barhoum A, Makhlouf A (eds) Fundamentals of Nanoparticles, Micro and Nano Technologies. Elsevier, pp. 343–370

44. von Broekhuizen F, von Broekhuizen J (2009) Nanotechnology in the European Construction Industry- State of the art 2009- Executive Summary. European Federation of Building and Wood Workers and European Construction Industry Federation, Amsterdam

45. Álvarez-Docio CM, Reinosa JJ, del Campo A, Fernández JF (2017) 2D particles forming a nanostructured shell: A step forward cool NIR reflectivity for CoAl2O4 pigments. Dyes and Pigments 137:1–11. https://doi.org/10.1016/j.dyepig.2016.09.061

46. Hincapié I, Künniger T, Hischier R, et al (2015) Nanoparticles in facade coatings: a survey of industrial experts on functional and environmental benefits and challenges. Journal of Nanoparticle Research 17: https://doi.org/10.1007/s11051-015-3085-3

47. Halawa E, Ghaffarianhoseini A, Ghaffarianhoseini A, et al (2018) A review on energy conscious designs of building façades in hot and humid climates: Lessons for (and from)

Kuala Lumpur and Darwin. Renewable and Sustainable Energy Reviews 82:2147–2161. https://doi.org/10.1016/j.rser.2017.08.061

48. Murgia C, Valles D, Ho Park Y, Kuravi S (2019) Effect of high aged albedo cool roofs on commercial buildings energy savings in U.S.A. climates. International Journal of Renewable Energy Research 9:65–72

49. Synnefa A, Santamouris M, Akbari H (2007) Estimating the effect of using cool coatings on energy loads and thermal comfort in residential buildings in various climatic conditions. Energy and Buildings 39:1167–1174. https://doi.org/10.1016/j.enbuild.2007.01.004

50. Revel GM, Martarelli M, Bengochea MÁ, et al (2013) Nanobased coatings with improved NIR reflecting properties for building envelope materials: Development and natural aging effect measurement. Cement and Concrete Composites 36:128–135. https://doi.org/10.1016/j.cemconcomp.2012.10.002

51. Revel GM, Martarelli M, Emiliani M, et al (2014) Cool products for building envelope – Part I: Development and lab scale testing. Solar Energy 105:770–779. https://doi.org/10.1016/j.solener.2014.03.029

52. Rossi F, Pisello AL, Nicolini A, et al (2014) Analysis of retro-reflective surfaces for urban heat island mitigation: A new analytical model. Applied Energy 114:621–631. https://doi.org/10.1016/j.apenergy.2013.10.038

53. Tao Z, Zhang W, Huang Y, et al (2014) A novel pyrophosphate BaCr2(P2O7)2 as green pigment with high NIR solar reflectance and durable chemical stability. Solid State Sciences 34:78–84. https://doi.org/10.1016/j.solidstatesciences.2014.05.016

54. Pisello AL (2017) State of the art on the development of cool coatings for buildings and cities. Solar Energy 144:660–680. https://doi.org/10.1016/j.solener.2017.01.068

55. Pisello AL, Castaldo VL, Fabiani C, Cotana F (2016) Investigation on the effect of innovative cool tiles on local indoor thermal conditions: Finite element modeling and continuous monitoring. Building and Environment 97:55–68. https://doi.org/10.1016/j.buildenv.2015.11.038

56. Malz S, Krenkel W, Steffens O (2020) Infrared reflective wall paint in buildings: Energy saving potentials and thermal comfort. Energy and Buildings 224:110212. https://doi.org/10.1016/j.enbuild.2020.110212

57. Gobakis K, Synnefa A, Meier H, et al (2016) Cool Roofs in the European context. REHVA Journal 04:19–24

58. Carnielo E, Zinzi M, Fanchiotti A (2014) On the Solar Reflectance Angular Dependence of Opaque Construction Materials and Impact on the Energy Balance of Building Components. Energy Procedia 48:1244–1253. https://doi.org/10.1016/j.egypro.2014.02.141

59. Zinzi M, Carnielo E, Rossi G (2015) Directional and angular response of construction materials solar properties: Characterisation and assessment. Solar Energy 115:52–67. https://doi.org/10.1016/j.solener.2015.02.015

60. Takebayashi H (2016) High-Reflectance Technology on Building Façades: Installation Guidelines for Pedestrian Comfort. Sustainability 8:785. https://doi.org/10.3390/su8080785

61.Taha H, Sailor D, Akbari H (1992) High-albedo materials for reducing building cooling energy use. Lawrence Berkeley National Laboratory, Berkeley, CA

62.Uemoto KL, Sato NMN, John VM (2010) Estimating thermal performance of cool colored paints. Energy and Buildings 42:17–22. https://doi.org/10.1016/j.enbuild.2009.07.026

63. Yuan L, Han A, Ye M, et al (2018) Synthesis and characterization of environmentally benign inorganic pigments with high NIR reflectance: Lanthanum-doped BiFeO3. Dyes and Pigments 148:137–146. https://doi.org/10.1016/j.dyepig.2017.09.008

64. Fang F, Kennedy J, Futter J, Manning J (2013) A review of near infrared reflectance properties of metal oxide nanostructures. GNS Science Report 39:23–43

65. Hyde D, Brannon S (2006) Investigation of Infrared Reflective Pigmentation Technologies for Coatings and Composite Applications. In: Proceedings of the American Composites Manufacturers Association Composites and Polycon. St. Louis, USA

66. Moezzi A, McDonagh AM, Cortie MB (2012) Zinc oxide particles: Synthesis, properties and applications. Chemical Engineering Journal 185-186:1–22. https://doi.org/10.1016/j.cej.2012.01.076

67. Levinson R, Berdahl P, Akbari H (2005) Solar spectral optical properties of pigments—Part I: model for deriving scattering and absorption coefficients from transmittance and reflectance measurements. Solar Energy Materials and Solar Cells 89:319–349. https://doi.org/10.1016/j.solmat.2004.11.012

68. McNeil LE, French RH (2001) Light scattering from red pigment particles: Multiple scattering in a strongly absorbing system. Journal of Applied Physics 89:283–293. https://doi.org/10.1063/1.1331344

69. Kolokotsa D, Dimitriou V, Synnefa A (2012) Modelling Cool Materials' Properties. In: Advances in the Development of Cool Materials for the Built Environment. Bentham Science Publishers, pp. 195–230

70. Gonome H, Baneshi M, Okajima J, et al (2014) Control of thermal barrier performance by optimized nanoparticle size and experimental evaluation using a solar simulator. Journal of Quantitative Spectroscopy and Radiative Transfer 149:81–89. https://doi.org/10.1016/j.jqsrt.2014.07.025

71. Mie G (1908) Beiträge zur Optik trüber Medien, speziell kolloidaler Metallösungen. Annalen der Physik 330:377–445. https://doi.org/10.1002/andp.19083300302

72. Maradudin AA, méndez ER (2007) Light Scattering from Randomly Rough Surfaces. Science Progress 90:161–221. https://doi.org/10.3184/003685007x228711

73. Lyu M, Lin J, Krupczak J, Shi D (2020) Light angle dependence of photothermal properties in oxide and porphyrin thin films for energy-efficient window applications. MRS Communications 10:439–448. https://doi.org/10.1557/mrc.2020.39

74. Kubelka P (1948) New Contributions to the Optics of Intensely Light-Scattering Materials Part I. Journal of the Optical Society of America 38:448. https://doi.org/10.1364/josa.38.000448

75. Kubelka P, Munk F (1931) Ein Beitrag Zur Optik der Farbanstriche. Zeitschrift für

Technische Physik 12:593–601

76. Saunderson JL (1942) Calculation of the Color of Pigmented Plastics*. Journal of the Optical Society of America 32:727. https://doi.org/10.1364/josa.32.000727

77. Jansen M, Letschert HP (2000) Inorganic yellow-red pigments without toxic metals. Nature 404:980–982. https://doi.org/10.1038/35010082

78. Kiomarsipour N, Shoja Razavi R (2014) Hydrothermal synthesis of ZnO nanopigments with high UV absorption and vis/NIR reflectance. Ceramics International 40:11261–11268. https://doi.org/10.1016/j.ceramint.2014.03.178

79. Kiomarsipour N, Shoja Razavi R, Ghani K, Kioumarsipour M (2013) Evaluation of shape and size effects on optical properties of ZnO pigment. Applied Surface Science 270:33–38. https://doi.org/10.1016/j.apsusc.2012.11.167

80. Nielsen R, Wilfing G (2005) Zirconium and Zirconium Compounds. In: Ullmann's Encyclopedia of Industrial Chemistry. Wiley-VCH Verlag GmbH & Co. KGaA, Weinheim, pp. 1–27

81. Levinson R, Berdahl P, Akbari H (2005) Solar spectral optical properties of pigments—Part II: survey of common colorants. Solar Energy Materials and Solar Cells 89:351–389. https://doi.org/10.1016/j.solmat.2004.11.013

82. Liang S, Zhang H, Luo M, et al (2015) Preparation of Cr2O3-based pigments with high NIR reflectance via thermal decomposition of CrOOH. Transactions of Nonferrous Metals Society of China 25:2646–2647. https://doi.org/10.1016/s1003-6326(15)63887-0

83. Coser E, Moritz VF, Krenzinger A, Ferreira CA (2015) Development of paints with infrared radiation reflective properties. Polímeros 25:305–310. https://doi.org/10.1590/0104-1428.1869

84. Rong X, Jiao L, Kong X, Yuan G (2020) Research on Low-Brightness and High-Reflective Coatings Suitable for Buildings in Tropical Areas. Coatings 10:829. https://doi.org/10.3390/coatings10090829

85. Soumya S, Mohamed AP, Mohan K, Ananthakumar S (2015) Enhanced near-infrared reflectance and functional characteristics of Al-doped ZnO nano-pigments embedded

PMMA coatings. Solar Energy Materials and Solar Cells 143:335–346. https://doi.org/10.1016/j.solmat.2015.07.012

86. Zhou A, Yu Z, Chow CL, Lau D (2017) Enhanced solar spectral reflectance of thermal coatings through inorganic additives. Energy and Buildings 138:641–647. https://doi.org/10.1016/j.enbuild.2016.12.027

87. Jameel Z, Haider A, Taha S, et al (2016) Evaluation of hybrid sol-gel incorporated with nanoparticles as nano paint. In: AIP Conference Proceedings. p. 020001

88. Shen L, Zhang Y, Zhang P, et al (2016) Effect of TiO2 pigment gradation on the properties of thermal insulation coatings. International Journal of Minerals, Metallurgy, and Materials 23:1466–1474. https://doi.org/10.1007/s12613-016-1371-4

89. Liu L, Chen X (2014) Titanium Dioxide Nanomaterials: Self-Structural Modifications. Chemical Reviews 114:9890–9918. https://doi.org/10.1021/cr400624r

90. Reyes-Coronado D, Rodríguez-Gattorno G, Espinosa-Pesqueira ME, et al (2008) Phase-pure TiO2nanoparticles: anatase, brookite and rutile. Nanotechnology 19:145605. https://doi.org/10.1088/0957-4484/19/14/145605

91. Chen X, Mao S (2007) Titanium Dioxide nanomaterials: Synthesis, properties, modifications, and applications. Chemical Reviews 107:2891

92. Eppler RA (1987) Effect of Antimony Oxide on the Anatase-Rutile Transformation in Titanium Dioxide. Journal of the American Ceramic Society 70:C–64C–66. https://doi.org/10.1111/j.1151-2916.1987.tb04985.x

93. Landmann M, Rauls E, Schmidt WG (2012) The electronic structure and optical response of rutile, anatase and brookite TiO2. Journal of Physics: Condensed Matter 24:195503. https://doi.org/10.1088/0953-8984/24/19/195503

94. Yan X, Chen X (2015) Titanium Dioxide Materials. In: Encyclopedia of Inorganic and Bioinorganic Chemistry. John Wiley & Sons Ltd, pp. 1–38

95. Pelaez M, Nolan NT, Pillai SC, et al (2012) A review on the visible light active titanium dioxide photocatalysts for environmental applications. Applied Catalysis B: Environmental 125:331–349. https://doi.org/10.1016/j.apcatb.2012.05.036

96. Rahimi N, Pax RA, Gray EMacA (2016) Review of functional titanium oxides. I: TiO2 and its modifications. Progress in Solid State Chemistry 44:86–105. https://doi.org/10.1016/j.progsolidstchem.2016.07.002

97. Chen J, Poon C (2009) Photocatalytic construction and building materials: From fundamentals to applications. Building and Environment 44:1899–1906. https://doi.org/10.1016/j.buildenv.2009.01.002

98. Popov AP, Priezzhev AV, Lademann J, Myllylä R (2005) TiO2nanoparticles as an effective UV-B radiation skin-protective compound in sunscreens. Journal of Physics D: Applied Physics 38:2564–2570. https://doi.org/10.1088/0022-3727/38/15/006

99. Godnjavec J, Zabret J, Znoj B, et al (2014) Investigation of surface modification of rutile TiO2 nanoparticles with SiO2/Al2O3 on the properties of polyacrylic composite coating. Progress in Organic Coatings 77:47–52. https://doi.org/10.1016/j.porgcoat.2013.08.001

100. Kusior A, Banas J, Trenczek-Zajac A, et al (2018) Structural properties of TiO2 nanomaterials,. Journal of Molecular Structure, 1157:327–336

101. Song J, Qin J, Qu J, et al (2014) The effects of particle size distribution on the optical properties of titanium dioxide rutile pigments and their applications in cool non-white coatings. Solar Energy Materials and Solar Cells 130:42–50. https://doi.org/10.1016/j.solmat.2014.06.035

102. Piri N, Shams-nateri A, Mokhtari J (2017) Solar spectral performance of nanopigments. Solar Energy Materials and Solar Cells 162:72–82. https://doi.org/10.1016/j.solmat.2016.12.036

103. Allen NS, Edge M, Ortega A, et al (2004) Degradation and stabilisation of polymers and coatings: nano versus pigmentary titania particles. Polymer Degradation and Stability 85:927–946. https://doi.org/10.1016/j.polymdegradstab.2003.09.024

104. Marques J, Gomes TD, Forte MA, et al (2019) A new route for the synthesis of highly-active N-doped TiO2 nanoparticles for visible light photocatalysis using urea as nitrogen precursor. Catalysis Today 326:36–45. https://doi.org/10.1016/j.cattod.2018.09.002

105. Kumar S, Verma NK, Singla ML (2012) Study on reflectivity and photostability of Al-doped TiO2 nanoparticles and their reflectors. Journal of Materials Research 28:521–528. https://doi.org/10.1557/jmr.2012.361

106. Islam MM, Bredow T, Gerson A (2007) Electronic properties of oxygen-deficient and aluminum-doped rutileTiO2from first principles. Physical Review B 76: https://doi.org/10.1103/physrevb.76.045217

107. Grabstanowicz LR, Gao S, Li T, et al (2013) Facile Oxidative Conversion of TiH2 to High-Concentration Ti3+-Self-Doped Rutile TiO2 with Visible-Light Photoactivity. Inorganic Chemistry 52:3884–3890. https://doi.org/10.1021/ic3026182

108. Zaleska A (2008) Doped-TiO2: A Review. Recent Patents on Engineering 2:157–164. https://doi.org/10.2174/187221208786306289

109. Mohan AC, Renjanadevi B (2016) Preparation of Zinc Oxide Nanoparticles and its Characterization Using Scanning Electron Microscopy (SEM) and X-Ray Diffraction (XRD). Procedia Technology 24:761–766. https://doi.org/10.1016/j.protcy.2016.05.078

110. Dimapilis EAS, Hsu C-S, Mendoza RMO, Lu M-C (2018) Zinc oxide nanoparticles for water disinfection. Sustainable Environment Research 28:47–56. https://doi.org/10.1016/j.serj.2017.10.001

111. Wei ZP, Lu YM, Shen DZ, et al (2007) Room temperature p-n ZnO blue-violet light-emitting diodes. Applied Physics Letters 90:042113. https://doi.org/10.1063/1.2435699

112. Osmond G (2012) Zinc white: a review of zinc oxide pigment properties and implications for stability in oil-based paintings. AICCM Bulletin 33:20–29. https://doi.org/10.1179/bac.2012.33.1.004

113. N. Jones F, E. Nichols M, Pappas SP (2017) Pigments. In: Organic Coatings: Science and Technology, 4th Edition. John Wiley & Sons, Inc., pp. 417–434

114. Clementi C, Rosi F, Romani A, et al (2012) Photoluminescence Properties of Zinc Oxide in Paints: A Study of the Effect of Self-Absorption and Passivation. Applied Spectroscopy 66:1233–1241. https://doi.org/10.1366/12-06643

115. de Liedekerke M (2006) Zinc Oxide (Zinc White): Pigments, Inorganic. In:

Ullmann’s Encyclopedia of Industrial Chemistry. Wiley-VCH Verlag GmbH & Co. KGaA, Weinheim, pp. 56–60

116. Lv J, Tang M, Quan R, Chai Z (2019) Synthesis of solar heat-reflective ZnTiO3 pigments with novel roof cooling effect. Ceramics International 45:15768–15771. https://doi.org/10.1016/j.ceramint.2019.05.081

117. Terki R, Bertrand G, Aourag H, Coddet C (2006) Structural and electronic properties of zirconia phases: A FP-LAPW investigations. Materials Science in Semiconductor Processing 9:1006–1013. https://doi.org/10.1016/j.mssp.2006.10.033

118. Han Y, Zhu J (2013) Surface Science Studies on the Zirconia-Based Model. Topics in Catalysts 56:1525-1541. https://doi.org/10.1002/chin.201349222

119. Moles P (2017) The use of zirconium in surface coatings. In: Luxfer MEL Technologies. http://www.zrchem.com/. Accessed 17 Jun 2021

120. George G, Vishnu VS, Reddy MLP (2011) The synthesis, characterization and optical properties of silicon and praseodymium doped Y6MoO12 compounds: Environmentally benign inorganic pigments with high NIR reflectance. Dyes and Pigments 88:109–115. https://doi.org/10.1016/j.dyepig.2010.05.010

121. Makhlouf SA, Bakr ZH, Al-Attar H, Moustafa MS (2013) Structural, morphological and electrical properties of Cr2O3 nanoparticles. Materials Science and Engineering: B 178:337–343. https://doi.org/10.1016/j.mseb.2013.01.012

122. Zhao P, Zhao H, Yu J, et al (2018) Crystal structure and properties of Al2O3-Cr2O3 solid solutions with different Cr2O3 contents. Ceramics International 44:1356–1361. https://doi.org/10.1016/j.ceramint.2017.08.195

123. Newnham R, Hann Y (1962) Refinement of the α-A1203, Ti203, V203 and Cr203 structures. Zeitschrift für Kristallographie, 117:235–237

124. Santulli A, Feygenson M, Camino F, et al (2011) Synthesis and Characterization of One-Dimensional Cr2O3 Nanostructures. Chemistry of Materials 23:1000–1008

125. Thongkanluang T, Wutisatwongkul J, Chirakanphaisarn N, Pokaipisit A (2013) Performance of Near-Infrared Reflective Tile Roofs. Advanced Materials Research

770:30–33. https://doi.org/10.4028/www.scientific.net/amr.770.30

126. Deepak HN, Choudhari KS, Shivashankar SA, et al (2019) Facile microwave-assisted synthesis of Cr2O3 nanoparticles with high near-infrared reflection for roof-top cooling applications. Journal of Alloys and Compounds 785:747–753. https://doi.org/10.1016/j.jallcom.2019.01.254

127. Thongkanluang T, Limsuwan P, Rakkwamsuk P (2011) Preparation and Application of High Near-Infrared Reflective Green Pigment for Ceramic Tile Roofs. International Journal of Applied Ceramic Technology 8:1451–1458. https://doi.org/10.1111/j.1744-7402.2010.02599.x

128. Singh J, Verma V, Kumar R (2019) Preparation and structural, optical studies of Al substituted chromium oxide (Cr2O3) nanoparticles. Vacuum 159:282–286. https://doi.org/10.1016/j.vacuum.2018.09.033

129. Li P, Xu H, Zhang Y, et al (2009) The effects of Al and Ba on the colour performance of chromic oxide green pigment. Dyes and Pigments 80:287–291. https://doi.org/10.1016/j.dyepig.2008.07.016

130. Sangeetha S, Basha R, Sreeram KJ, et al (2012) Functional pigments from chromium (III) oxide nanoparticles. Dyes and Pigments 94:548–552. https://doi.org/10.1016/j.dyepig.2012.03.019

131. Muñoz R, Masó N, Julián B, et al (2004) Environmental study of Cr2O3–Al2O3 green ceramic pigment synthesis. Journal of the European Ceramic Society 24:2087–2094. https://doi.org/10.1016/s0955-2219(03)00360-1

122. Elakkiya V., Abhishekram R., Sumathi. S, (2019) Copper doped nickel aluminate: Synthesis, characterisation, optical and colour properties. Chinese Journal of Chemical Engineering 27:2596–2605. https://doi.org/10.1016/j.cjche.2019.01.008

133. Karmaoui M, Silva NJO, Amaral VS, et al (2013) Synthesis of cobalt aluminate nanopigments by a non-aqueous sol–gel route. Nanoscale 5:4277. https://doi.org/10.1039/c3nr34229h

134. Dey S, Dhal GC (2019) Catalytic conversion of carbon monoxide into carbon

dioxide over spinel catalysts: An overview. Materials Science for Energy Technologies 2:575–588. https://doi.org/10.1016/j.mset.2019.06.003

135. Paudel TR, Zakutayev A, Lany S, et al (2011) Doping Rules and Doping Prototypes in A2BO4 Spinel Oxides. Advanced Functional Materials 21:4493–4501. https://doi.org/10.1002/adfm.201101469

136. Ali AA, El Fadaly E, Ahmed IS (2018) Near-infrared reflecting blue inorganic nano-pigment based on cobalt aluminate spinel via combustion synthesis method. Dyes and Pigments 158:451–462. https://doi.org/10.1016/j.dyepig.2018.05.058

137. Tong Y, Zhang H, Wang S, et al (2016) Highly Dispersed Re-Doped CoAl2O4Nanopigments: Synthesis and Chromatic Properties. Journal of Nanomaterials 2016:1–7. https://doi.org/10.1155/2016/4169673

138. Yang R, Han A, Ye M, et al (2017) The influence of Mn/N-codoping on the thermal performance of ZnAl2O4 as high near-infrared reflective inorganic pigment. Journal of Alloys and Compounds 696:1329–1341. https://doi.org/10.1016/j.jallcom.2016.12.100

139. Hedayati HR, Sabbagh Alvani AA, Sameie H, et al (2015) Synthesis and characterization of Co1−xZnxCr2−yAlyO4 as a near-infrared reflective color tunable nano-pigment. Dyes and Pigments 113:588–595. https://doi.org/10.1016/j.dyepig.2014.09.030

140. Menon SG, Swart HC (2020) Microwave-assisted synthesis of blue-green NiAl2O4 nanoparticle pigments with high near-infrared reflectance for indoor cooling. Journal of Alloys and Compounds 819:152991. https://doi.org/10.1016/j.jallcom.2019.152991

141. Thejus PK, Krishnapriya KV, Nishanth KG (2021) A cost-effective intense blue colour inorganic pigment for multifunctional cool roof and anticorrosive coatings. Solar Energy Materials and Solar Cells 219:110778. https://doi.org/10.1016/j.solmat.2020.110778

142. Wendusu T, Honda T, Masui T, Imanaka N (2013) Novel environmentally friendly (Bi, Ca, Zn, La) VO4 inorganic yellow pigments. RSC Advances 3:24941. https://doi.org/10.1039/c3ra43978j

143. Ding C, Han A, Ye M, et al (2018) Hydrothermal synthesis and characterization of novel yellow pigments based on V5+ doped BiPO4 with high near-infrared reflectance. RSC Advances 8:19690–19700. https://doi.org/10.1039/c8ra02406e

144. Sandhya Kumari L, Prabhakar Rao P, Narayana Pillai Radhakrishnan A, et al (2013) Brilliant yellow color and enhanced NIR reflectance of monoclinic BiVO4 through distortion in VO43− tetrahedra. Solar Energy Materials and Solar Cells 112:134–143. https://doi.org/10.1016/j.solmat.2013.01.022

145. Ianoş R, Muntean E, Păcurariu C, et al (2017) Combustion synthesis of a blue Co-doped zinc aluminate near-infrared reflective pigment. Dyes and Pigments 142:24–31. https://doi.org/10.1016/j.dyepig.2017.03.016

146. Bao W, Ma F, Zhang Y, et al (2016) Synthesis and characterization of Fe3+ doped Co0.5Mg0.5Al2O4 inorganic pigments with high near-infrared reflectance. Powder Technology 292:7–13. https://doi.org/10.1016/j.powtec.2016.01.013

147. Elakkiya V, Sumathi S (2020) Ce and Fe doped gahnite: Cost effective solar reflective pigment for cool coating applications. Journal of Alloys and Compounds 820:153174. https://doi.org/10.1016/j.jallcom.2019.153174

148. Merikhi J, Jungk H-O, Feldmann C (2000) Sub-micrometer CoAl2O4 pigment particles — synthesis and preparation of coatings. Journal of Materials Chemistry 10:1311–1314. https://doi.org/10.1039/a910201i

149. Eliziário SA, de Andrade JM, Lima SJG, et al (2011) Black and green pigments based on chromium–cobalt spinels. Materials Chemistry and Physics 129:619–624. https://doi.org/10.1016/j.matchemphys.2011.05.001

150. Yuvaraj S, Nithya VD, Fathima KS, et al (2013) Investigations on the temperature dependent electrical and magnetic properties of NiTiO3 by molten salt synthesis. Materials Research Bulletin 48:1110–1116. https://doi.org/10.1016/j.materresbull.2012.12.001

151. Du Y, Zhang M, Wu J, et al Optical properties of SrTiO3 thin films by pulsed laser deposition. Applied Physics A 76:1105–1108

152. Ramadass N (1978) ABO3-type oxides—Their structure and properties—A bird's eye view. Materials Science and Engineering 36:231–239. https://doi.org/10.1016/0025-5416(78)90076-9

153. Cousin P, Ross RA (1990) Preparation of mixed oxides: a review. Materials Science and Engineering: A 130:119–125. https://doi.org/10.1016/0921-5093(90)90087-j

154. Singh L, Rai US, Mandal KD, Singh NB (2014) Progress in the growth of CaCu3Ti4O12 and related functional dielectric perovskites. Progress in Crystal Growth and Characterization of Materials 60:15–62. https://doi.org/10.1016/j.pcrysgrow.2014.04.001

155. Meenakshi P, Selvaraj M (2018) Bismuth titanate as an infrared reflective pigment for cool roof coating. Solar Energy Materials and Solar Cells 174:530–537. https://doi.org/10.1016/j.solmat.2017.09.048

156. Yang R, Han A, Ye M, et al (2017) Synthesis, characterization and thermal performance of Fe/N co-doped MgTiO3 as a novel high near-infrared reflective pigment. Solar Energy Materials and Solar Cells 160:307–318. https://doi.org/10.1016/j.solmat.2016.10.045

157. Sun H, Tao Y, Zhang J (2020) Magnesium titanate as a new high solar reflectance pigment to fabricate cooling engineering composites for energy saving areas. Journal of Alloys and Compounds 847:156527. https://doi.org/10.1016/j.jallcom.2020.156527

158. Moghtada A, Shahrouzianfar A, Ashiri R (2017) Facile synthesis of NiTiO3 yellow nano-pigments with enhanced solar radiation reflection efficiency by an innovative one-step method at low temperature. Dyes and Pigments 139:388–396. https://doi.org/10.1016/j.dyepig.2016.12.044

159. Wang J-L, Li Y-Q, Byon Y-J, et al (2013) Synthesis and characterization of NiTiO3 yellow nano pigment with high solar radiation reflection efficiency. Powder Technology 235:303–306. https://doi.org/10.1016/j.powtec.2012.10.044

160. Zou J, Zheng W (2016) TiO2@CoTiO3 complex green pigments with low cobalt content and tunable color properties. Ceramics International 42:8198–8205. https://doi.org/10.1016/j.ceramint.2016.02.029

161. Mao Z, Yang Z, Zhang J (2019) SrTiO3 as a new solar reflective pigment on the cooling property of PMMA-ceramic composites. Ceramics International 45:16078–16087. https://doi.org/10.1016/j.ceramint.2019.05.124

162. Viruthagiri G, Praveen P, Mugundan S, Gopinathan E (2013) ynthesis and Characterization of Pure and Nickel Doped SrTiO3 Nanoparticles via Solid State Reaction Route. Indian Journal of Advances in Chemical Science 1:132–138

163. Zou J, Zhang T, He X (2019) Dark brown Cr doped CaTiO3 pigments with high NIR reflectance. Materials Letters 248:173–176. https://doi.org/10.1016/j.matlet.2019.04.031

164. Chen Y, Ma Y, Wang Z, et al (2018) Molten salt synthesis of YMnO3 powder with high near-infrared reflectivity. Materials Letters 229:171–173. https://doi.org/10.1016/j.matlet.2018.07.002

165. Han A, Zhao M, Ye M, et al (2013) Crystal structure and optical properties of YMnO3 compound with high near-infrared reflectance. Solar Energy 91:32–36. https://doi.org/10.1016/j.solener.2013.01.011

166. Xu Z, Wang D, Zhong M, Zhang Z (2020) Preparation and characterization of Mg2+-doped CaCu3Ti4O12 pigment with high NIR reflectance. Ceramics International 46:25306–25312. https://doi.org/10.1016/j.ceramint.2020.06.324

167. Oka R, Masui T (2016) Synthesis and characterization of black pigments based on calcium manganese oxides for high near-infrared (NIR) reflectance. RSC Advances 6:90952–90957. https://doi.org/10.1039/c6ra21443f

168. Dohnalová Ž, Šulcová P, Bělina P (2019) Pink NIR pigment based on Cr-doped SrSnO3. Journal of Thermal Analysis and Calorimetry 138:4475–4484. https://doi.org/10.1007/s10973-019-08522-z

169. Tian M, Han A, Ma S, et al (2021) Preparation of Cr-doped BaTiO3 near infrared reflection pigment powder and its anti-aging performance for acrylonitrile-styrene-acrylate. Powder Technology 378:182–190. https://doi.org/10.1016/j.powtec.2020.09.072

170. Li J, Lorger S, Stalick JK, et al (2016) From Serendipity to Rational Design: Tuning the Blue Trigonal Bipyramidal Mn3+Chromophore to Violet and Purple through Application of Chemical Pressure. Inorganic Chemistry 55:9798–9804. https://doi.org/10.1021/acs.inorgchem.6b01639

171. Smith AE, Comstock MC, Subramanian MA (2016) Spectral properties of the UV absorbing and near-IR reflecting blue pigment, YIn1-xMnxO3. Dyes and Pigments 133:214–221. https://doi.org/10.1016/j.dyepig.2016.05.029

172. Rosati A, Fedel M, Rossi S (2021) YIn0.9Mn0.1O3–ZnO NIR reflective nano-pigment exhibiting three different colors: Ochre, cyan blue, and deep blue. Journal of Solid State Chemistry 299:122176. https://doi.org/10.1016/j.jssc.2021.122176

173. Ma Y, Chen Y, Wang Z, et al (2020) Controllable near-infrared reflectivity and infrared emissivity with substitutional iron-doped orthorhombic YMnO3 coatings. Solar Energy 206:778–786. https://doi.org/10.1016/j.solener.2020.06.063

174. Sreeram KJ, Aby CP, Nair BU, Ramasami T (2008) Colored cool colorants based on rare earth metal ions. Solar Energy Materials and Solar Cells 92:1462–1467. https://doi.org/10.1016/j.solmat.2008.06.008

175. Jovaní M, Sanz A, Beltrán-Mir H, Cordoncillo E (2016) New red-shade environmental-friendly multifunctional pigment based on Tb and Fe doped Y2Zr2O7 for ceramic applications and cool roof coatings. Dyes and Pigments 133:33–40. https://doi.org/10.1016/j.dyepig.2016.05.042

176. Raj AKV, Rao PPrabhakar, Sreena TS, Thara TRAju (2019) Pigmentary colors from yellow to red in Bi2Ce2O7 by rare earth ion substitutions as possible high NIR reflecting pigments. Dyes and Pigments 160:177–187. https://doi.org/10.1016/j.dyepig.2018.08.010

177. Olegário RC, Ferreira de Souza EC, Marcelino Borges JF, et al (2013) Synthesis and characterization of Fe3+ doped cerium–praseodymium oxide pigments. Dyes and Pigments 97:113–117. https://doi.org/10.1016/j.dyepig.2012.12.011

178. Jose S, Narendranath SB, Joshy D, et al (2018) Low temperature synthesis of NIR reflecting bismuth doped cerium oxide yellow nano-pigments. Materials Letters 233:82–

85. https://doi.org/10.1016/j.matlet.2018.08.136

179. Farbod M, Rafati Z (2016) Color parameters of Y2Cu2O5 green-blue nanopigments fabricated by the sol-gel combustion method and their efficiency for coloring the glazed tiles. Ceramics International 42:15732–15738. https://doi.org/10.1016/j.ceramint.2016.07.033

180. Jose S, Prakash A, Laha S, et al (2014) Green colored nano-pigments derived from Y2BaCuO5: NIR reflective coatings. Dyes and Pigments 107:118–126. https://doi.org/10.1016/j.dyepig.2014.03.025

181. Těšitelová K, Šulcová P (2016) Synthesis and study of Bi2Ce2O7 as inorganic pigment. Journal of Thermal Analysis and Calorimetry 125:1047–1052. https://doi.org/10.1007/s10973-016-5322-0

182. Xiao Y, Huang B, Chen J, Sun X (2018) Novel Bi3+ doped and Bi3+/Tb3+ co-doped LaYO3 pigments with high near-infrared reflectances. Journal of Alloys and Compounds 762:873–880. https://doi.org/10.1016/j.jallcom.2018.05.233

183. Liu L, Han A, Ye M, Zhao M (2015) Synthesis and characterization of Al3+ doped LaFeO3 compounds: A novel inorganic pigments with high near-infrared reflectance. Solar Energy Materials and Solar Cells 132:377–384. https://doi.org/10.1016/j.solmat.2014.08.048

184. Zhao M, Han A, Ye M, Wu T (2013) Preparation and characterization of Fe3+ doped Y2Ce2O7 pigments with high near-infrared reflectance. Solar Energy 97:350–355. https://doi.org/10.1016/j.solener.2013.08.007

185. Sarasamma Vishnu V, Lakshmipathi Reddy M (2011) Near-infrared reflecting inorganic pigments based on molybdenum and praseodymium doped yttrium cerate: Synthesis, characterization and optical properties. Solar Energy Materials and Solar Cells 95:2685–2692. https://doi.org/10.1016/j.solmat.2011.05.042

186. Huang B, Xiao Y, Huang C, et al (2017) Environment-friendly pigments based on praseodymium and terbium doped La2Ce2O7 with high near-infrared reflectance: Synthesis and characterization. Dyes and Pigments 147:225–233. https://doi.org/10.1016/j.dyepig.2017.08.004

187. Vishnu VS, George G, Reddy MLP (2010) Effect of molybdenum and praseodymium dopants on the optical properties of Sm2Ce2O7: Tuning of band gaps to realize various color hues. Dyes and Pigments 85:117–123. https://doi.org/10.1016/j.dyepig.2009.10.012

188. Radhika SP, Sreeram KJ, Unni Nair B (2014) Mo-Doped Cerium Gadolinium Oxide as Environmentally Sustainable Yellow Pigments. ACS Sustainable Chemistry & Engineering 2:1251–1256. https://doi.org/10.1021/sc500085m

189. Raj AKV, Prabhakar Rao P, Sameera S, Divya S (2015) Pigments based on terbium-doped yttrium cerate with high NIR reflectance for cool roof and surface coating applications. Dyes and Pigments 122:116–125. https://doi.org/10.1016/j.dyepig.2015.06.021

190. Chen J, Xiao Y, Huang B, Sun X (2018) Sustainable cool pigments based on iron and tungsten co-doped lanthanum cerium oxide with high NIR reflectance for energy saving. Dyes and Pigments 154:1–7. https://doi.org/10.1016/j.dyepig.2018.02.032

191. Chen J, Xie W, Guo X, et al (2020) Near infrared reflective pigments based on Bi3YO6 for heat insulation. Ceramics International 46:24575–24584. https://doi.org/10.1016/j.ceramint.2020.06.245

102. Ding C, Tian M, Han A, et al (2020) V-doped LaPO4 new solar heat-reflective pigments and its improvement on the aging resistance of poly-methyl methacrylate. Solar Energy 195:660–669. https://doi.org/10.1016/j.solener.2019.12.002

193. Fortuño-Morte M, Beltrán-Mir H, Cordoncillo E (2020) Study of the role of praseodymium and iron in an environment-friendly reddish orange pigment based on Fe doped Pr2Zr2O7: A multifunctional material. Journal of Alloys and Compounds 845:155841. https://doi.org/10.1016/j.jallcom.2020.155841

194. Vishnu VS, George G, Divya V, Reddy MLP (2009) Synthesis and characterization of new environmentally benign tantalum-doped Ce0.8Zr0.2O2 yellow pigments: Applications in coloring of plastics. Dyes and Pigments 82:53–57. https://doi.org/10.1016/j.dyepig.2008.11.001

195. Yao B, Geng S, Wang J, Wang L (2018) Synthesis, Characterization, and Optical

Properties of Near-Infrared Reflecting Composite Inorganic Pigments Composed of TiO2/CuO Core–Shell Particles. Australian Journal of Chemistry 71:373. https://doi.org/10.1071/ch17626

196. He X, Wang F, Liu H, et al (2017) Fabrication of highly dispersed NiTiO3@TiO2 yellow pigments with enhanced NIR reflectance. Materials Letters 208:82–85. https://doi.org/10.1016/j.matlet.2017.05.047

197. He X, Wang F, Liu H, et al (2017) Synthesis and coloration of highly dispersed NiTiO 3 @TiO 2 yellow pigments with core-shell structure. Journal of the European Ceramic Society 37:2965–2972. https://doi.org/10.1016/j.jeurceramsoc.2017.03.020

198. Zou J, Chen Y, Zhang P (2021) Influence of crystallite size on color properties and NIR reflectance of TiO2@NiTiO3 inorganic pigments. Ceramics International 47:12661–12666. https://doi.org/10.1016/j.ceramint.2021.01.126

199. Sadeghi-Niaraki S, Ghasemi B, adeh AH, et al (2019) Preparation of (Fe,Cr)2O3@TiO2 cool pigments for energy saving applications. Journal of Alloys and Compounds 779:367–379. https://doi.org/10.1016/j.jallcom.2018.11.114

200. Sadeghi-Niaraki S, Ghasemi B, Habibolahzadeh A, et al (2020) Cool and photocatalytic reddish-brown nanostructured Fe2O3@SiO2@TiO2 pigments. Materials Science and Engineering: B 262:114752. https://doi.org/10.1016/j.mseb.2020.114752

201. Soranakom P, Vittayakorn N, Rakkwamsuk P, et al (2021) Effect of surfactant concentration on the formation of Fe2O3@SiO2 NIR-reflective red pigments. Ceramics International 47:13147–13155. https://doi.org/10.1016/j.ceramint.2021.01.179

202. Zhang T, Wang Y, Pan Z (2019) Preparation of hollow glass microspheres@ZnS Se1− or copper-/indium-co-doped ZnS Se1− composite color pigments with enhanced near-infrared reflectance. Solar Energy 184:570–583. https://doi.org/10.1016/j.solener.2019.04.038

203. Lu D, Gao Q, Wu X, Fan Y (2017) ZnO nanostructures decorated hollow glass microspheres as near infrared reflective pigment. Ceramics International 43:9164–9170. https://doi.org/10.1016/j.ceramint.2017.04.067

204. Gao Q, Wu X, Fan Y, Meng Q (2018) Novel near infrared reflective pigments based on hollow glass microsphere/BiOCl1-xIx composites: Optical property and superhydrophobicity. Solar Energy Materials and Solar Cells 180:138–147. https://doi.org/10.1016/j.solmat.2018.02.033

205. Gao Q, Wu X, Fan Y (2014) Solar spectral optical properties of rutile TiO2 coated mica–titania pigments. Dyes and Pigments 109:90–95. https://doi.org/10.1016/j.dyepig.2014.04.028

206. Yuan L, Han A, Ye M, et al (2017) Synthesis and characterization of novel nontoxic BiFe1−xAlxO3/mica-titania pigments with high NIR reflectance. Ceramics International 43:16488–16494. https://doi.org/10.1016/j.ceramint.2017.09.032

207. Bedon C, Honfi D, Machalická KV, et al (2019) Structural characterisation of adaptive facades in Europe – Part I: Insight on classification rules, performance metrics and design

208.. Ascione F, Bianco N, Iovane T, et al (2021) The evolution of building energy retrofit via double-skin and responsive façades: A review. Solar Energy 224:703–717. https://doi.org/10.1016/j.solener.2021.06.035

209. Balali A, Valipour A (2020) Identification and selection of building façade’s smart materials according to sustainable development goals. Sustainable Materials and Technologies 26:e00213. https://doi.org/10.1016/j.susmat. 2020.e00213

210. Karlessi T, Santamouris M, Apostolakis K, et al (2009) Development and testing of thermochromic coatings for buildings and urban structures. Solar Energy 83:538–551. https://doi.org/10.1016/j.solener.2008.10.005

211. Berardi U, Garai M, Morselli T (2020) Preparation and assessment of the potential energy savings of thermochromic and cool coatings considering inter-building effects. Solar Energy 209:493–504. https://doi.org/10.1016/j.solener.2020.09.015

212. Granadeiro V, Almeida M, Souto T, et al (2020) Thermochromic Paints on External Surfaces: Impact Assessment for a Residential Building through Thermal and Energy Simulation. Energies 13:1912. https://doi.org/10.3390/en13081912

213. Chang T-C, Cao X, Bao S-H, et al (2018) Review on thermochromic vanadium dioxide based smart coatings: from lab to commercial application. Advances in Manufacturing 6:1–19. https://doi.org/10.1007/s40436-017-0209-2

214. Luceño-Sánchez J, Díez-Pascual A, Peña Capilla R (2019) Materials for Photovoltaics: State of Art and Recent Developments. International Journal of Molecular Sciences 20:976. https://doi.org/10.3390/ijms20040976

215. Joost U, Šutka A, Oja M, et al (2018) Reversible Photodoping of TiO2 Nanoparticles for Photochromic Applications. Chemistry of Materials 30:8968–8974. https://doi.org/10.1021/acs.chemmater.8b04813

216. Wang S, Fan W, Liu Z, et al (2018) Advances on tungsten oxide based photochromic materials: strategies to improve their photochromic properties. Journal of Materials Chemistry C 6:191–212. https://doi.org/10.1039/c7tc04189f

217. Moreira MANS, Heitmann AP, Bezerra ACS, et al (2020) Photocatalytic performance of cementitious materials with addition of red mud and Nb2O5 particles. Construction and Building Materials 259:119851. https://doi.org/10.1016/j.conbuildmat.2020.119851

218. Kousis I, Fabiani C, Gobbi L, Pisello AL (2020) Phosphorescent-based pavements for counteracting urban overheating – A proof of concept. Solar Energy 202:540–552. https://doi.org/10.1016/j.solener.2020.03.092

219.. Lu X, Guo S, Tong X, et al (2017) Tunable Photocontrolled Motions Using Stored Strain Energy in Malleable Azobenzene Liquid Crystalline Polymer Actuators. Advanced Materials 29:1606467. https://doi.org/10.1002/adma.201606467

220. Fabiani C, Chiatti C, Pisello AL (2021) Development of photoluminescent composites for energy efficiency in smart outdoor lighting applications: An experimental and numerical investigation. Renewable Energy 172:1–15. https://doi.org/10.1016/j.renene.2021.02.071

221.Chiatti C, Fabiani C, Cotana F, Pisello AL (2021) Exploring the potential of photoluminescence for urban passive cooling and lighting applications: A new approach towards materials' optimization. Energy 231:120815.

https://doi.org/10.1016/j.energy.2021.120815

222. Wang J (Jialiang), Shi D (2017) Spectral selective and photothermal nano structured thin films for energy efficient windows. Applied Energy 208:83–96. https://doi.org/10.1016/j.apenergy.2017.10.066

223. Kulczyk-Malecka J, Kelly PJ, West G, et al (2014) Investigation of silver diffusion in TiO2/Ag/TiO2 coatings. Acta Materialia 66:396–404. https://doi.org/10.1016/j.actamat.2013.11.030

224. Sahu DR, Lin S-Y, Huang J-L (2006) ZnO/Ag/ZnO multilayer films for the application of a very low resistance transparent electrode. Applied Surface Science 252:7509–7514. https://doi.org/10.1016/j.apsusc.2005.09.021

225. White JR, de Poumeyrol B, Hale JM, Stephenson R (2004) Piezoelectric paint: Ceramic-polymer composites for vibration sensors. Journal of Materials Science 39:3105–3114. https://doi.org/10.1023/b:jmsc.0000025839.98785.b9

226. Ahmed R, Mir F, Banerjee S (2017) A review on energy harvesting approaches for renewable energies from ambient vibrations and acoustic waves using piezoelectricity. Smart Materials and Structures 26:085031. https://doi.org/10.1088/1361-665x/aa7bfb

227. Gu L, Zhou D, Cao J (2016) Piezoelectric Active Humidity Sensors Based on Lead-Free NaNbO3 Piezoelectric Nanofibers. Sensors 16:833. https://doi.org/10.3390/s16060833

228.Rodrigues C, Nunes D, Clemente D, et al (2020) Emerging triboelectric nanogenerators for ocean wave energy harvesting: state of the art and future perspectives. Energy & Environmental Science 13:2657–2683. https://doi.org/10.1039/d0ee01258k

229. Chen J, Guo H, Ding P, et al (2016) Transparent triboelectric generators based on glass and polydimethylsiloxane. Nano Energy 30:235–241. https://doi.org/10.1016/j.nanoen.2016.10.005

230. Wang J, Meng C, Gu Q, et al (2020) Normally Transparent Tribo-Induced Smart Window. ACS Nano 14:3630–3639. https://doi.org/10.1021/acsnano.0c00107

231. Akeiber H, Nejat P, Majid MZAbd, et al (2016) A review on phase change material

(PCM) for sustainable passive cooling in building envelopes. Renewable and Sustainable Energy Reviews 60:1470–1497. https://doi.org/10.1016/j.rser.2016.03.036

232. Cheng X, Zhai X, Wang R (2016) Thermal performance analysis of a packed bed cold storage unit using composite PCM capsules for high temperature solar cooling application. Applied Thermal Engineering 100:247–255. https://doi.org/10.1016/j.applthermaleng.2016.02.036

233. Chung MH, Park JC (2016) Development of PCM cool roof system to control urban heat island considering temperate climatic conditions. Energy and Buildings 116:341–348. https://doi.org/10.1016/j.enbuild.2015.12.056

234. Lei J, Kumarasamy K, Zingre KT, et al (2017) Cool colored coating and phase change materials as complementary cooling strategies for building cooling load reduction in tropics. Applied Energy 190:57–63. https://doi.org/10.1016/j.apenergy.2016.12.114

235. Cannavale A, Ayr U, Fiorito F, Martellotta F (2020) Smart Electrochromic Windows to Enhance Building Energy Efficiency and Visual Comfort. Energies 13:1449. https://doi.org/10.3390/en13061449

236. Tavares PF, Gaspar AR, Martins AG, Frontini F (2014) Evaluation of electrochromic windows impact in the energy performance of buildings in Mediterranean climates. Energy Policy 67:68–81. https://doi.org/10.1016/j.enpol.2013.07.038

237. Jelle BP, Gao T (2015) The Utilization of Electrochromic Materials for Smart Window Applications in Energy-Efficient Buildings. In: Proceedings of TechConnect World Innovation

238. Nishizawa K, Yamada Y, Yoshimura K (2017) Low-temperature chemical fabrication of Pt-WO 3 gasochromic switchable films using UV irradiation. Solar Energy Materials and Solar Cells 170:21–26. https://doi.org/10.1016/j.solmat.2017.05.058

239. Zahir MdH, Mohamed SA, Saidur R, Al-Sulaiman FA (2019) Supercooling of phase-change materials and the techniques used to mitigate the phenomenon. Applied Energy 240:793–817. https://doi.org/10.1016/j.apenergy.2019.02.045

240. Cannavale A (2020) Chromogenic Technologies for Energy Saving. Clean

Technologies 2:462–475. https://doi.org/10.3390/cleantechnol2040029

241. Piccolo A, Marino C, Nucara A, Pietrafesa M (2018) Energy performance of an electrochromic switchable glazing: Experimental and computational assessments. Energy and Buildings 165:390–398. https://doi.org/10.1016/j.enbuild.2017.12.049

242. Lin Y-J, Chang Y-H, Yang W-D, Tsai B-S (2006) Synthesis and characterization of ilmenite NiTiO3 and CoTiO3 prepared by a modified Pechini method. Journal of Non-Crystalline Solids 352:789–794. https://doi.org/10.1016/j.jnoncrysol.2006.02.001

243. Sakka S (2013) Sol–Gel Process and Applications. In: Handbook of Advanced Ceramics (Second Edition). Academic Press, pp. 883–910

244. Yu Y-H, Xia M (2012) Preparation and characterization of ZnTiO3 powders by sol–gel process. Materials Letters 77:10–12. https://doi.org/10.1016/j.matlet.2012.02.113

245. Brinker C (1990) Sol-Gel Science. In: The Physics and Chemistry of Sol–Gel Processing. Academic Press, USA, pp. xvi–18

246. Spooren J, Walton RI (2005) Hydrothermal synthesis of the perovskite manganites Pr0.5Sr0.5MnO3 and Nd0.5Sr0.5MnO3 and alkali-earth manganese oxides CaMn2O4, 4H-SrMnO3, and 2H-BaMnO3. Journal of Solid State Chemistry 178:1683–1691. https://doi.org/10.1016/j.jssc.2005.03.006

247. Xia C-T, Shi E-W, Zhong W-Z, Guo J-K (1996) Hydrothermal synthesis of BaTiO3 nano/microcrystals. Journal of Crystal Growth 166:961–966. https://doi.org/10.1016/0022-0248(95)00521-8

248. Xue P, Hu Y, Xia W, et al (2017) Molten-salt synthesis of BaTiO3 powders and their atomic-scale structural characterization. Journal of Alloys and Compounds 695:2870–2877. https://doi.org/10.1016/j.jallcom.2016.11.395

249. Xing X, Zhang C, Qiao L, et al (2006) Facile Preparation of ZnTiO3 Ceramic Powders in Sodium/Potassium Chloride Melts. Journal of the American Ceramic Society 89:1150–1152. https://doi.org/10.1111/j.1551-2916.2005. 00853.x

250. Pholnak C, Sirisathitkul C, Danworaphong S, Harding DJ (2013) Sonochemical Synthesis of Zinc Oxide Nanoparticles Using an Ultrasonic Homogenizer. Ferroelectrics

455:15–20. https://doi.org/10.1080/00150193.2013.843405

251. Hassanjani-Roshan A, Vaezi MR, Shokuhfar A, Rajabali Z (2011) Synthesis of iron oxide nanoparticles via sonochemical method and their characterization. Particuology 9:95–99. https://doi.org/10.1016/j.partic.2010.05.013

252. Mason, T.J., Lorimer, J.P. (2002) Introduction to Applied Ultrasonics. In: Applied Sonochemistry: Uses of Power Ultrasound in Chemistry and Processing, Wiley-VCH Verlag GmbH & Co. KGaA, UK, pp. 20–21

Acknowledgements

This work was financially supported by project PTDC/ECI-CON/28766/2017 - POCI-01-0145-FEDER-028766 funded by FEDER funds through Compete2020 - Programa Operacional Competitividade e Internacionalização (POCI), project Circular 2B funded by EEA Grants and by Base Funding - UIDB/04708/2020 of the CONSTRUCT - Instituto de I&D em Estruturas e Construções - funded by national funds through the FCT/MCTES (PIDDAC). R. C. Veloso would like to acknowledge the support of FCT - Fundação para a Ciência e Tecnologia for the funding the doctoral grant SFRH/BD/148785/2019.

Graphical Abstract

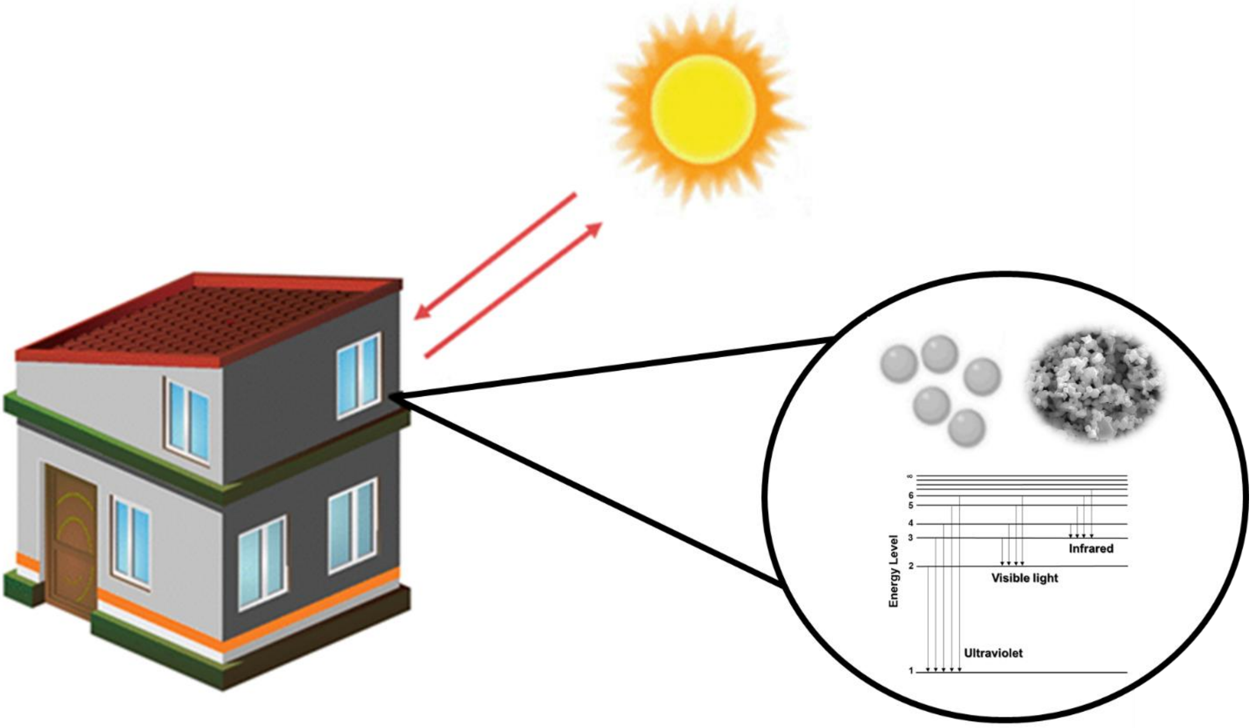

Copyrights

Table A 1: Evidence of reprint permissions for illustrations.

Figure	Page	License number
1	3	5150271162295
3	7	5140811338468
4	8	Open Access- MDPI
5	9	5150280142822
7	14	5150280331439
8	15	5150280598746
9	17	5150290094443
11	19	5150290259414
14 and 15	22 and 23	5150290490122
16	24	Figure under common license, already requested permission
17 a)	25	Open Access
17 b)	25	1148065
18	26	5150300035847
19	27	5150300320203
20	28	5150300464175
21	29	5150710833614
22	30	5150710971057
23	31	5150711078449
24	31	5150711196566
25	32	5150711302982
26	33	Permission/license is granted at no charge
27	36	5150720213700
28	37	5150720390351
29	38	5150720512162
30	39	5150720683495
31	41	Permission granted by email

32	43	5150730172363
35	47	1148208
37	49	Permission/license is granted at no charge
39	50	This article is licensed under a Creative Commons, permission is granted since provided the correct acknowledgement